Off-axis electron holography for the quantitative study of magnetic properties of nanostructures.

From single nano-magnets to complex devices

Etienne SNOECK, Christophe GATEL,
Robin Cours, Aurélien Masseboeuf

CEMES-CNRS

29 rue Jeanne Marvig, 31055,
Toulouse, France

CEMES - Toulouse

1. **Spin configurations in size controlled single Fe nanomagnets => 0D**
2. ***In situ* electron holography of the dynamic field emanating from a HDD writer => 3D**

Electron Holography : Mapping fields

Interaction electron-matter

$$\psi(\mathbf{r}) = \sum_{\mathbf{g}} \tilde{\psi}_g(\mathbf{r}) e^{2\pi i \mathbf{g}.\mathbf{r}}$$

amplitude and **phase**

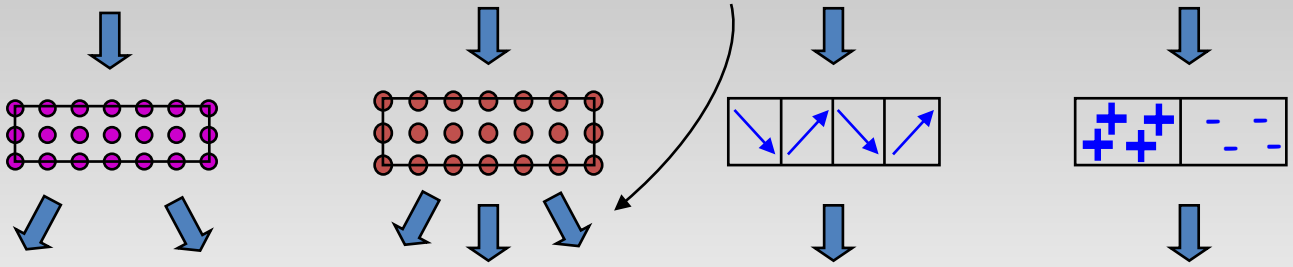

Phase shift

Geometric	Crystalline	Magnetic	Electric
$\varphi = \varphi_{geom}$	$+ \varphi_{cryst}$	$+ \varphi_{mag}$	$+ \varphi_{elec}$
Strain field	**Crystal structure**	**Magnetic field**	**Electrostatic field**

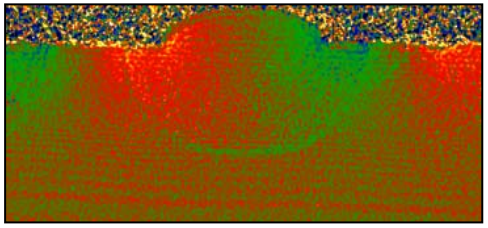

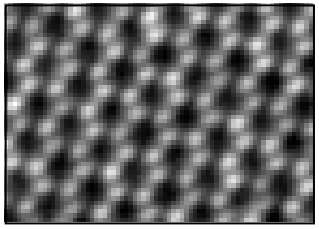

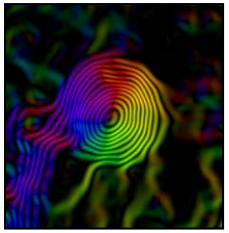

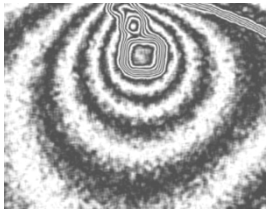

Electron wave in a TEM

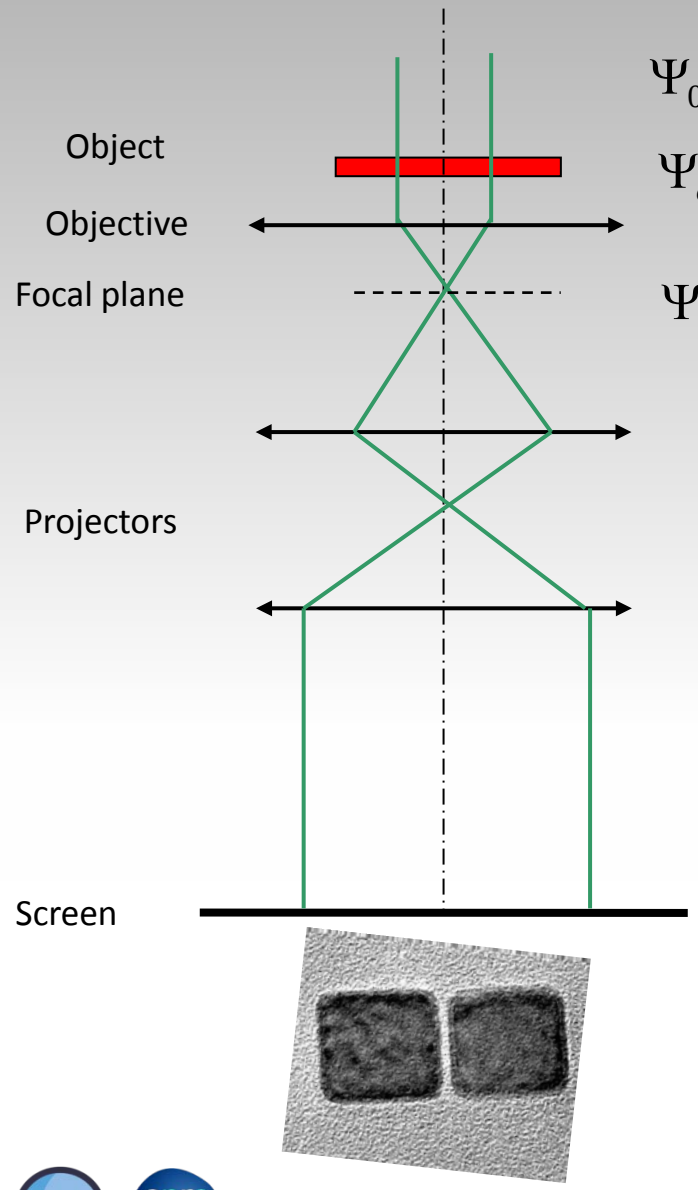

$$\Psi_0 = \exp(i\vec{k}.\vec{r})$$

$$\Psi_{obj} = a_0(\vec{r})\exp i(\vec{k}.\vec{r} + \phi_0(\vec{r}))$$

Phase shift after interaction with the object

$$\Psi_s = a_s(\vec{r})\exp i(\vec{k}.\vec{r} + \phi_s(\vec{r}))$$

Phase shift below the objective

$$I(x,y) \propto |\Psi_s|^2 \propto a_s{}^2(\vec{r})$$

Image

$\phi_s(\vec{r})$ is lost!

What information is carried by $\phi_s(\vec{r})$?

$$\Psi_0 = \exp(i\vec{k}.\vec{r})$$

Electromagnetic field

- Electrostatic potential : V
- Magnetic Potential vector : $\vec{A}$

Aharonov-Bohm

$$\Psi_s = a_s(\vec{r})\exp i(\vec{k}.\vec{r} + \phi_s(\vec{r}))$$

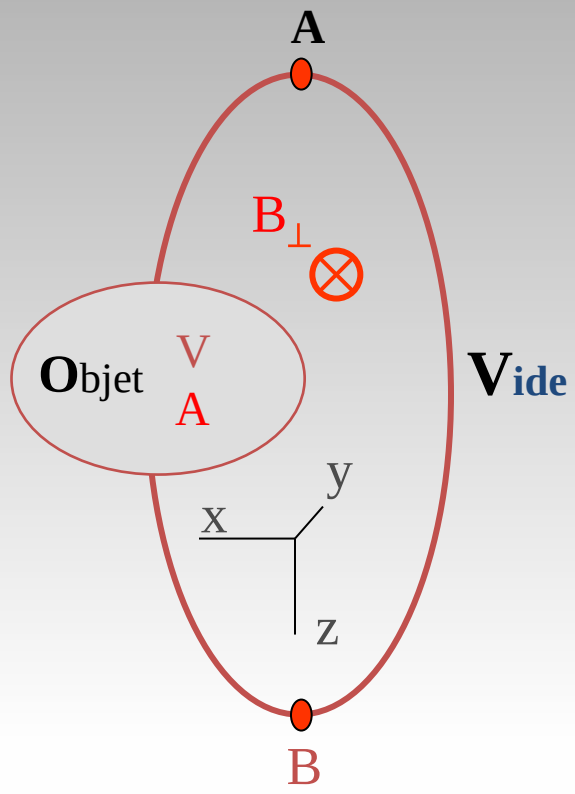

$$\phi_s(x,y) = C_E \int V(x,y,z).dz - \frac{e}{h}\int A_z(x,z).dz$$

$$= C_E \int V(x,y,z).dz - \frac{e}{h}\iint B_\perp(x,z).dx.dz$$

$$C_E = \left(\frac{2\pi}{\lambda}\right)\left(\frac{E+E_0}{E(E+2E_0)}\right)$$

Electrostatic potential contribution to the phase shift

Magnetic contribution to the phase shift

$\phi_s(\vec{r})$

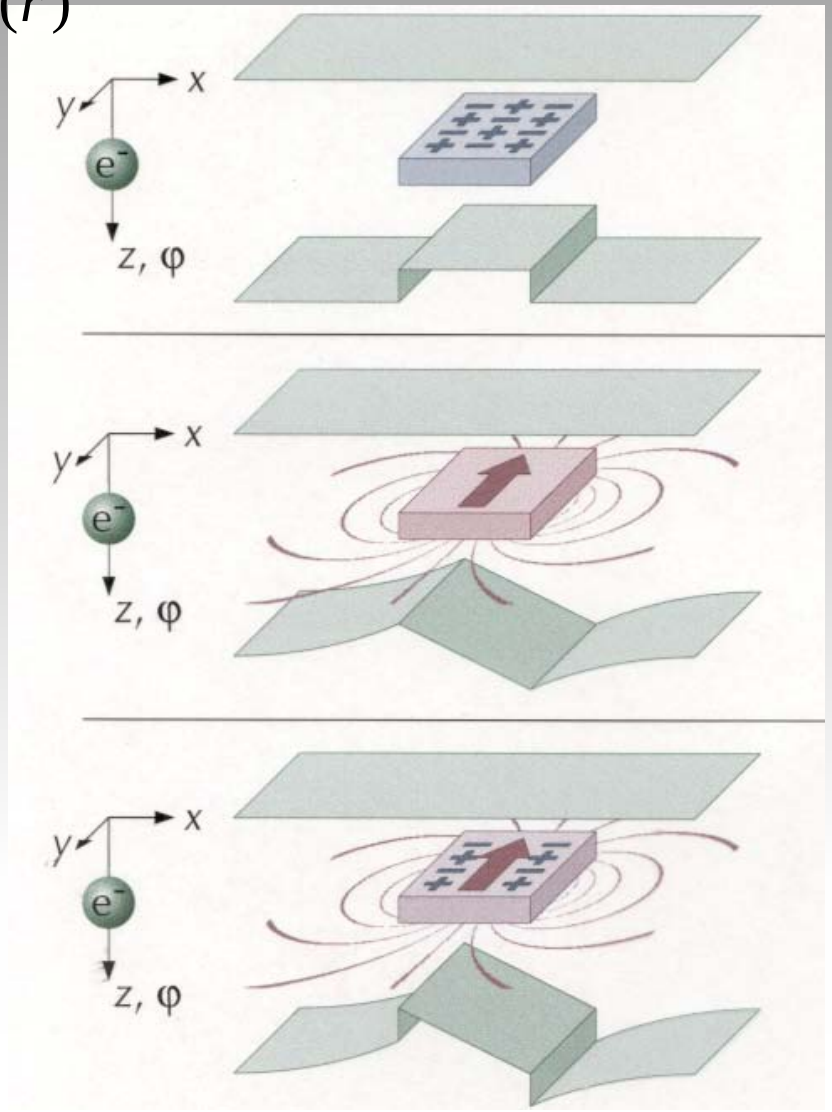

Phase shift induced by the local electrostatic potential:

$$\phi_{Elec}(x) = C_E \int V(x,y,z).dz$$

Phase shift induced by the local magnetic field :

$$\phi_{Mag}(x) = -\frac{e}{h} \iint B_{\perp}(x,z).dx.dz$$

Total phase shift

$$\phi_{Total}(x) = \phi_{Elec}(x) + \phi_{Mag}(x)$$

But phase image $\phi(x,y) = \phi^C(x,y) + \phi^M(x,y)$

➔ Need to separate different contributions to the phase shift

2. Off-axis Electron Holography

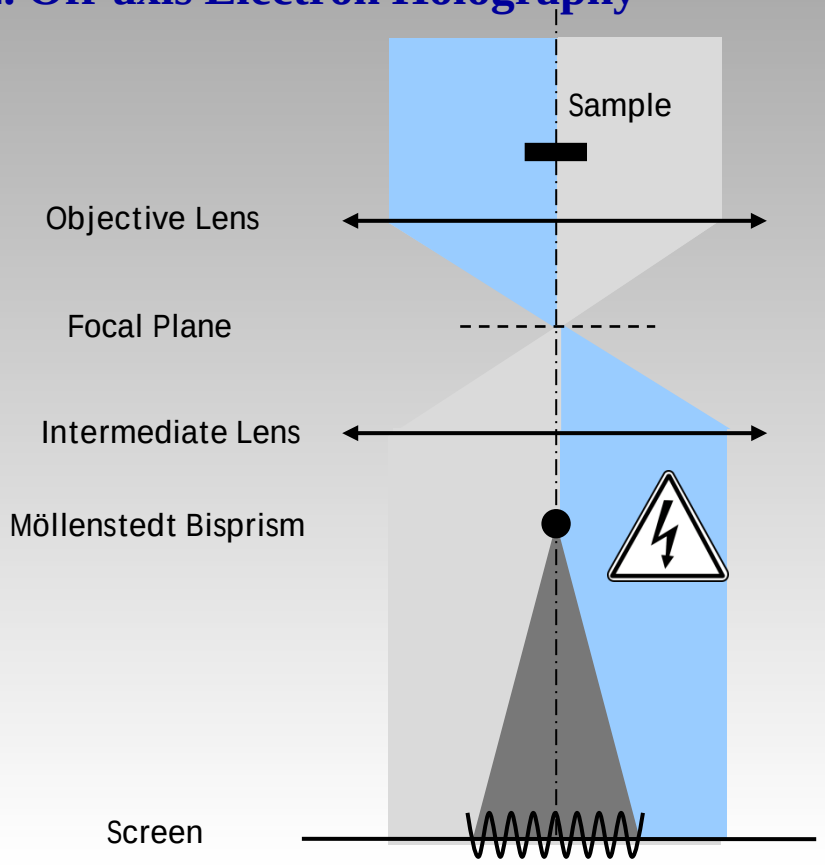

$$\psi_0 = \exp(i\mathbf{k}.\mathbf{r})$$

$$\psi(\mathbf{r}) = A(\mathbf{r})\exp i\left((\mathbf{k}.\mathbf{r}) + \varphi(r)\right)$$

$$\Psi(\mathbf{r}) = A_S(\mathbf{r})\exp i\left((\mathbf{k}.\mathbf{r}) + \varphi_S(r)\right)$$

Incident beam

↓

After the sample

↓

After the objective lens

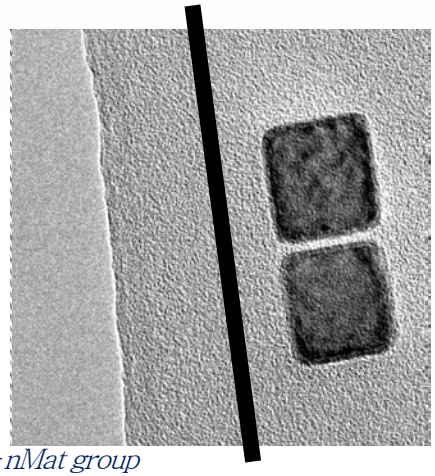

$$I_{Holo} = \left|\Psi_0 + \Psi^*\right|^2 \quad \text{+ background}$$

$$= 1 + A_s^2(x,y)$$

$$+ 2A_s(x,y).\cos(2\pi R_0.x + \boxed{\varphi_S(x,y)})$$

$$+ I_{Inélast}(x,y)$$

30nm Fe nanocubes

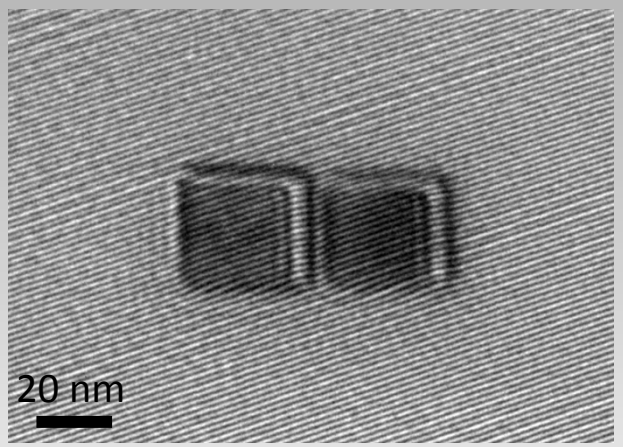

FFT

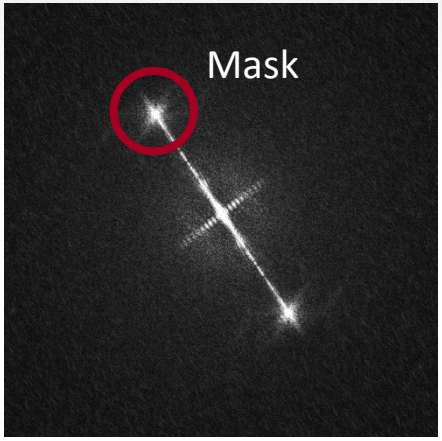

FFT^{-1}

Hologram Image

Interference between a reference wave and the wave through the sample

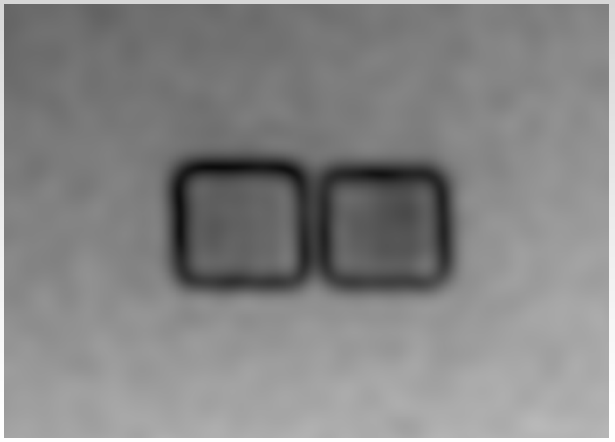

Amplitude image

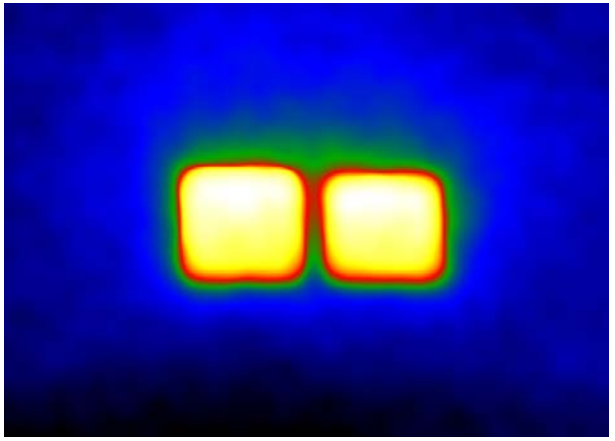

Phase image

Phase shift extraction and different contributions

30nm Fe nanocubes

$$\phi(\mathbf{R}) = \phi_{MIP,Elec}(\mathbf{R}) + \phi_{Mag}(\mathbf{R})$$

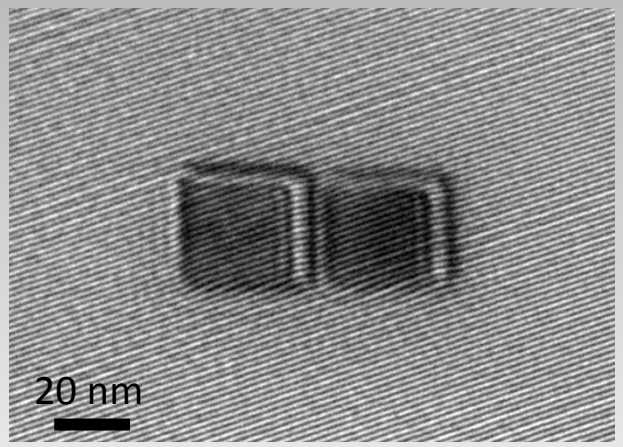

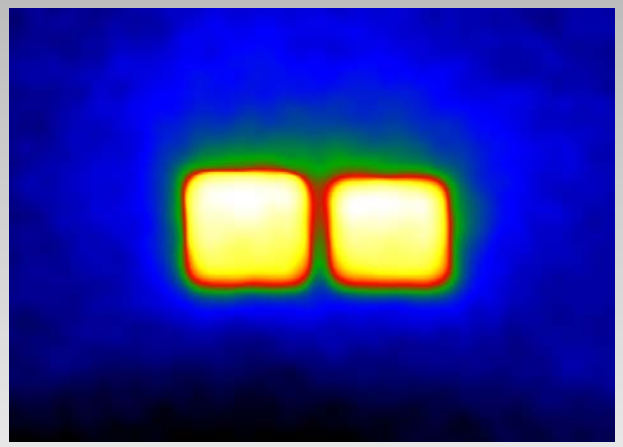

- Different methods to separate the contributions
- Need to record many holograms

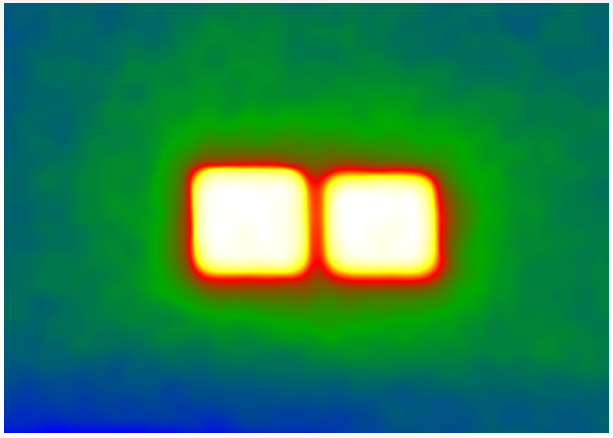

$$\phi_{MIP,Elec}(\mathbf{R}) = C_E \int V(\mathbf{r})\,\mathrm{dz}$$

$$\phi_{Mag}(\mathbf{R}) = -\frac{e}{h}\iint \mathbf{B}_{\mathbf{R}}(\mathbf{R}_{\perp}, z)\,\mathrm{dR}\,\mathrm{dz}$$

Measurements of the **magnetic induction (B)** components from $\phi_{Mag}(\vec{r})$

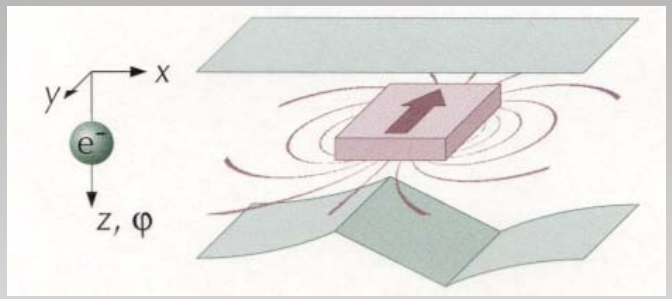

$$\phi_{Mag}(x) = -\frac{e}{h}\iint B_{\perp}(x,z).dx.dz$$

• The equiphase contours give the $B_{\perp}$ direction ➔ contours lines = in-plane projection of the magnetic flux

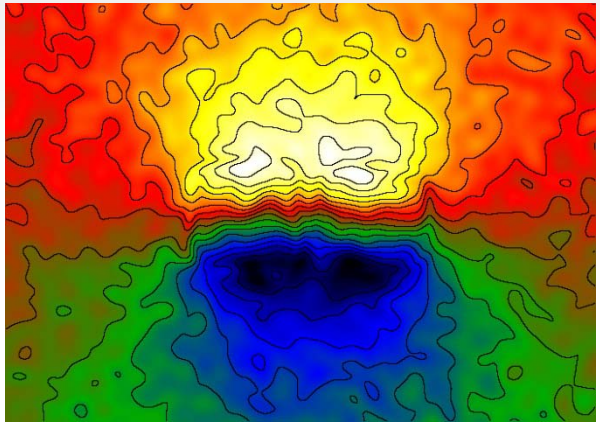

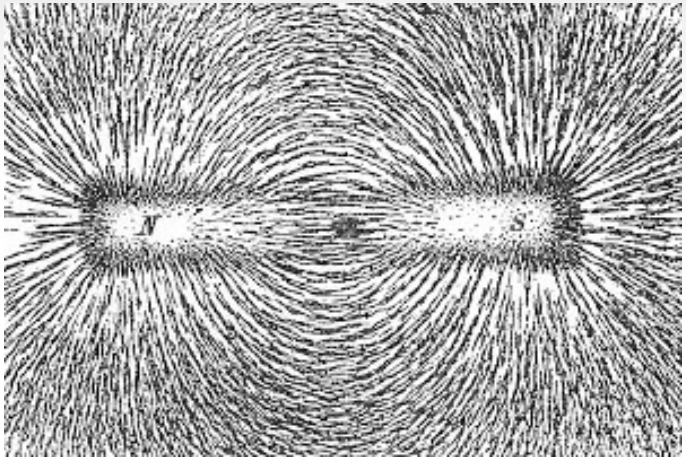

Magnetic components from ϕ^M

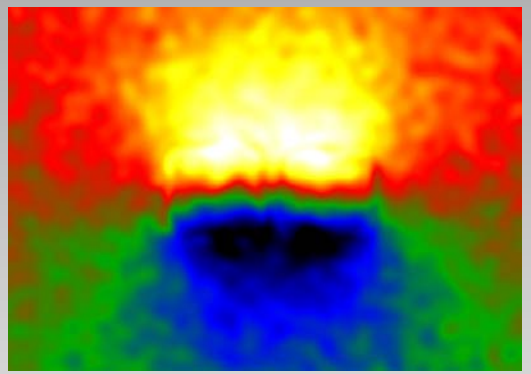

• The phase gradient is proportionnal to the in-plane $B_{\perp}$ components of the induction

➔ B_x, B_y components

$$\frac{\partial \varphi_{Mag}(y)}{\partial y} = \frac{e}{\hbar} B_x(y).t$$

(t = thickness)

$$\frac{\partial \phi_{Mag}(x)}{\partial x} = \frac{e}{h} B_y(x).t$$

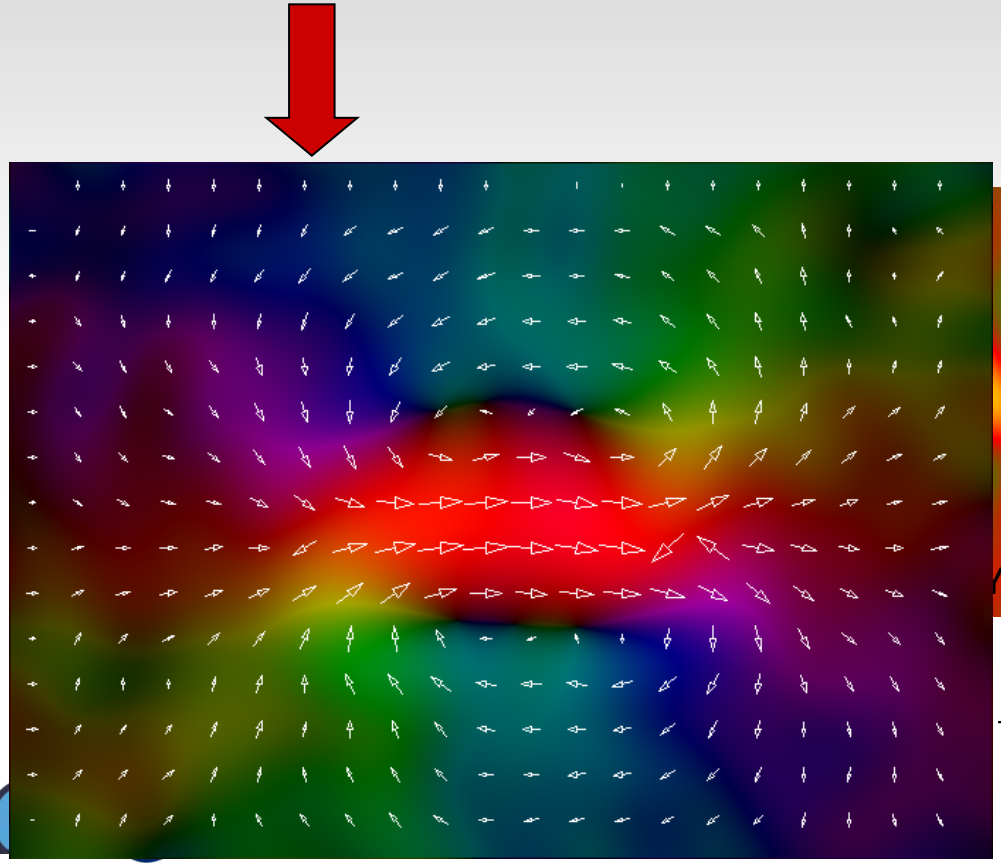

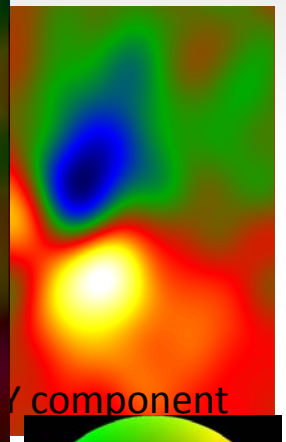

Y component

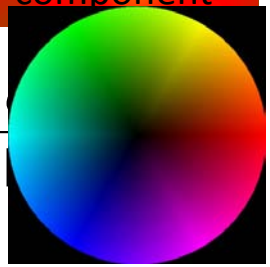

•<u>Only planar components of the induction can be measured</u>

Magnetic nanomaterials

Hybrid DW in Ni nanocylinder - N. Biziere *Nano Lett* 2013

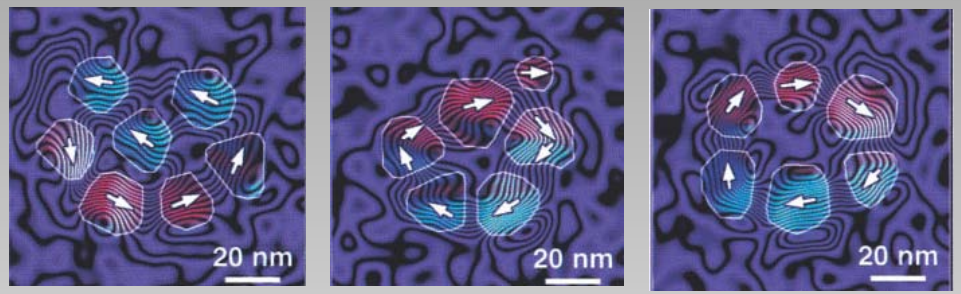

Magnetic coupling in polycrystalline Co nano-rings (*Rafal DB*)

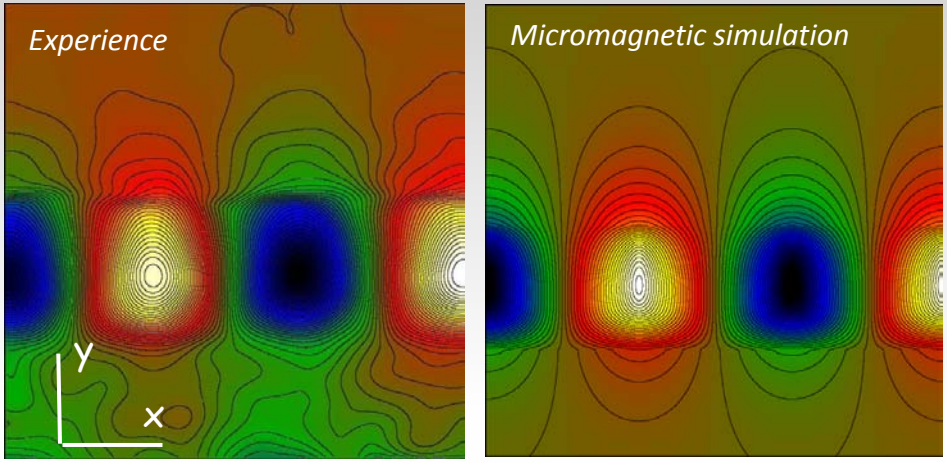

Magnetic bits in FePd epitaxial thin with perpendicular magnetic anisotropy - A. Masseboeuf et al. *Nano Lett., 2009, **9** (8), pp 2803*

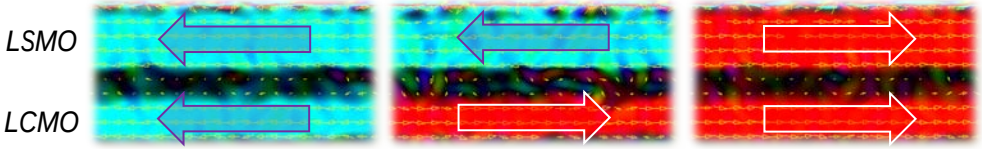

LSMO/STO/LCMo Magnetic tunnel junction reversal

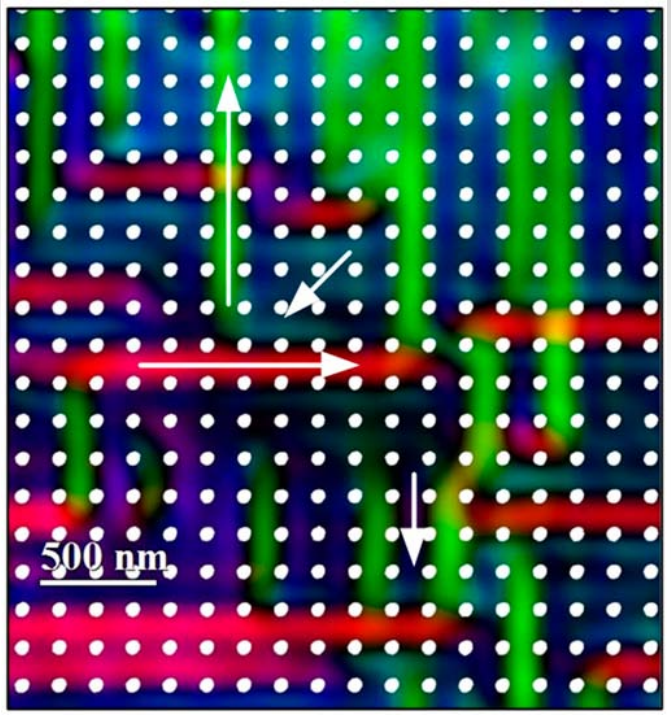

Super domain configuration in antidot array of FeNi – *L.A Rodriguez Nanotechnology. 2014*

Fe nanoparticles synthesized in liquid phase by organometallic chemistry

➔ « Model » objects for the study of magnetic transition as a function of the size

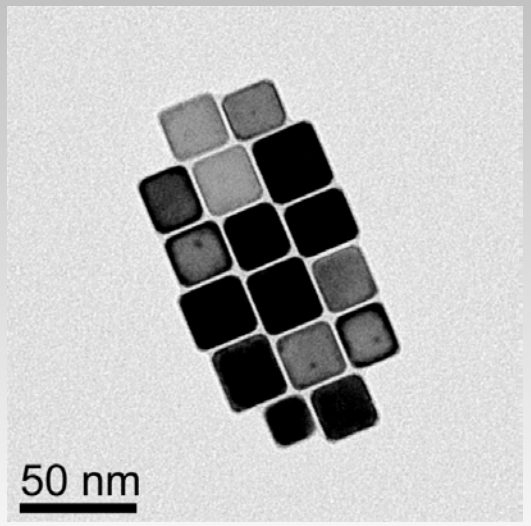

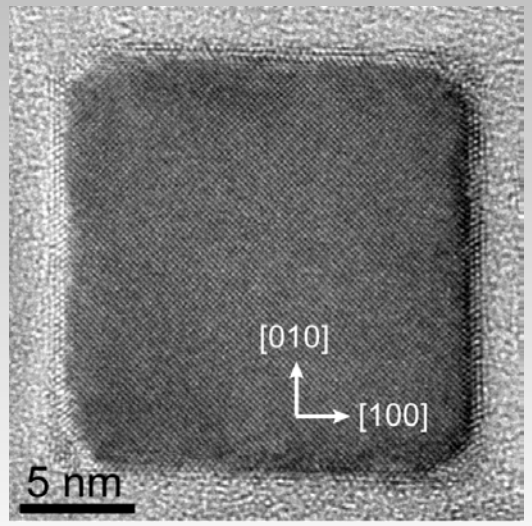

• Nanocube: single-crystal *bcc* structure with {100} facets

• <100> edges = magnetocrystalline easy axis.

~1 nm layer of Fe_3O_4 shell resulting from the air exposition during sample transfer.

➔ Magnetometry experiments on powders of nanocubes showed the **same saturation magnetization M_S than bulk Fe** (2.2 T).

Magnetic configuration of a single 30nm Fe cube

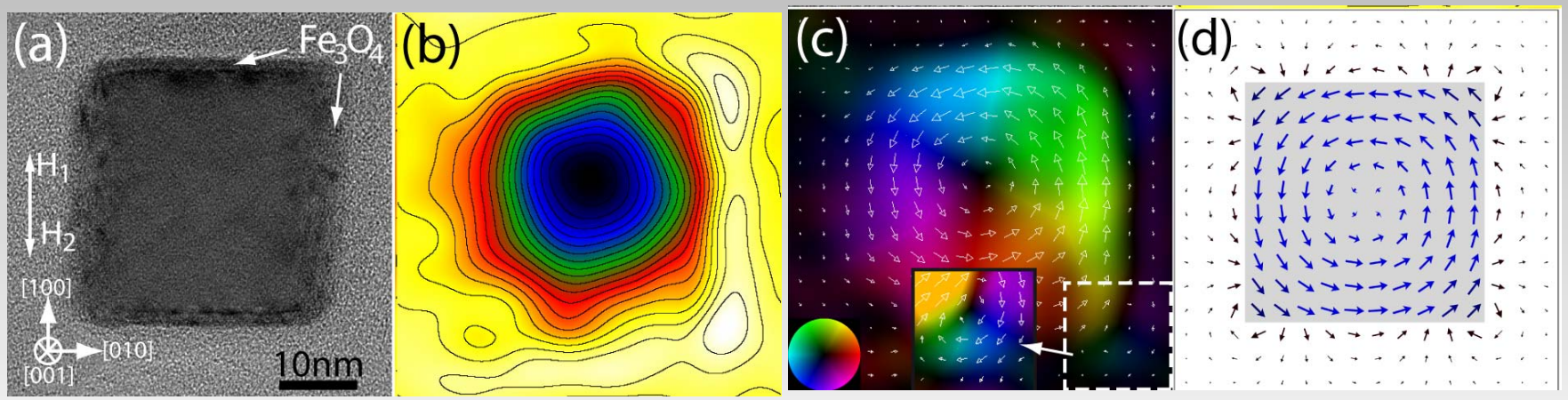

Nanoletters, ***8,*** *4293-4298 (2008)*

Spatial resolution on phase image ≈ 5 nm

Tecnai F20 in Lorentz mode

- Axial symmetry of the induction: axis perpendicular to the (001) face.
- Complete flux closure in the vortex plane to minimize the magnetostatic energy.
- Agreement between simulation and experimental results.

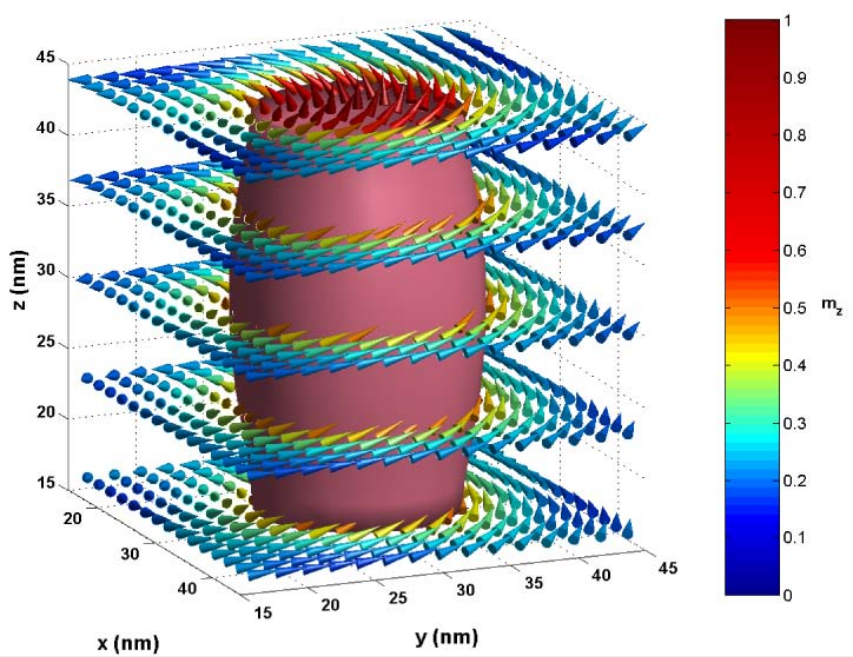

- 3D view of a micromagnetic simulation of the vortex
- Competition between dipolar interactions and exchange energy
- Diameter : 16 nm at the centre

  14 nm at the surfaces

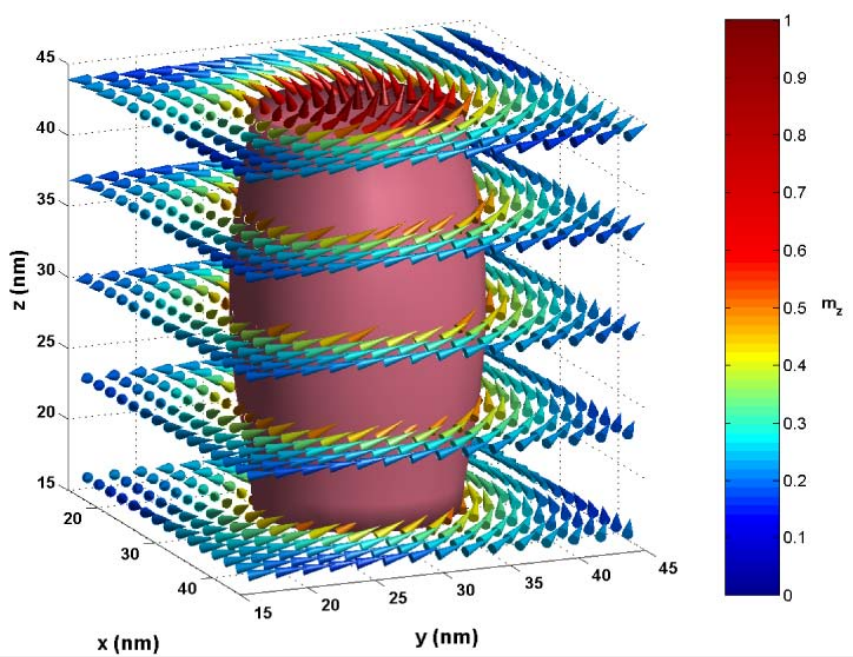

- 3D view of a micromagnetic simulation of the vortex
- Competition between dipolar interactions and exchange energy
- Diameter : 16 nm at the centre

  14 nm at the surfaces

When the nanocube size decreases:

300K : Vortex => Single Domain => Superparamagnetism

25 nm 15nm

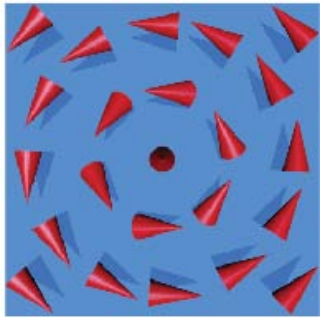

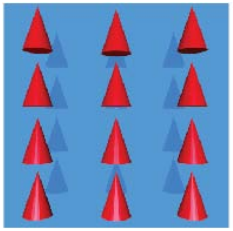

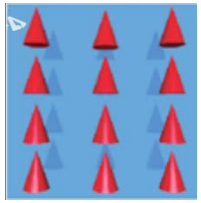

To study the Vortex -> SD transition, 2 main issues have to be solved:

- Determination of the 3rd dimension:

Evaluation of the squareness distribution, defined as a/b ratio : 18%

Nanocube thickness assumed as similar thickness to length c/a ratio, leaded to a thickness estimation $c = (1 \pm 0.18) \times a$.

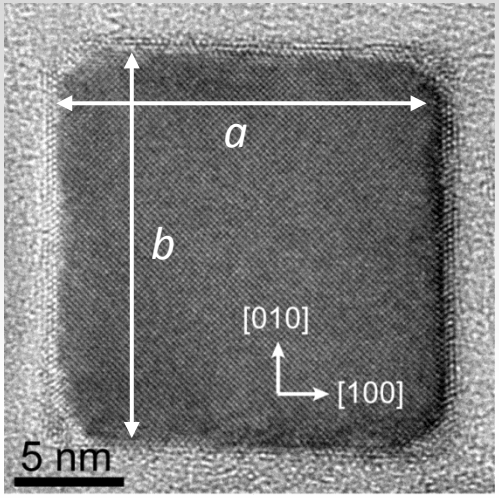

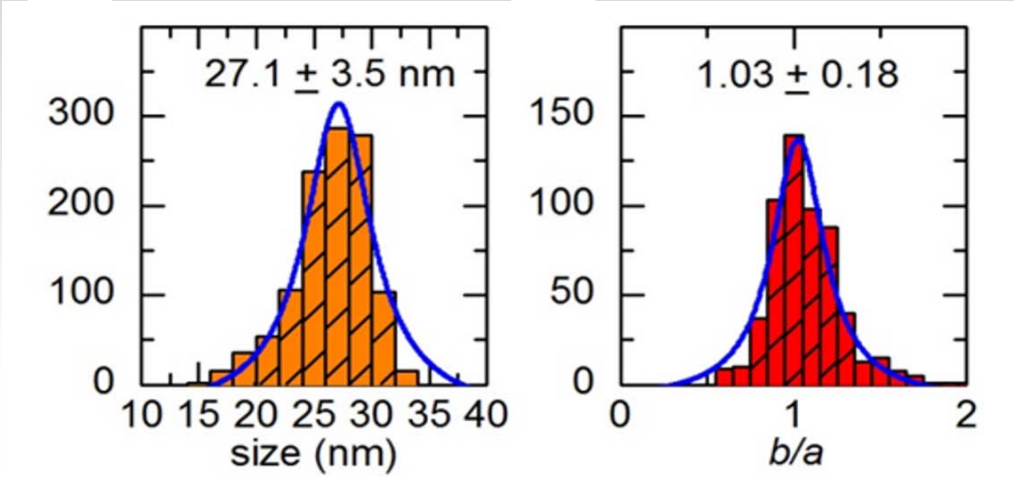

- Sensitive to the magnetic phase shift:

Decrease the size from 30 nm to 25 nm corresponds to a magnetic volume decay of more than 40%

=> Need to increase the phase sensitivity …

Tecnai F-20

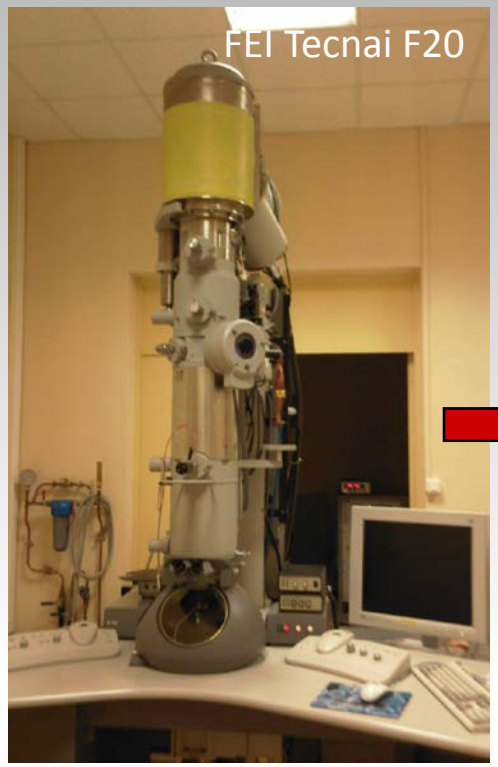

Spatial resolution ≈ 5 nm in Lorentz mode

Schottky-FEG

Hitachi HF3300

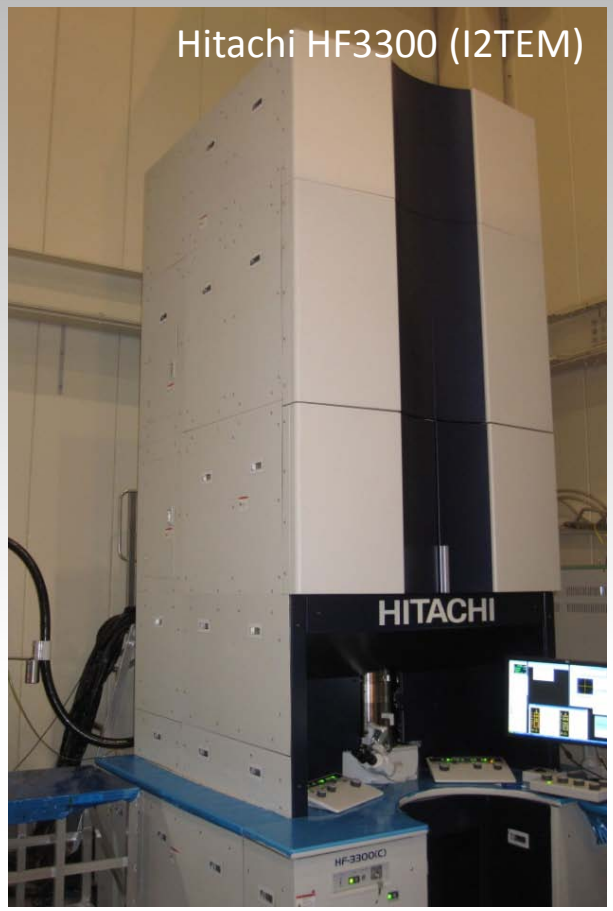

愛2TEM

Cold FEG => Signal/Noise ↗

Multiple biprisms:

=> No Fresnel fringes

New corrector (B-COR) with dedicated lorentz mode

Double stage: Normal Stage and Lorentz Stage

- Spatial resolution ≈ 0.5 nm in Lorentz mode
- Sample in free field space => 1-2 Oe (I2TEM) vs 150 Oe (Tecnaï)

I2TEM: TEM dedicated to holography and "*in-situ*" TEM

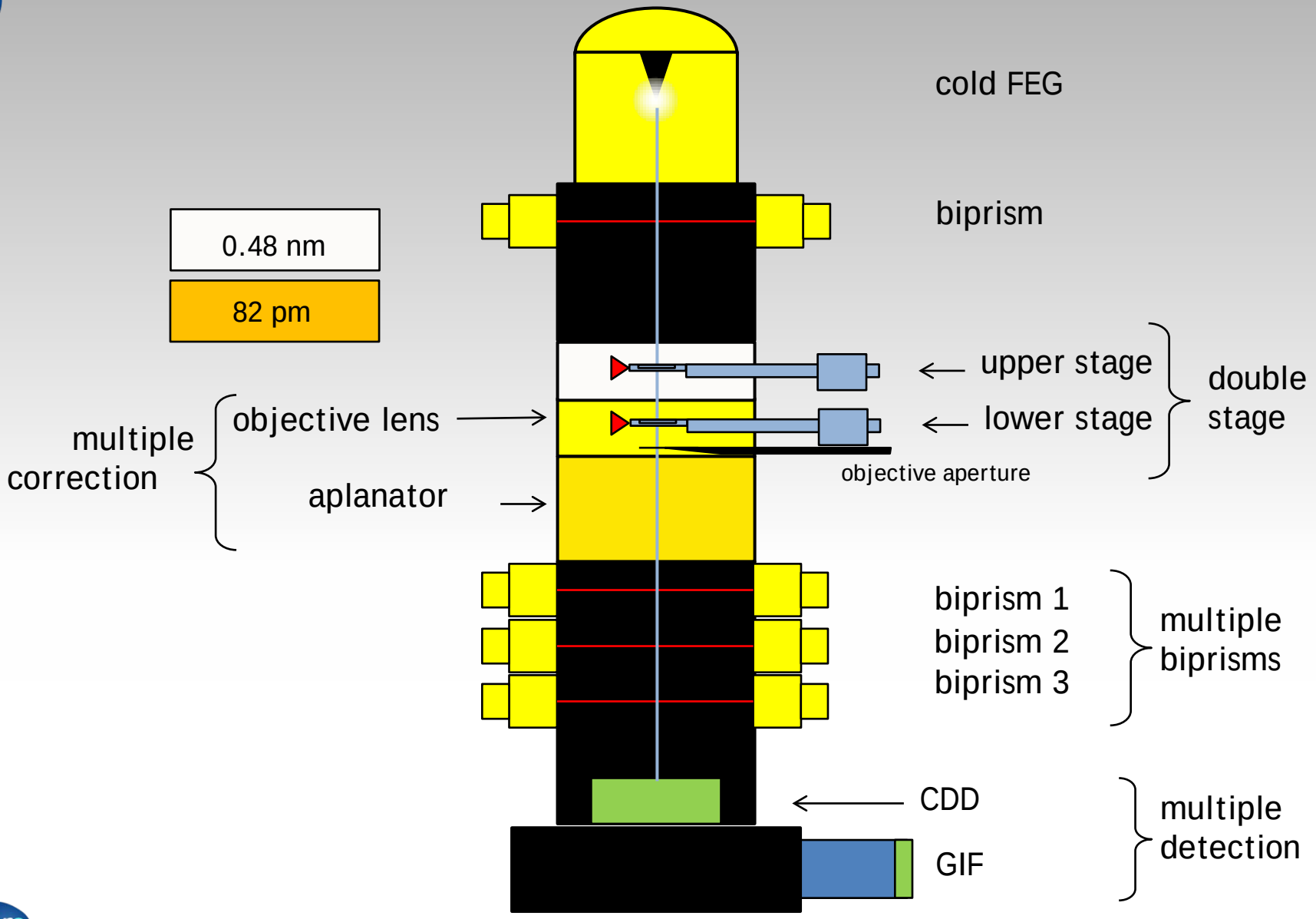

Hologram

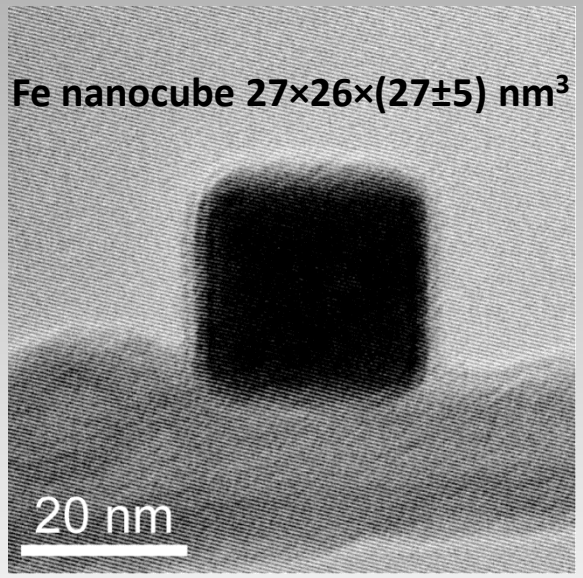

Magnetic Phase Shift

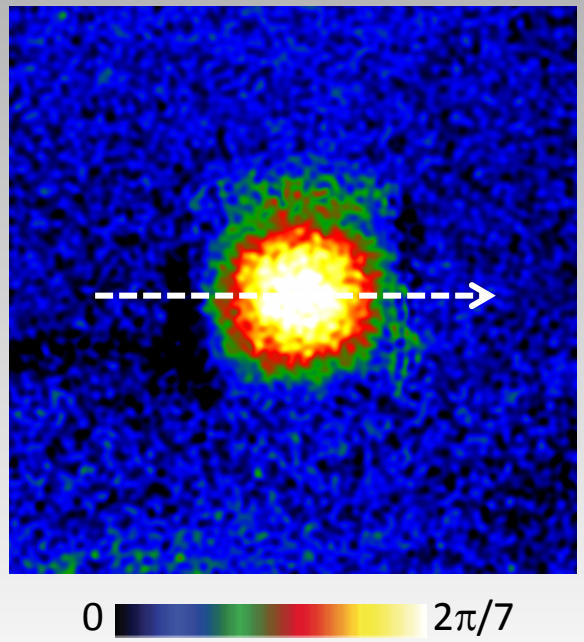

Vector Map with Cosine of

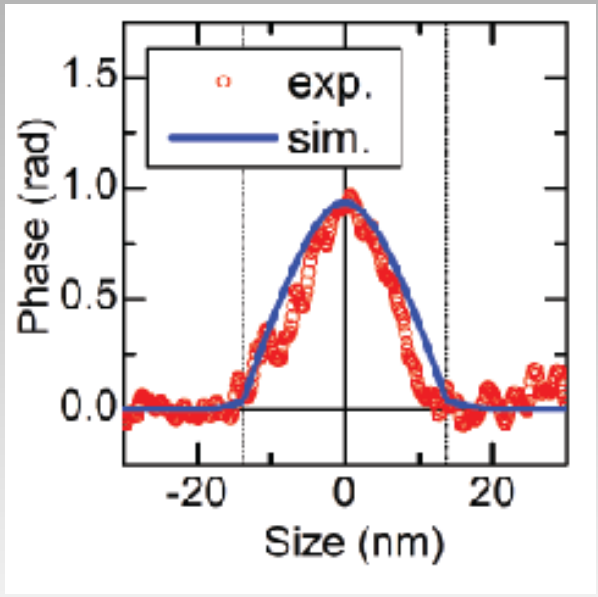

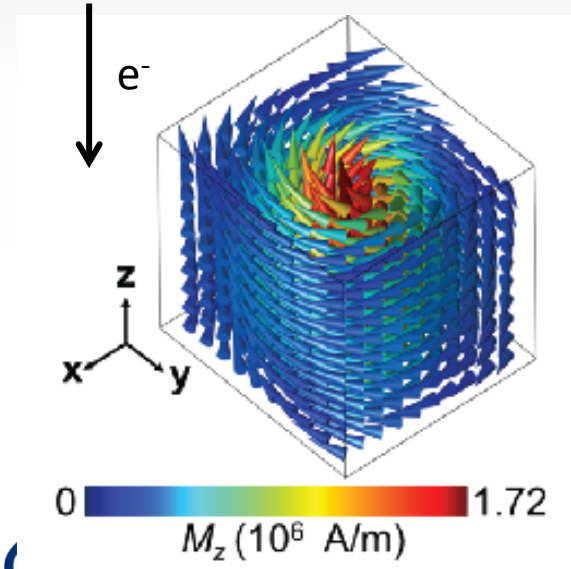

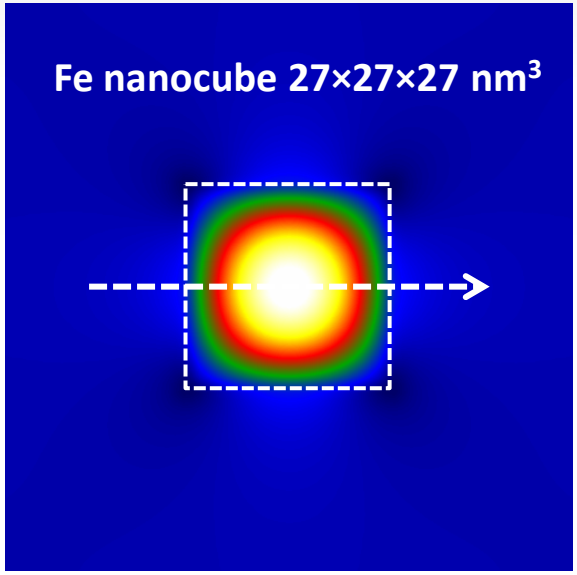

- Axial symmetry of the induction: axis ⊥ to the (001) face
- Complete flux closure in the vortex plane
- Perfect quantitative agreement with simulated phase shift caculated from 3D micromagnetic simulation integration along the electron path

Hologram

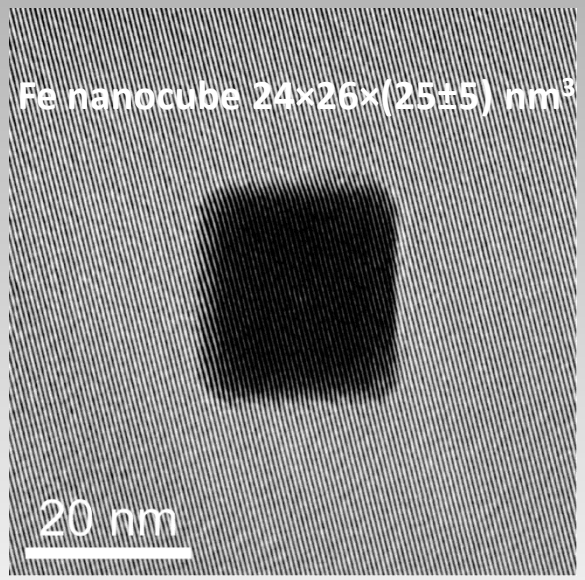

Magnetic Phase Shift

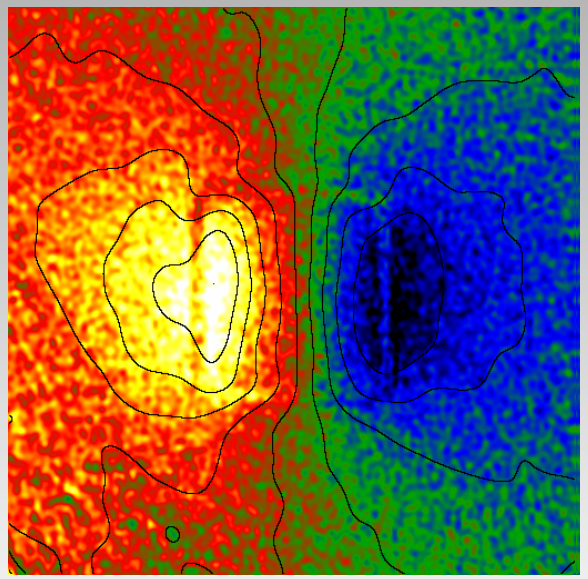

Vector Map with Cosine of Magnetic Phase Shift

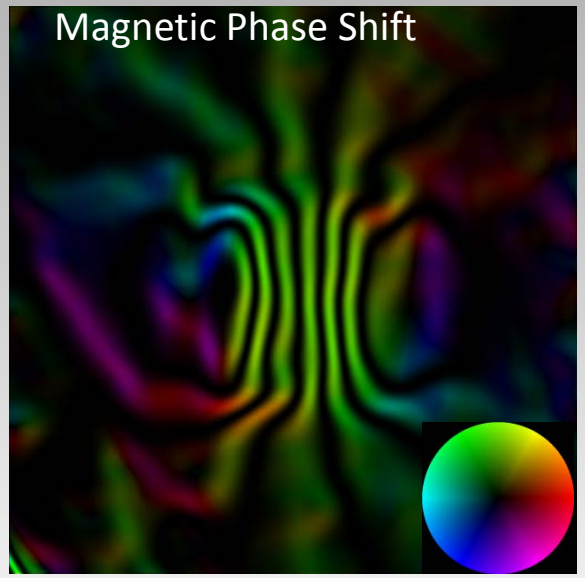

-π/6 π/6

- Magnetic induction lines fairly aligned within the cube.
- They tend to curl outside in order to close the induction flux.
- Magnetic configuration: Single Domain or Vortex with core // in-plane <001> directions

=> Micromagnetic simulations are then mandatory to unambiguously distinguish between both configurations.

Spin configurations in size controlled single Fe nanomagnets

Simulated Vortex

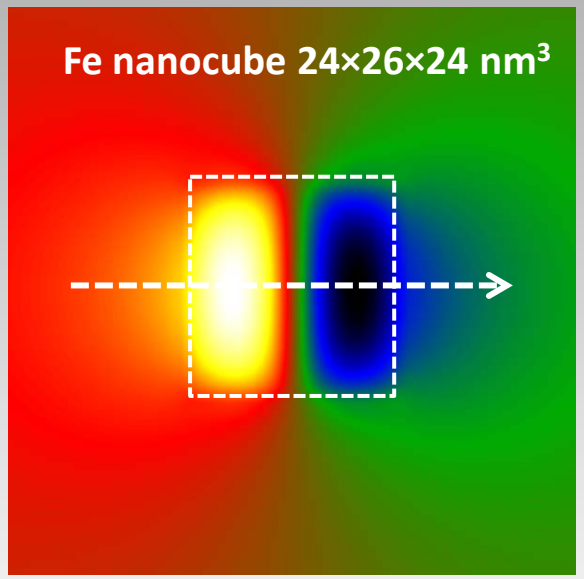

-π/25 π/25

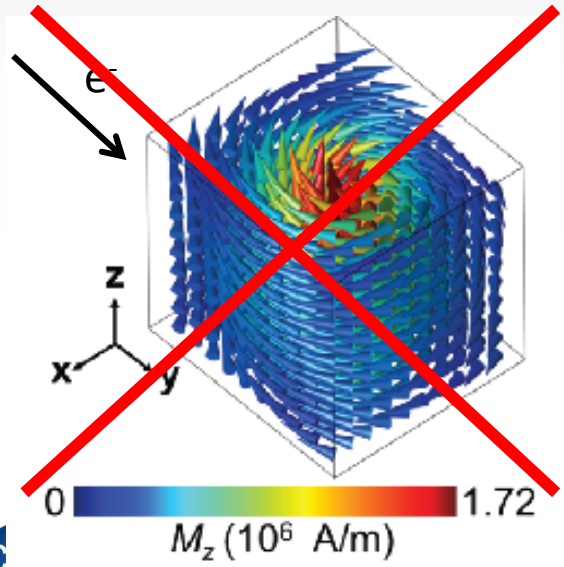

Simulated Single Domain

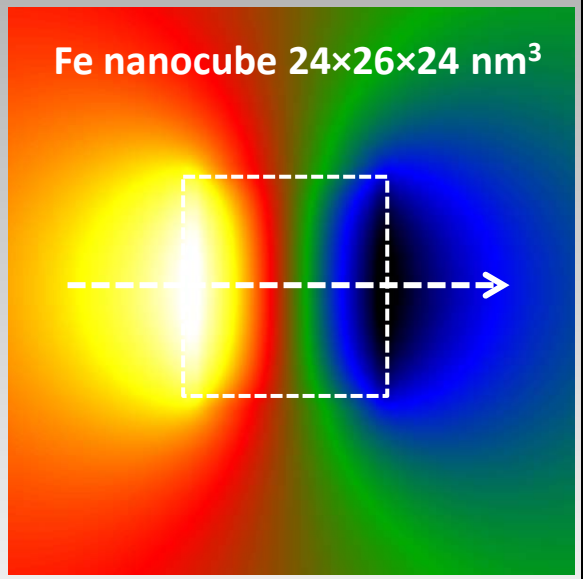

-π/6 π/6

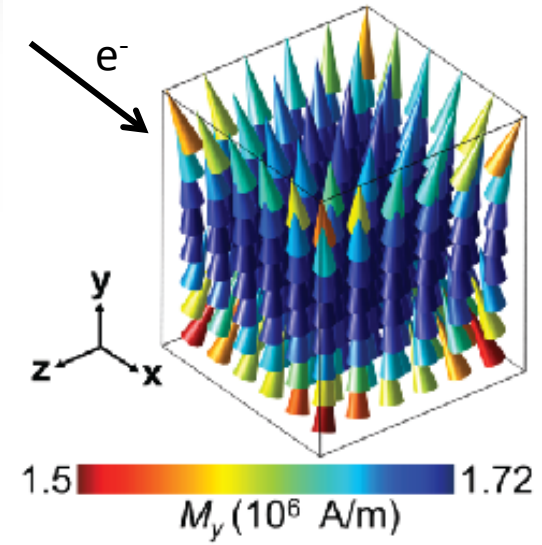

Experimental Phase Shift

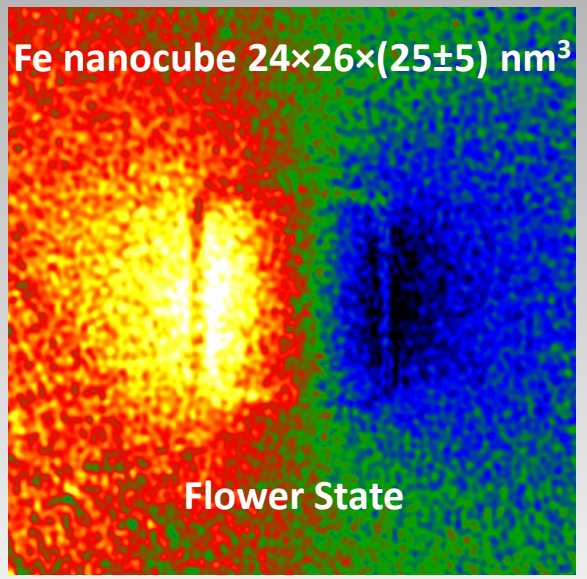

-π/6 π/6

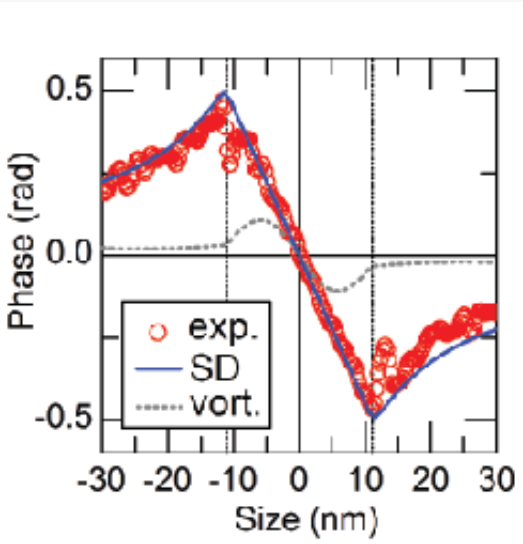

A surprisingly magnetic state…

Hologram

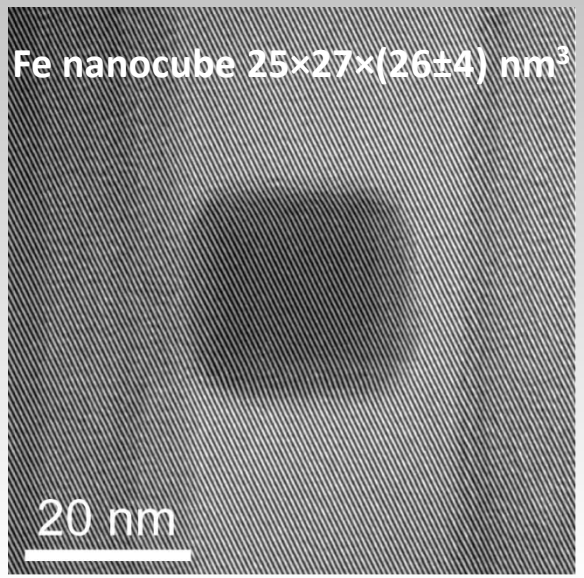

Experimental Phase Shift

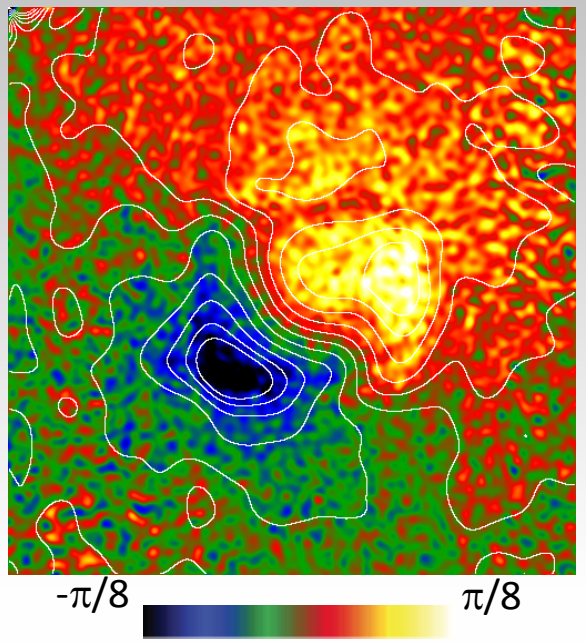

- Some cubes give an unexpected magnetic configuration for intermediate size
- Complex pattern which cannot be directly interpreted:
  - Low phase shift of the integrated induction
  - C state ?

Experimental Phase Shift

Simulated Phase Shift

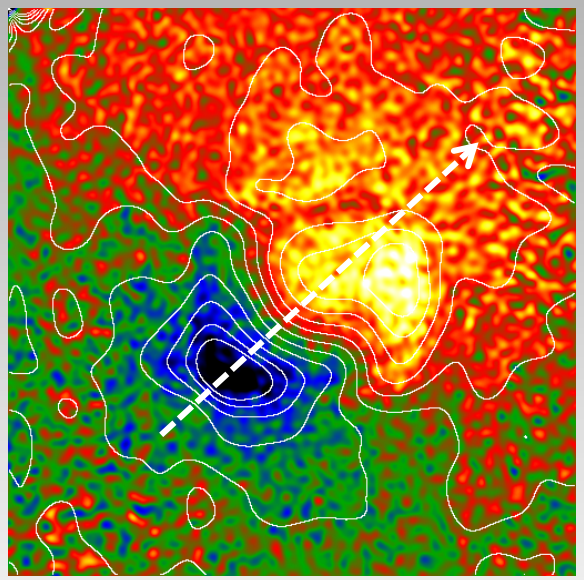

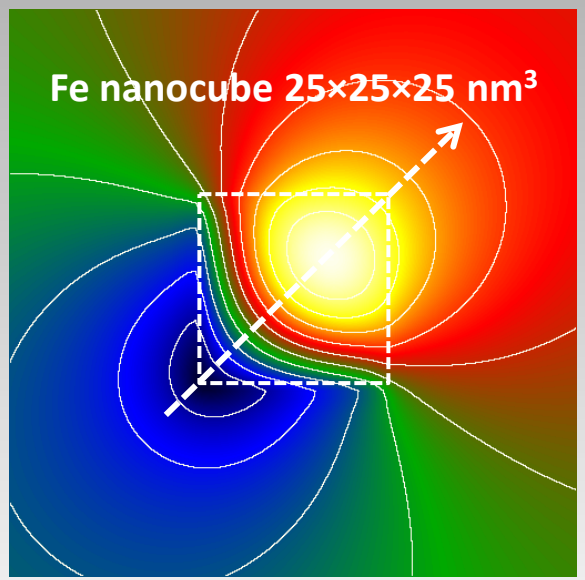

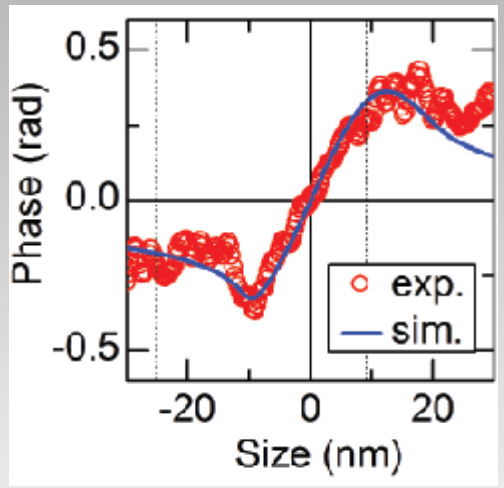

-π/8 π/8

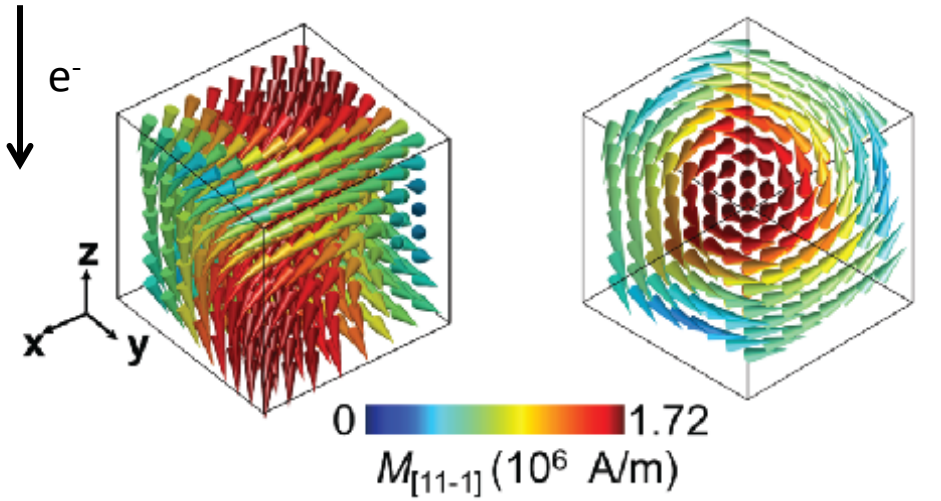

- Very good quantitative agreement between experimental and simulated magnetic phase shift
- Projection along the cube diagonal reveals that spins curl around <111> direction
- Vortex whose core axis is aligned along the diagonal of the cubes

=> Vortex <111>

Magnetic phase diagram of a perfect Fe nanocube

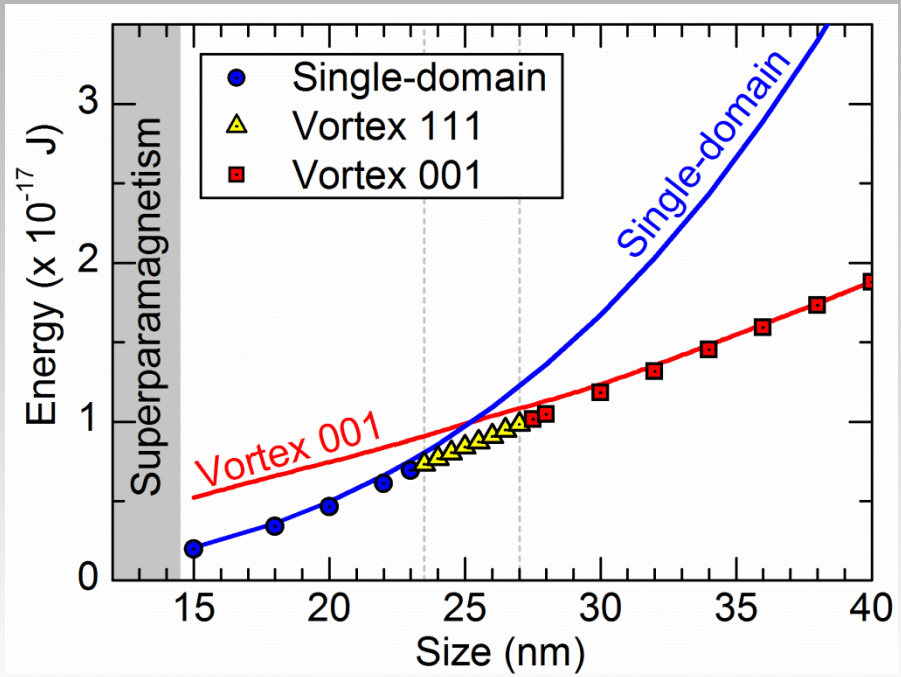

1st approach: Fixe Initial spin configuration (uniform SD or V<001>) imposed: resulting energy vs size.

	Exchange energy	Magnetostatic energy
Single Domain	↘	↗
Vortex <001>	↗	↘

Magnetic phase diagram of a perfect Fe nanocube

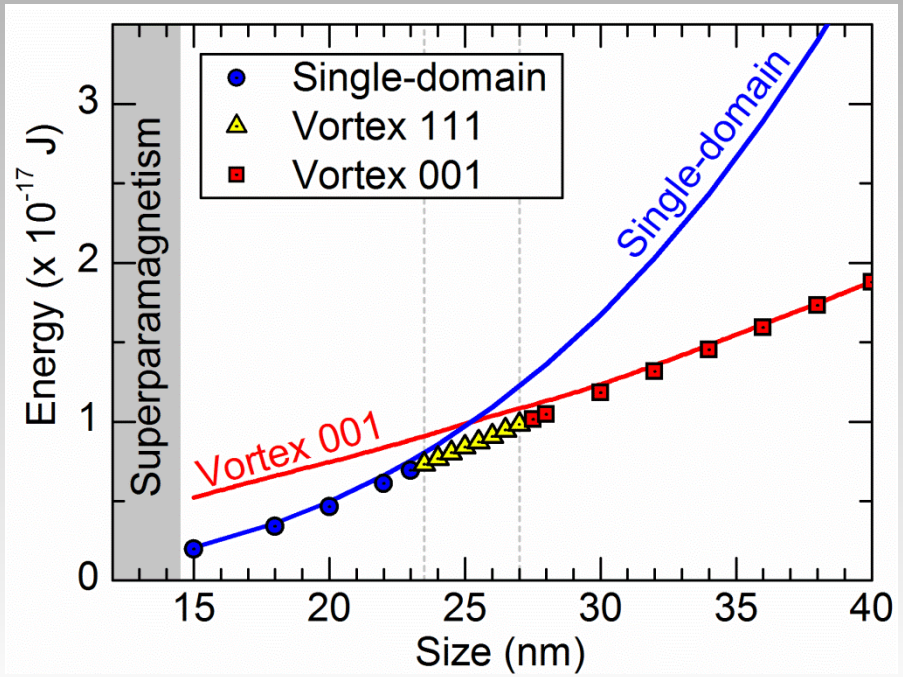

2nd approach:

Random spin configuration originally introduced: Relaxation of the spins will lead to the stable configuration and the corresponding energy

➔ Stable SD configurations below 23.5 nm

➔ V<001> obtained within cubes above 27 nm (same energies with <001>core axis)

- Between 24 and 27 nm, **<111> vortex is the most stable configuration**.
=> Balancing exchange and magnetostatic interactions, at the expanse of the magneto-crystalline energy (quite low in Fe).

Summary

- Clear description of equilibrium states of a nanomagnet of cubic anisotropy.
- Deeper understanding of the single domain limit, more complex than expected with the appearance of an unreported <111> vortex state.
- Optimization of nanomagnets in the perspective of various applications: hyperthermia, data storage,…

➔ **Future**: Next transition SP/SD ? What is the limit ? Other type of materials morphologies?

If the nanocube size decreases:

300K : Vortex => Single Domain => Superparamagnetism

25 nm 15nm

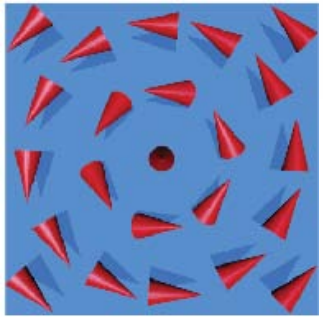

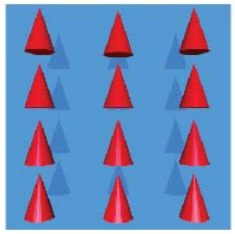

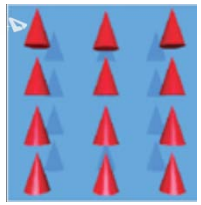

- **Interaction with an external field ? => Need to produce a controlled localized field**

NANO LETTERS

Letter

pubs.acs.org/NanoLett

Size-Specific Spin Configurations in Single Iron Nanomagnet: From Flower to Exotic Vortices

Christophe Gatel,[*,†] Francisco Javier Bonilla,[‡] Anca Meffre,[‡] Etienne Snoeck,[†] Bénédicte Warot-Fonrose,[†] Bruno Chaudret,[‡] Lise-Marie Lacroix,[‡] and Thomas Blon[*,‡]

[†]Centre d'Elaboration de Matériaux et d'Etudes Structurales, CEMES-CNRS, 29 rue Jeanne Marvig, B.P. 94347, 31055 Toulouse, France

[‡]Laboratoire de Physique et Chimie des Nano-Objets, LPCNO, UMR5215 INSA-UPS-CNRS, Université de Toulouse; Institut National des Sciences Appliquées, 135 avenue de Rangueil, 31077 Toulouse, France

S *Supporting Information*

ABSTRACT: The different spin configurations in the vicinity of the single-domain/vortex transition are reported in isolated magnetic nanoparticles. By combining chemical synthesis, electron holography in a dedicated transmission electron microscope and micromagnetic simulations, we establish the "magnetic configurations vs size" phase diagram of Fe single-crystalline nanocubes. Room temperature high resolution magnetic maps reveal the transition between single-domain and vortex states for Fe nanocubes from 25 to 27 nm, respectively. An intermediate spin configuration consisting of an ⟨111⟩ vortex is for the first time evidenced.

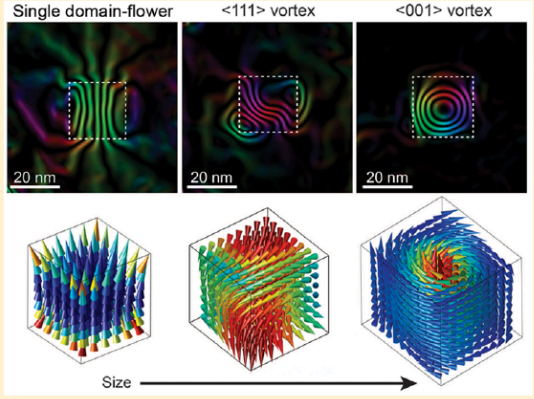

KEYWORDS: *magnetic configuration, electron holography, vortex state, single domain state, flower state, nanocube*

In situ electron holography of the dynamic field emanating from a HDD writer

Etienne SNOECK, C. GATEL,
A. Masseboeuf, R. Cours, F. Houdellier

CEMES - Toulouse

CEMES - CNRS
29 rue J. Marvig,
31055 Toulouse (France)

J. Einsle, R. Bowman

Centre for Nanostructred Media
School of Maths and Physics,
Queens University Belfast (UK)

M. Bashir, M. Gubbins

Seagate Tehnology (Ireland)
Londonderry (UK)

esteem2
european network for electron microscopy

In situ electron holography of the dynamic field emanating from a HDD writer

"Forecasts are that areal densities will need to increase by as much as 35% compound per annum and by 2020 cloud storage capacity will be around
7 zettabytes (7.10^{21}) corresponding to areal densities of 2 Tb/in^2."

SEAGATE

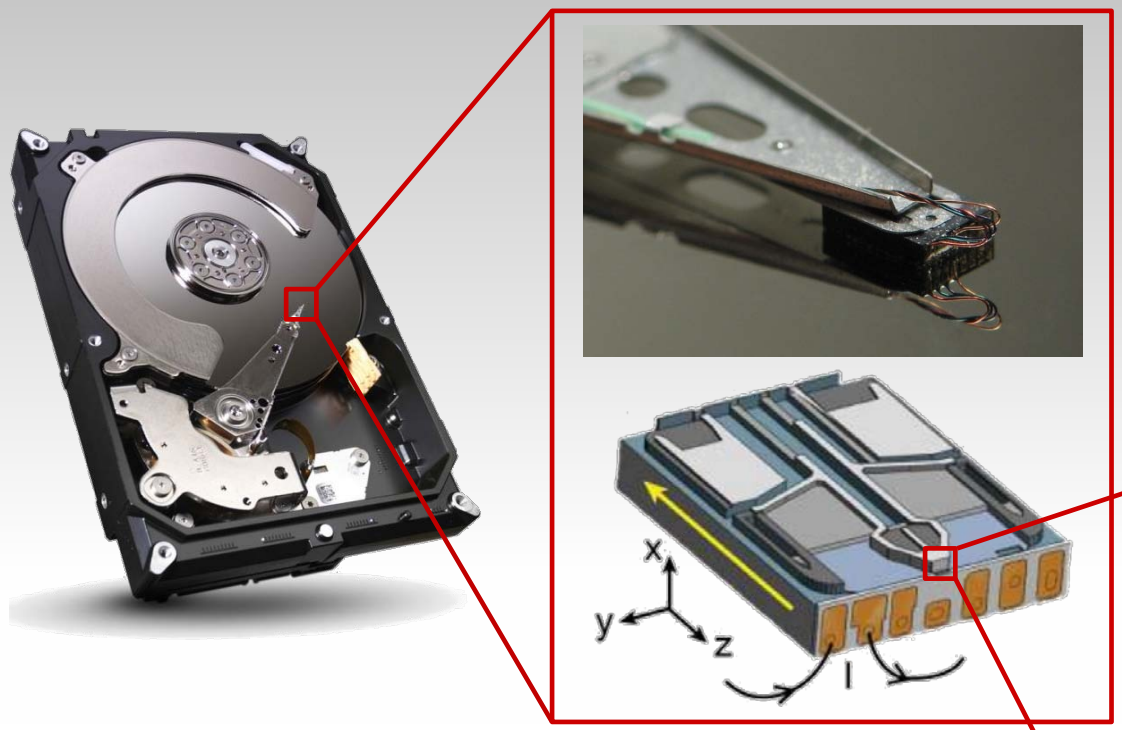

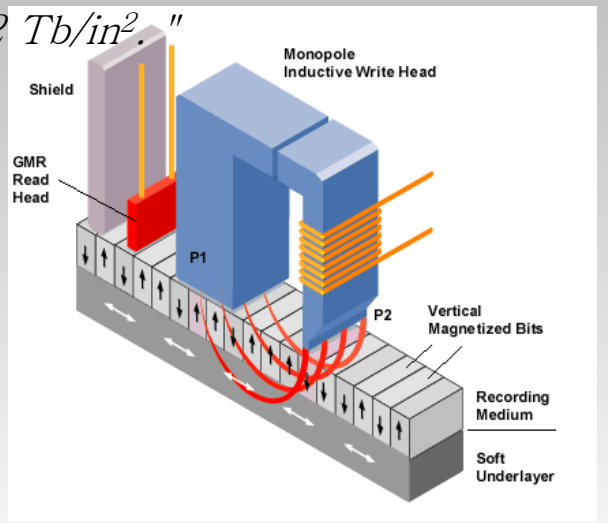

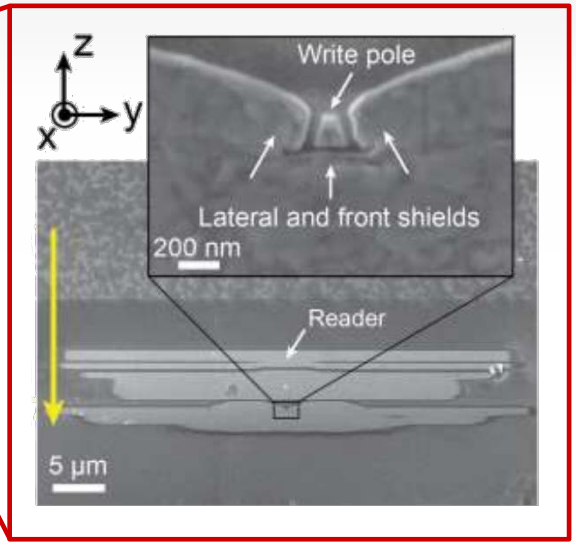

"A hard drive head can be seen as a spaceship

- *flying at a speed of Mach 2,*
- *10 cm above the ground,*
- *counting grass by 10-stalks packages*
- *over a field as big as Ireland."*

John Chapman

In situ electron holography of the dynamic field emanating from a HDD writer

"Forecasts are that areal densities will need to increase by as much as 35% compound per annum and by 2020 cloud storage capacity will be around 7 zettabytes (7.10^{21}) corresponding to areal densities of 2 Tb/in^2. "

SEAGATE

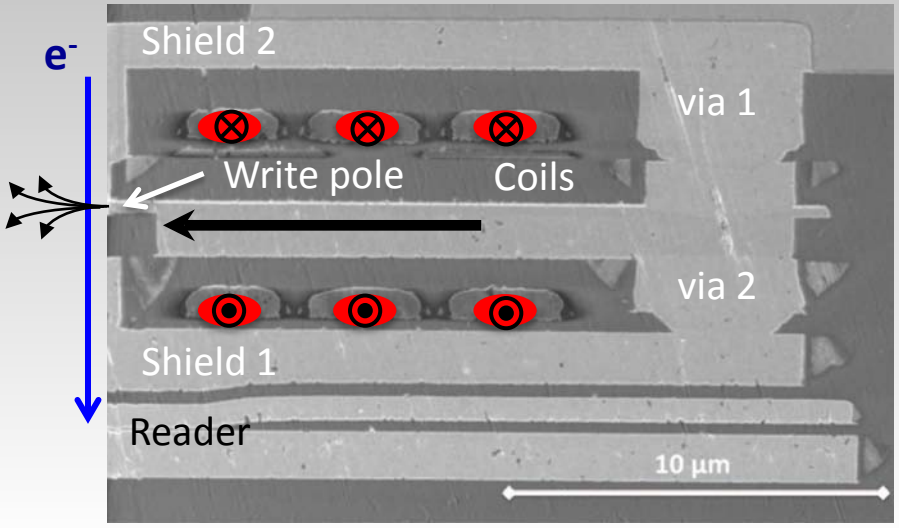

Electron beam phase shift measured in front of the write pole while applying a current through the device.

- Directional field
- No field for no current (no remnant state)
- Large saturation range

Sample preparation: 18 months !

1. Mechanical polishing down to 30 µm by tripod

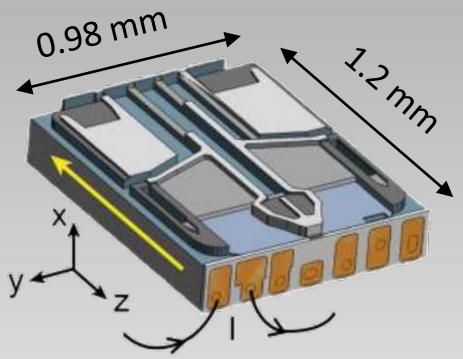

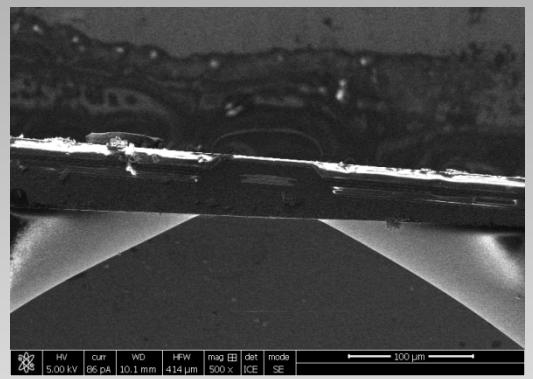

2. Growth of two carbon pillars by Ion Beam Induced Deposition using FIB on both sides of the write pole

3. Mounting the device into a home-made sample holder for electrical connections

4. Wedge bonding to connect the pads of the slider toward the dedicated contacts of the sample holder

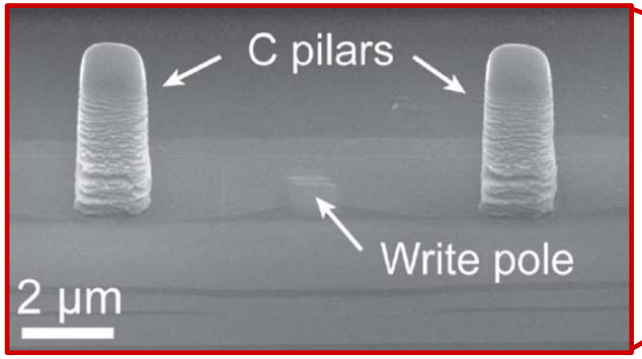

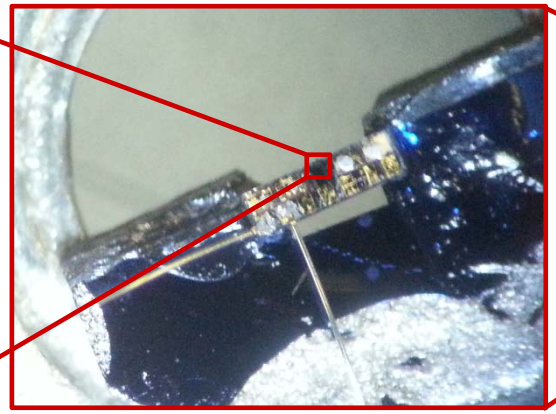

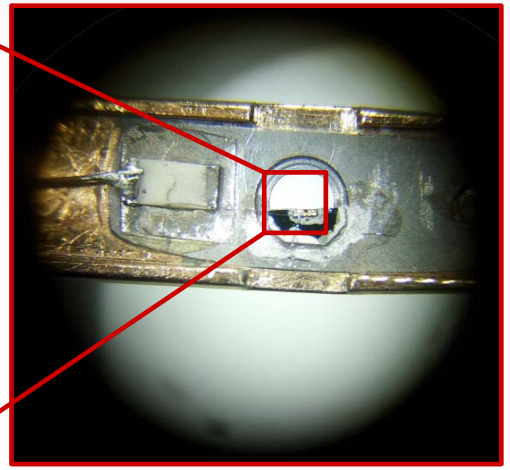

Microscope Set-up:

- Tecnai F20 – Cs corrected
- Lorentz mode
- Biprism voltage = 140 V
- Setting time: 7 hours
- Experiment time: 12 hours

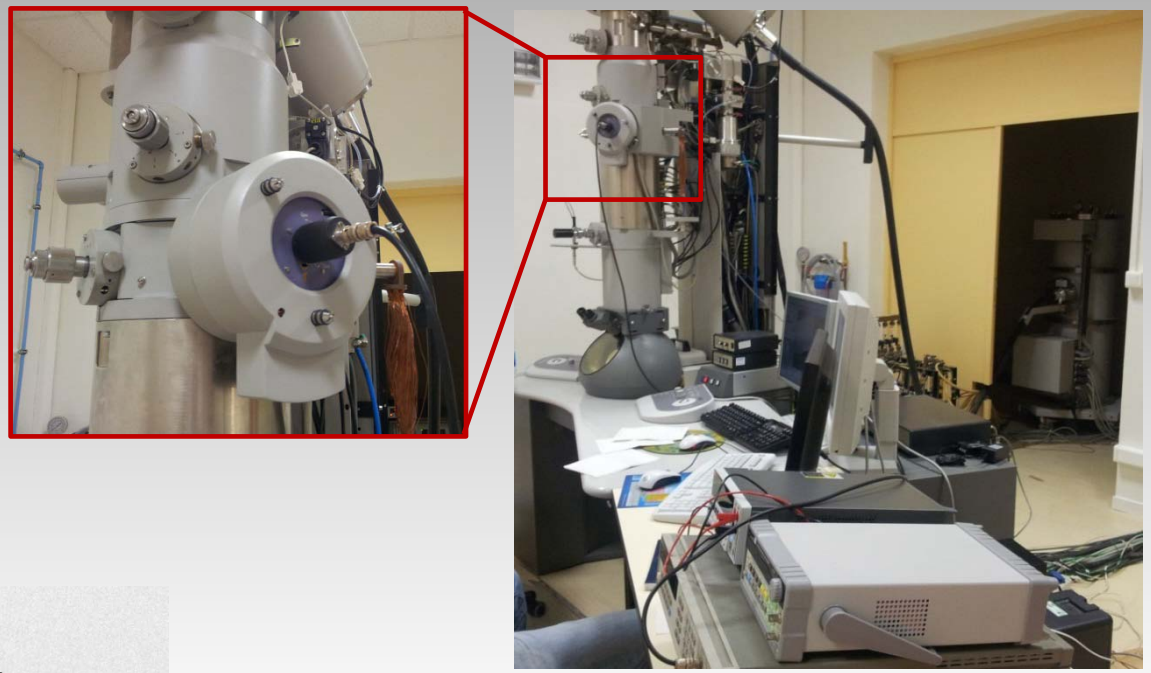

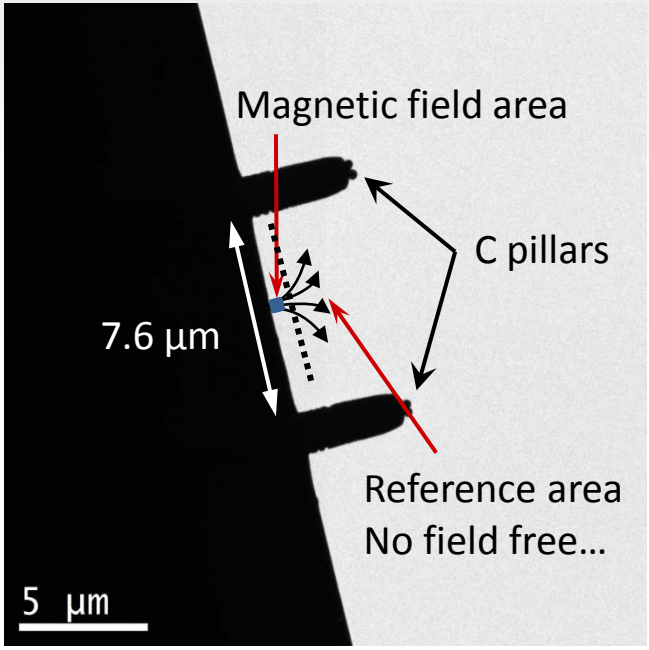

Slight magnetic field in the reference area

=> Need of simulations to take into account the phase variation

Variable steps of current adjusted on the switching process. Static measurement.

2 symetric datasets of 44 images each (+ 15 reference images at 20 µm from the head):

+60 to -60 mA: Current decreasing

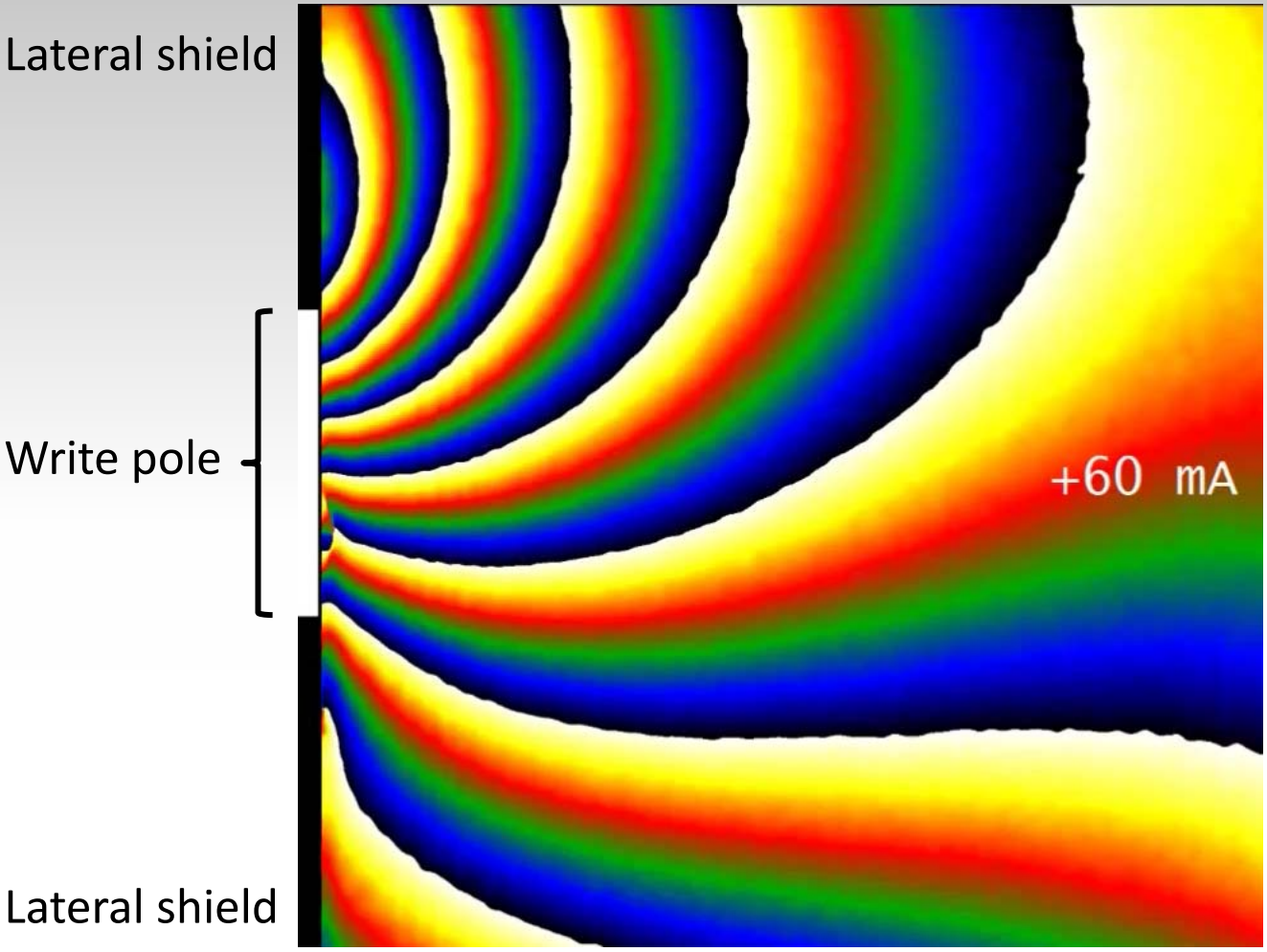

Variable steps of current adjusted on the switching process. Static measurement.

2 symetric datasets of 44 images each (+ 15 reference images at 20 µm from the head):

-60 to +60 mA: Current increasing

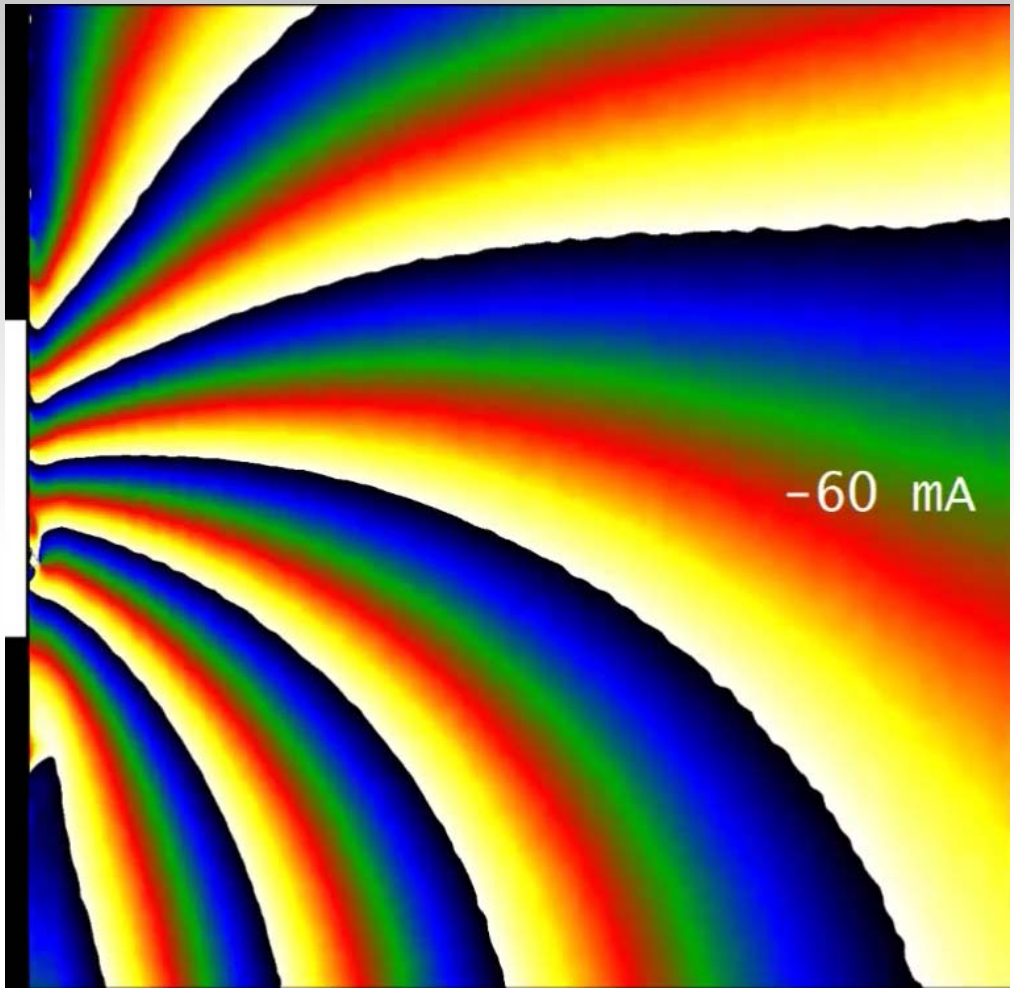

From phase images to magnetic components

$$\phi_{Mag}(\mathbf{r}) = -\frac{e}{h}\iint B_{\perp}(\mathbf{r}_{\perp}, z)\, dr\, dz$$

$$\int_{-\infty}^{\infty} B_x(r_{\perp}, z)\, dz = -\frac{h}{e}\frac{\partial \phi_{Mag}(\mathbf{r})}{\partial y}$$ *X component*

$$\int_{-\infty}^{\infty} B_y(r_{\perp}, z)\, dz = \frac{h}{e}\frac{\partial \phi_{Mag}(\mathbf{r})}{\partial x}$$ *Y component*

→ Projected in-plane magnetic induction

→ Magnetic unit in T.m

→ Magnetic flux in Wb

X component: $\int_{-\infty}^{\infty} B_x(r_\perp, z)\,dz = -\frac{h}{e}\frac{\partial \phi_{Mag}(\mathbf{r})}{\partial y}$

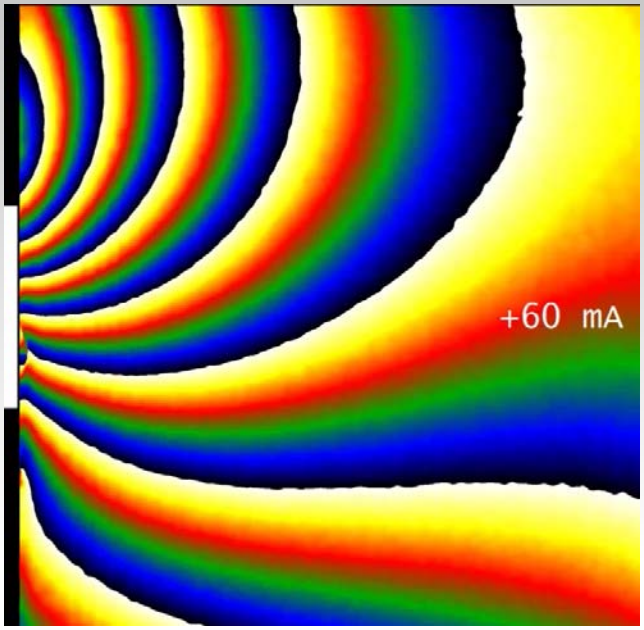

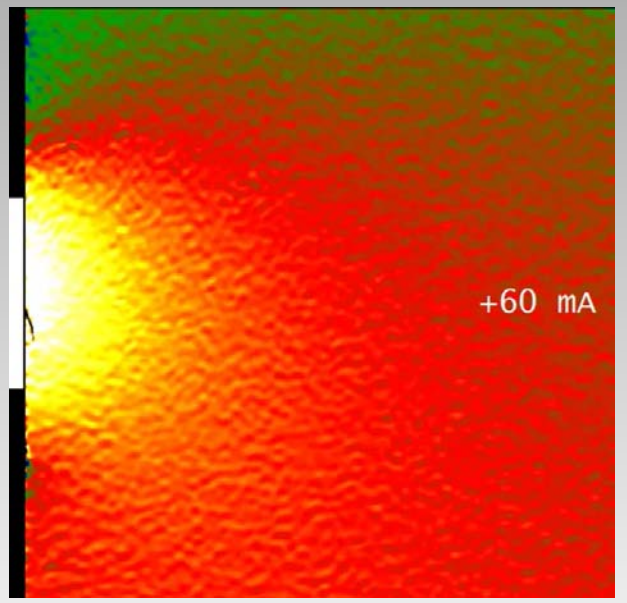

Y
X

-125 T.nm 125 T.nm

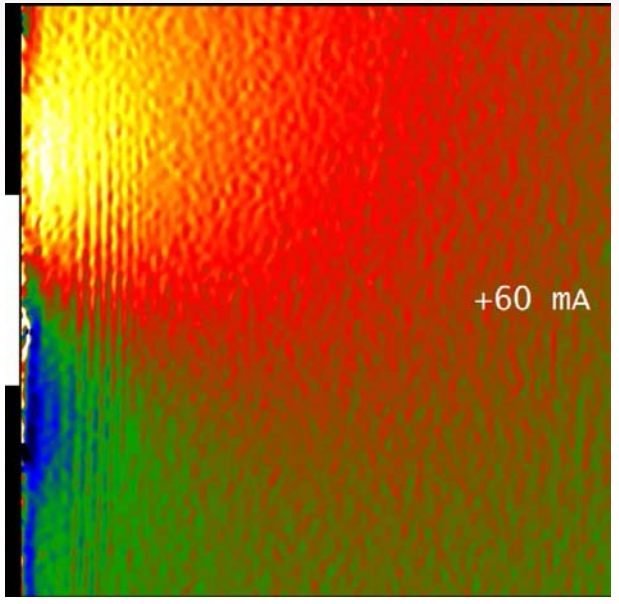

$\phi_{Mag}(\mathbf{r}) = -\frac{e}{h}\iint B_\perp(\mathbf{r}_\perp, z)\,dr\,dz$

Y component: $\int_{-\infty}^{\infty} B_y(r_\perp, z)\,dz = \frac{h}{e}\frac{\partial \phi_{Mag}(\mathbf{r})}{\partial x}$

In situ electron holography of the dynamic field emanating from a HDD writer

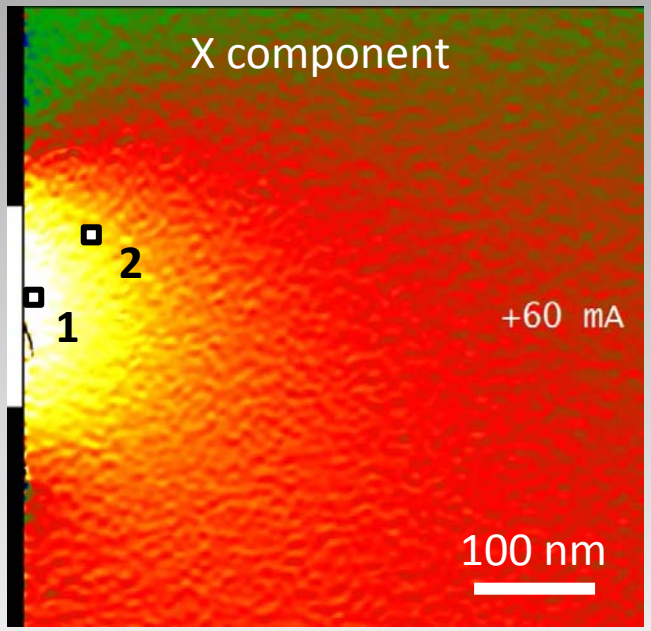

-125 T.nm  125 T.nm

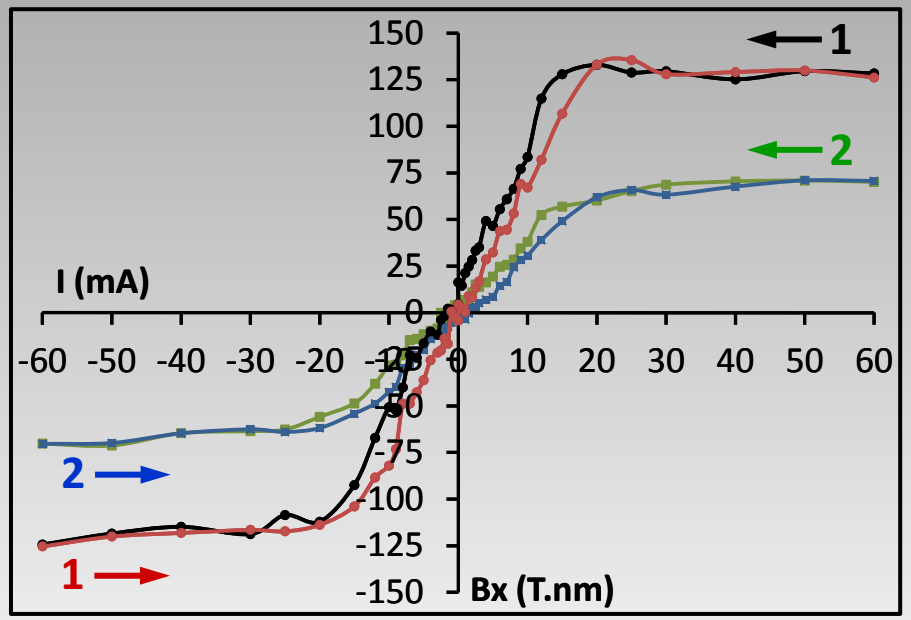

Cell used for the measurement: 5x5 nm²

In situ electron holography of the dynamic field emanating from a HDD writer

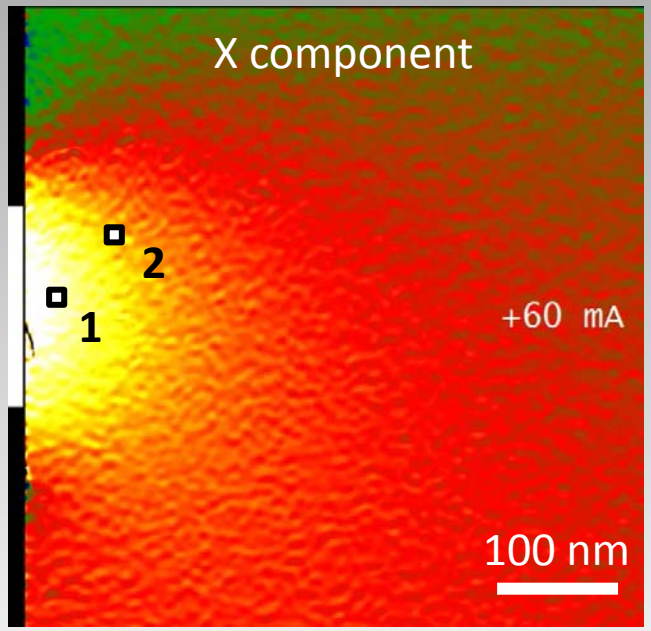

-125 T.nm 125 T.nm

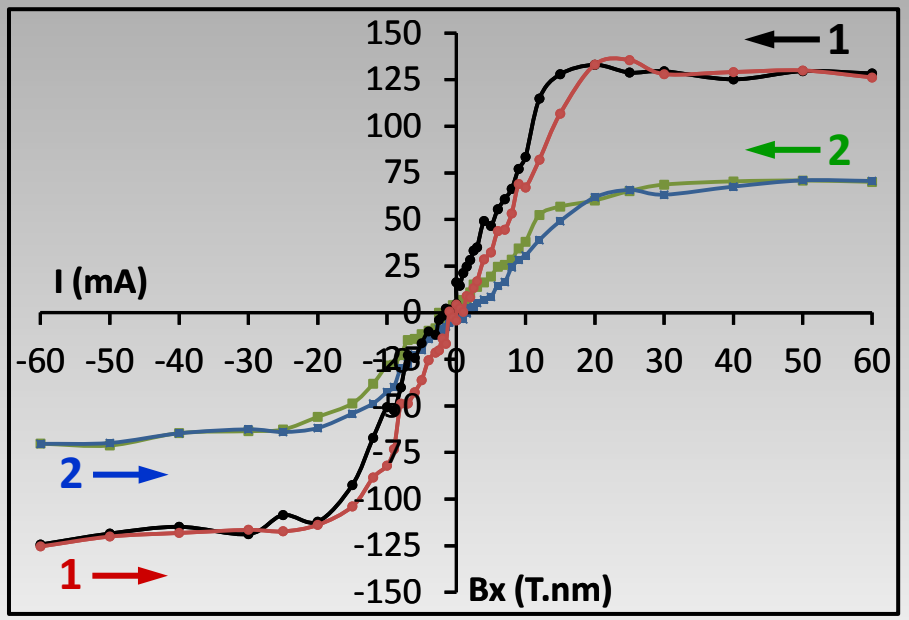

Cell used for the measurement: 5x5 nm²

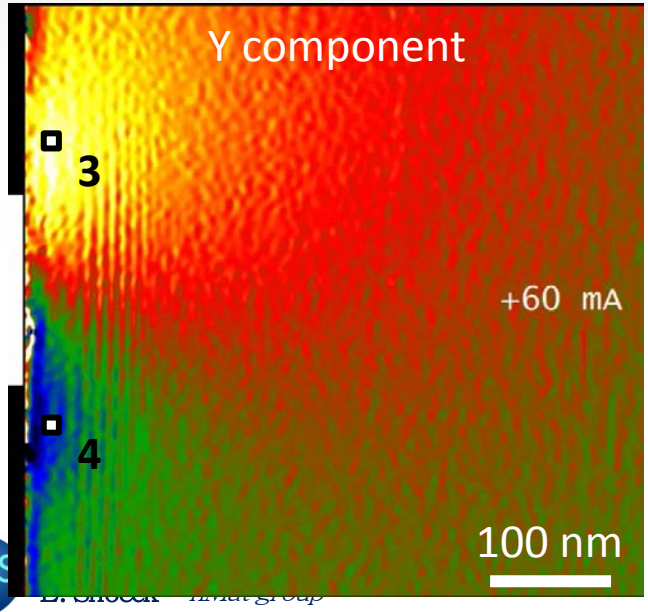

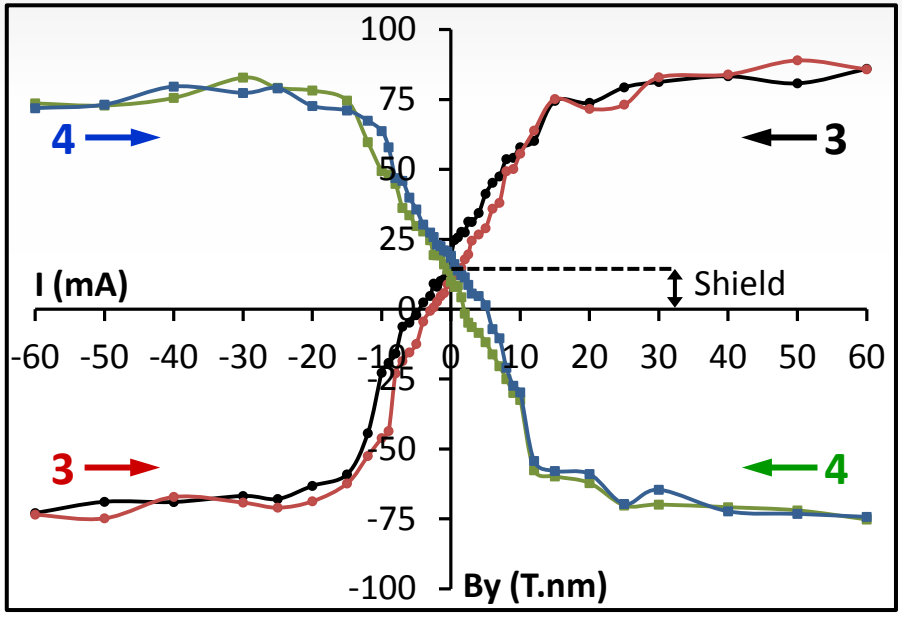

➔ Separate the lateral shield contribution from the writer part using « + i » and « – i » phase images

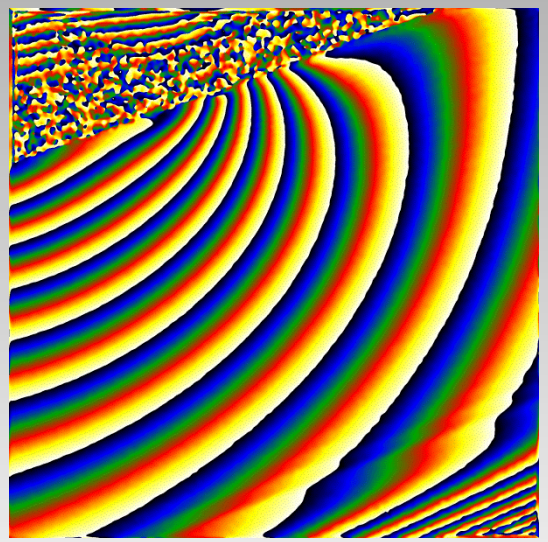

+ 60 mA

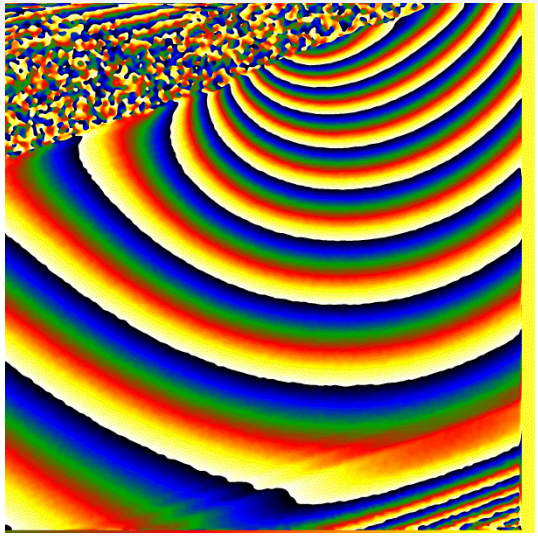

- 60 mA

A = Shield + Writer

B = Shield - Writer

Assuming a symetric signal:

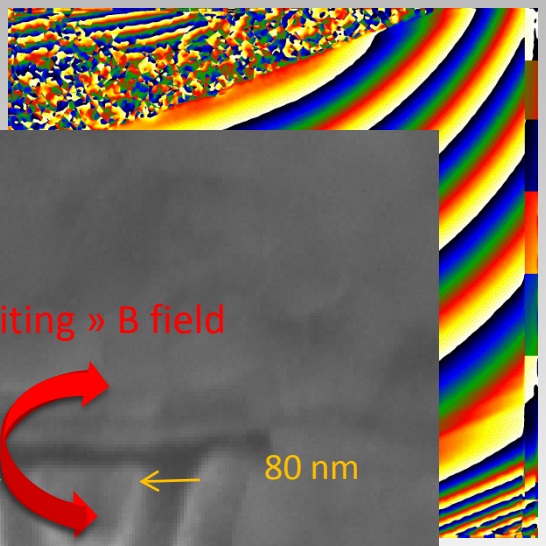

S = (A + B)/2

Shield contribution

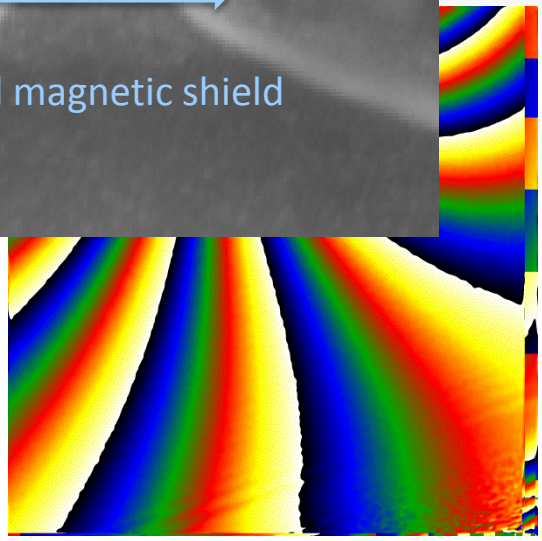

D = (A - B)/2

Writer contribution

for +60 mA

In situ electron holography of the dynamic field emanating from a HDD writer

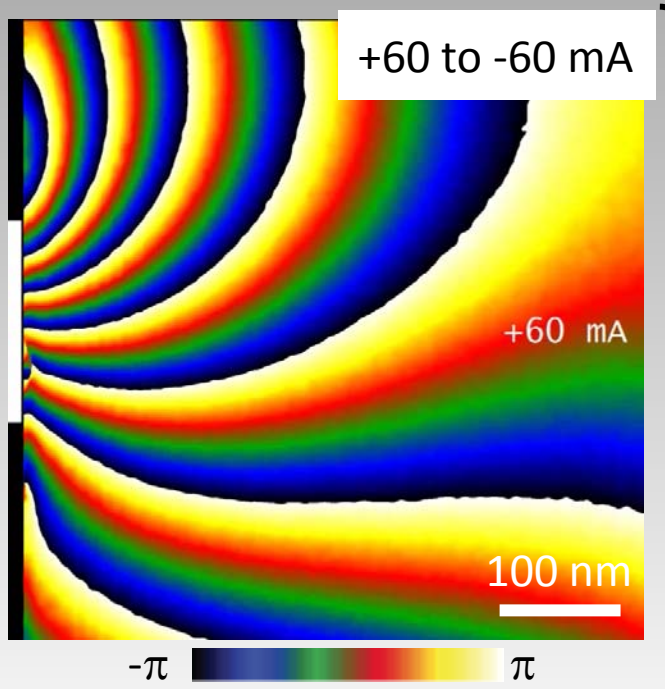

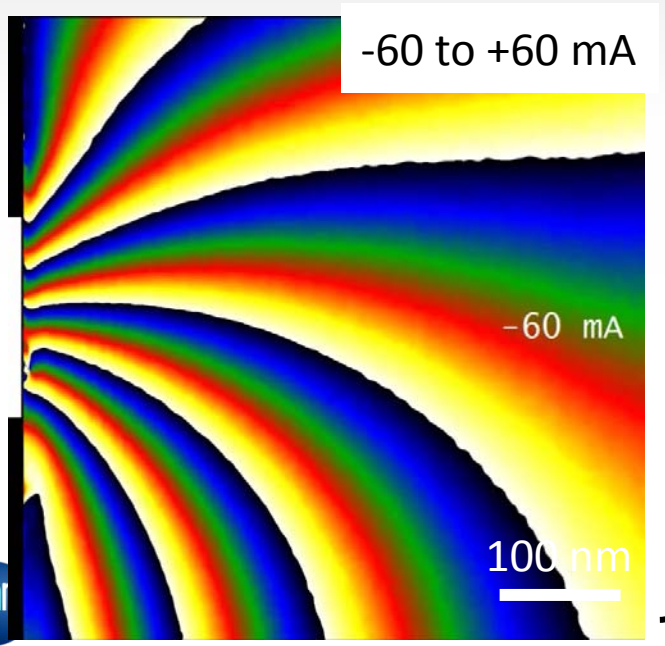

Shield contribution

Sum/2

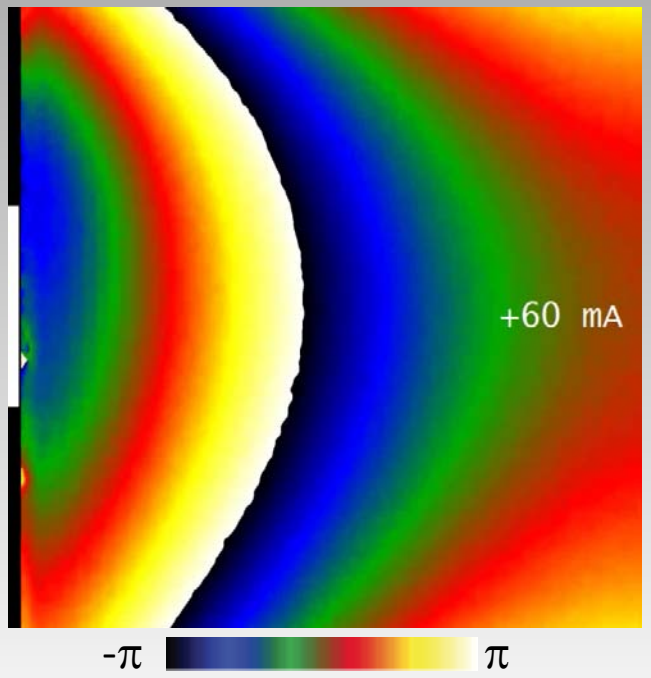

Difference/2

Pole contribution

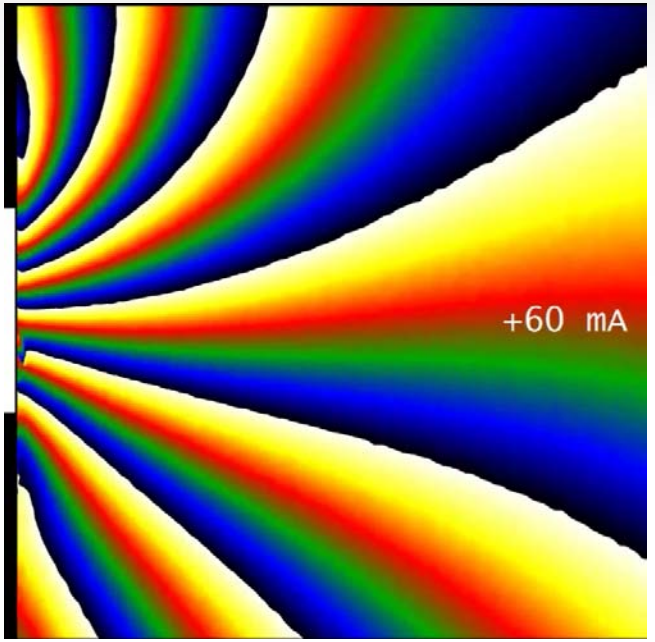

In situ electron holography of the dynamic field emanating from a HDD writer

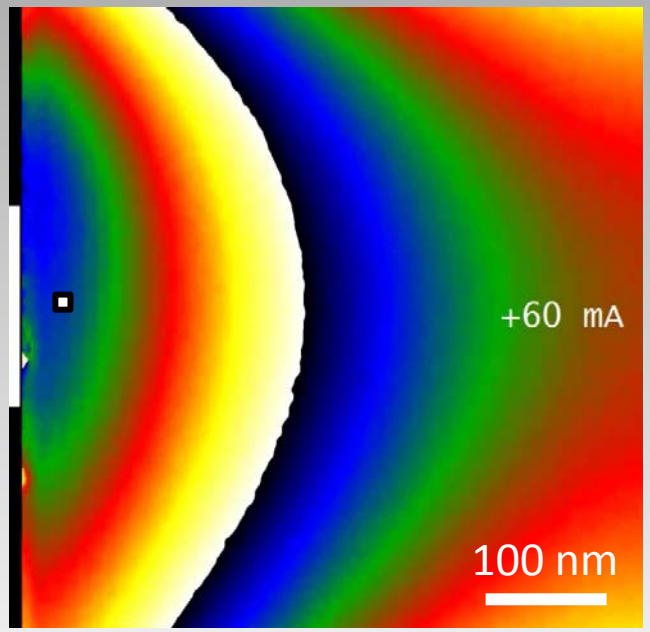

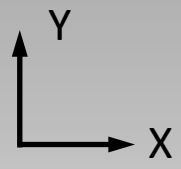

Hysteresis loop along the X direction (from the X component)

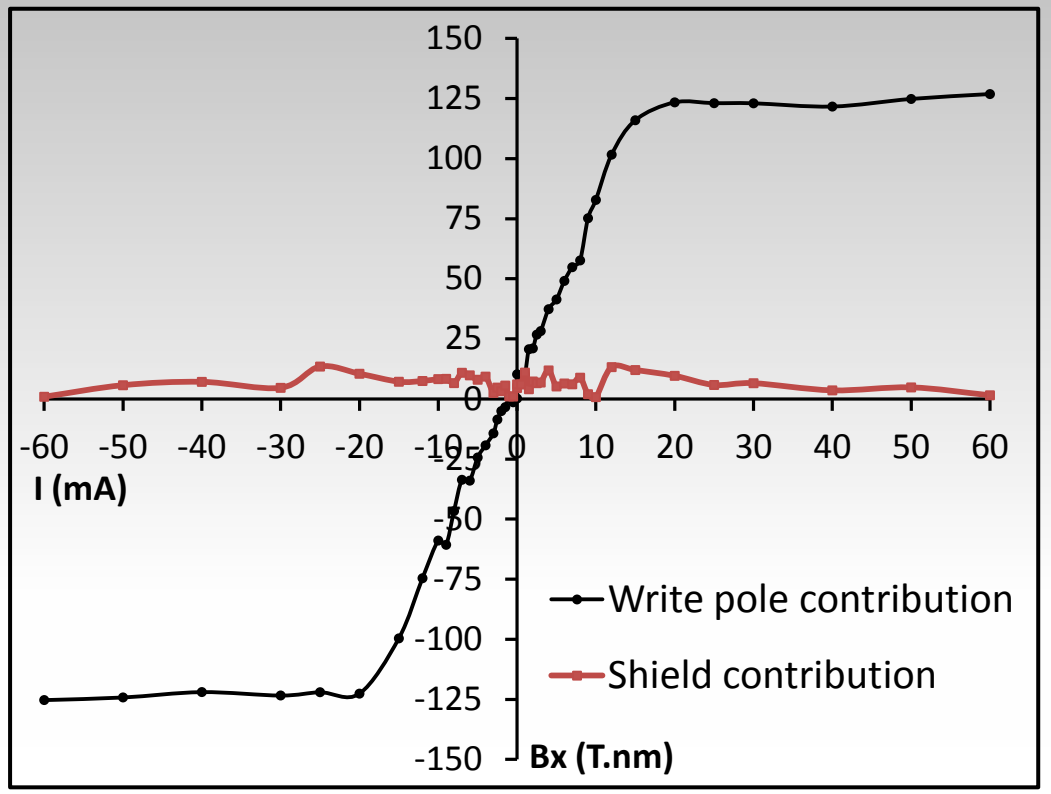

- Perfect symetric signal for the pole contribution: No remnant state, linear increase with a large plage of saturation
- No shield contribution

3D micromagnetic simulations using Magpar package

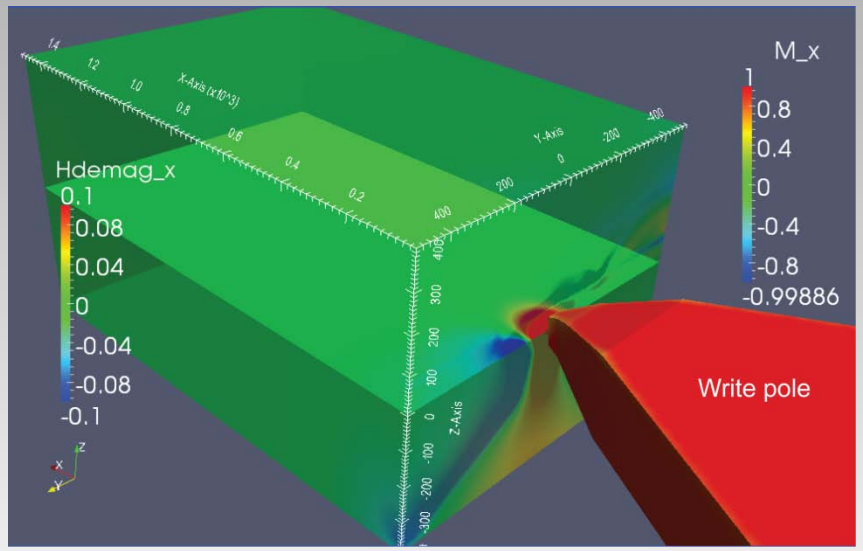

- Box of (1.5µm x 1 µm x 0.8 µm)
- Integration of the in-plane magnetic field components along the electron path
- Simulated phase shift calculated from Aharonov-Bohm equations
- Slight perturbation in the object wave area

Simulated phase +40 mA corrected

Simulated phase +40 mA

Experimental phase +40 mA

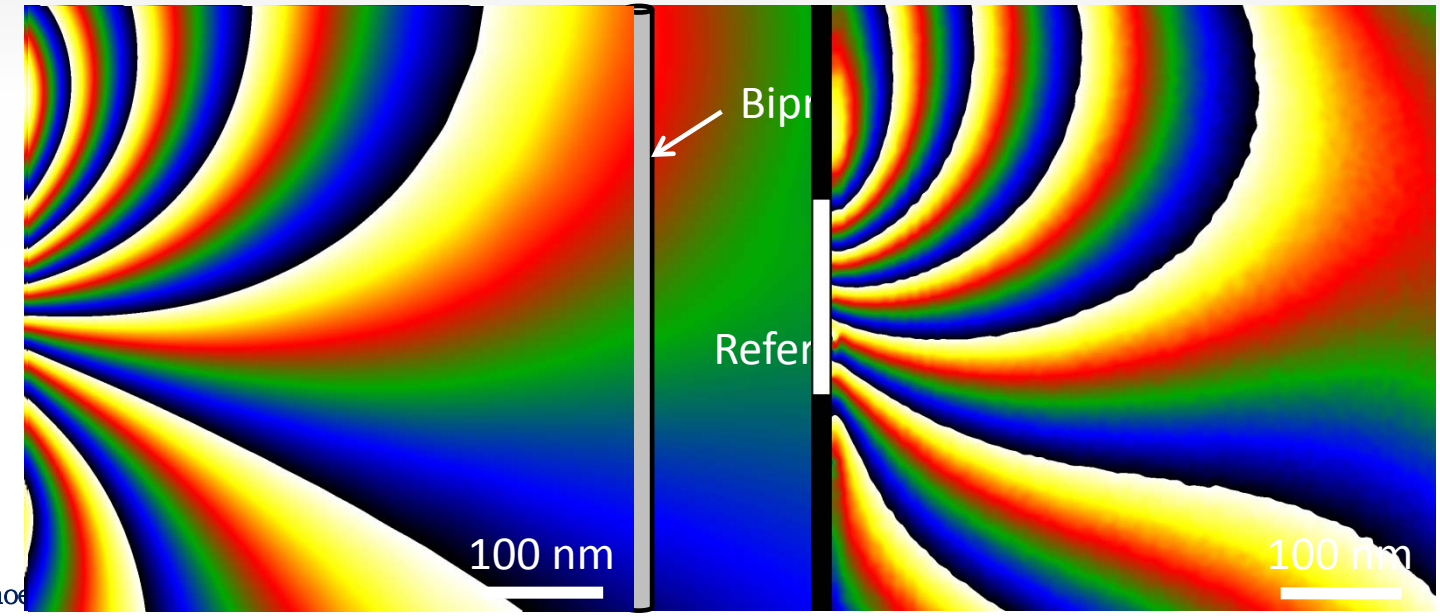

In situ electron holography of the dynamic field emanating from a HDD writer

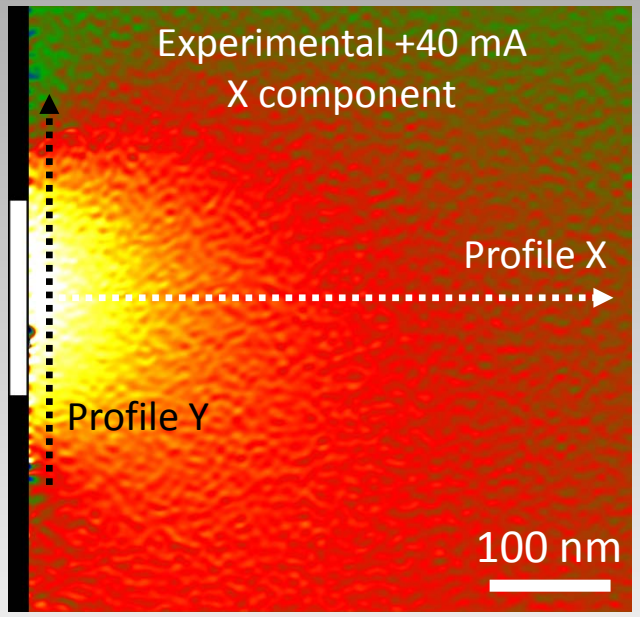

-125 T.nm 125 T.nm

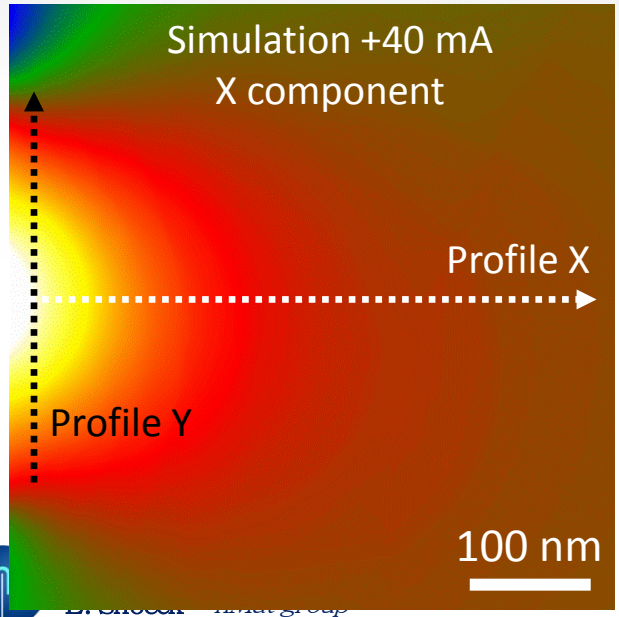

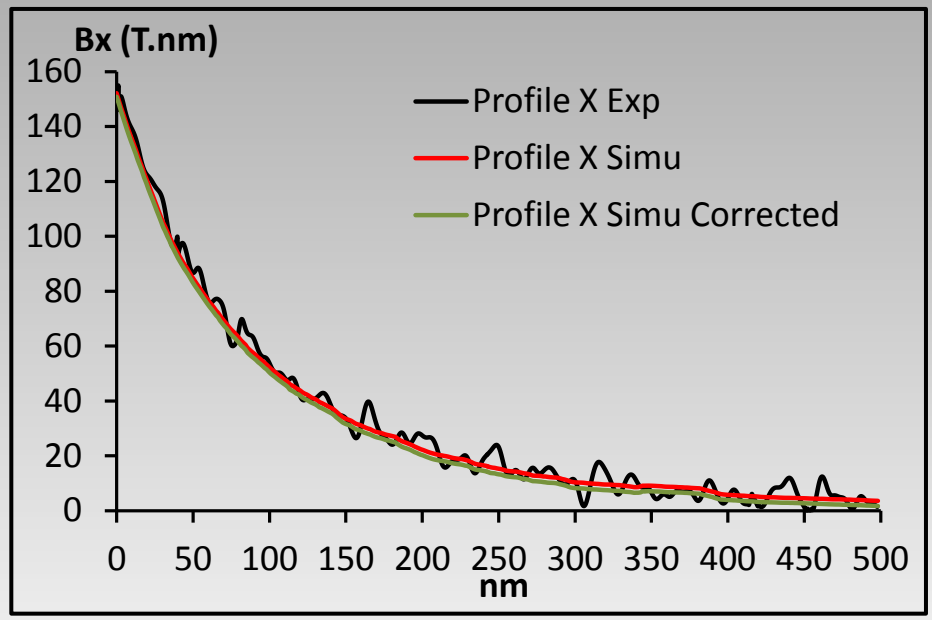

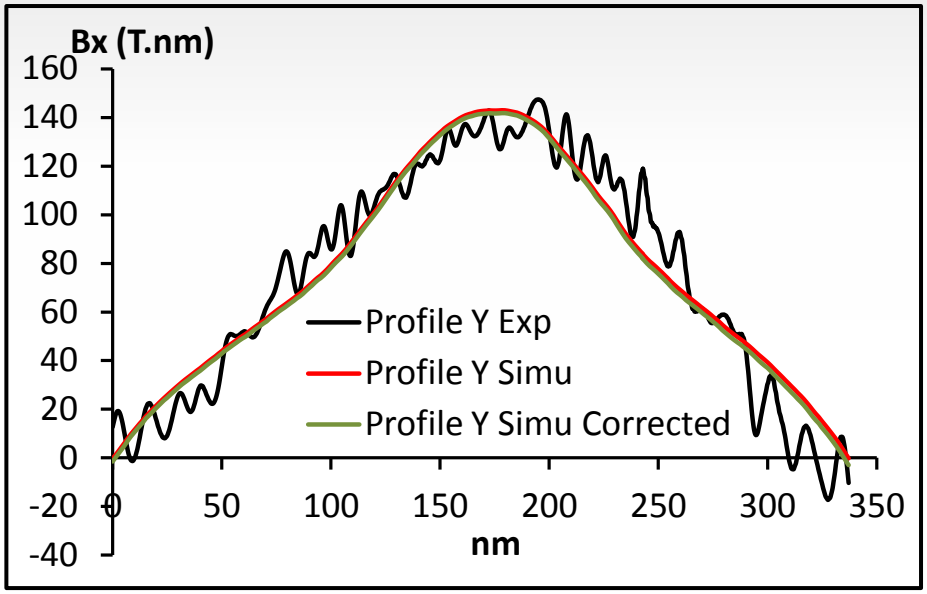

- **Neglictible effect of the field within the reference area**

Experimental data cube of the write pole contribution (X component)

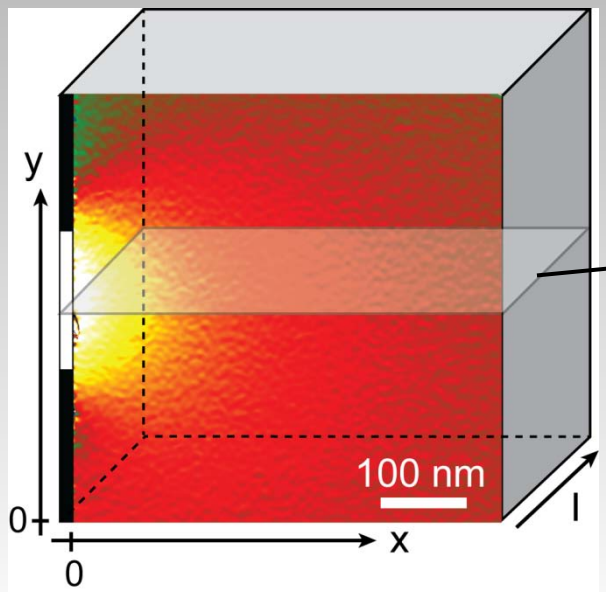

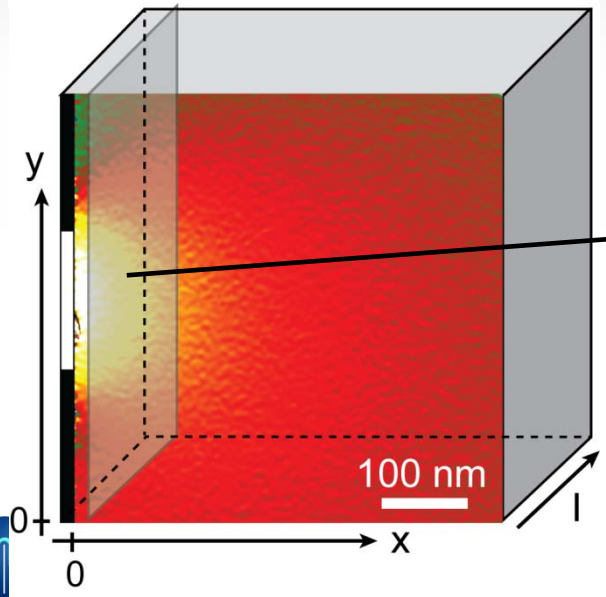

Surface plot of the hysteresis loops

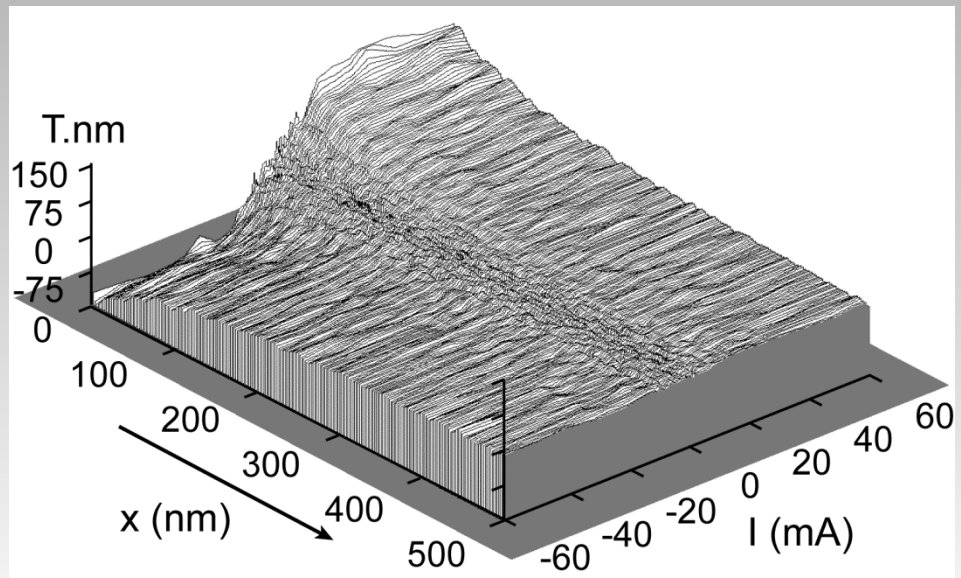

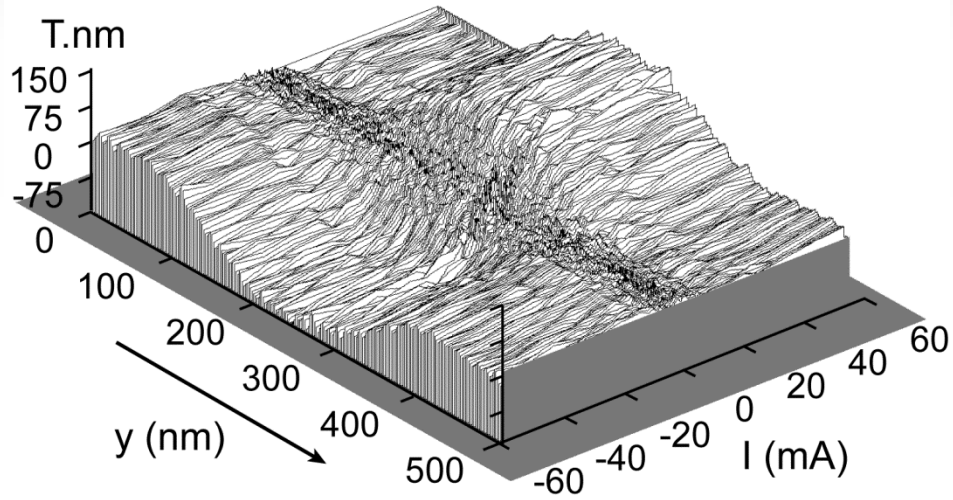

Variation of the radiated regions located at 5 nm in front of the pole as a function of the applied current and for various flux divergences.

Divergence from the X direction

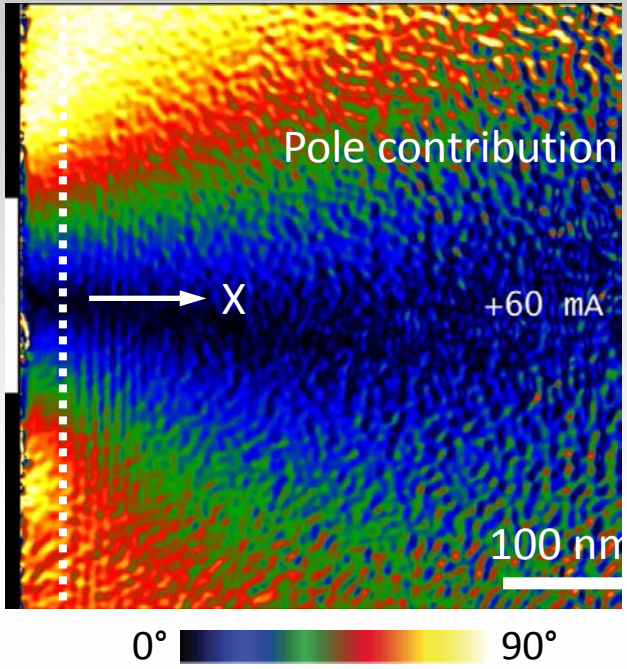

Angular spread

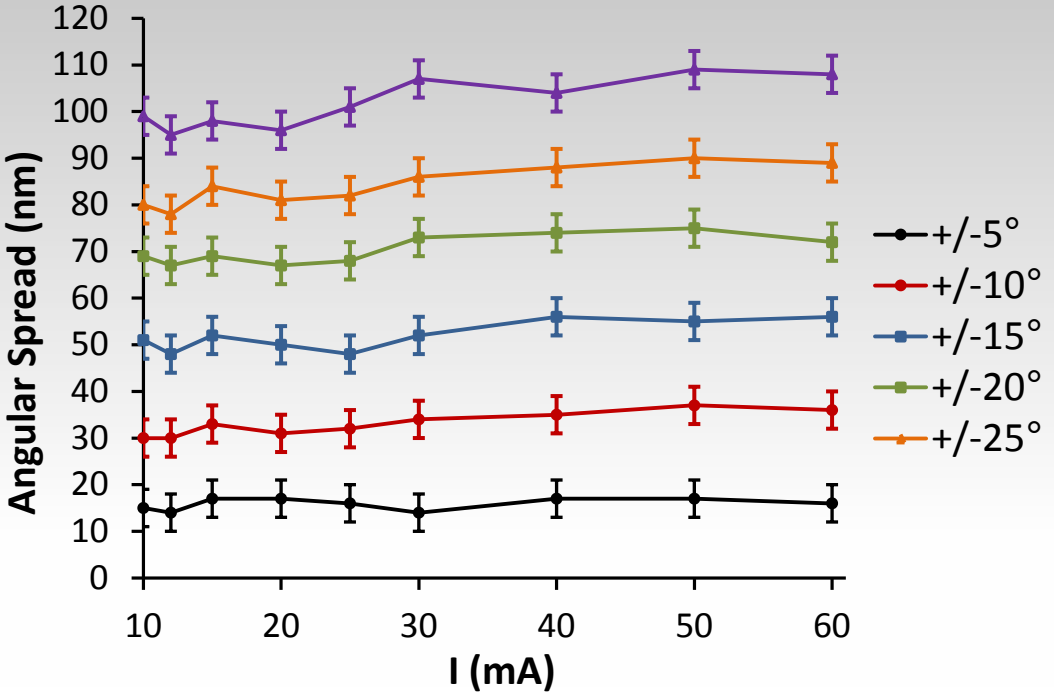

- Demonstration of the efficiency of the shields for focusing the field onto the media
- From the HDD application point of view, illustration that only the media directly under the write pole will experience any significant magnetic interaction for writing/erasure processes.

Summary

• Quantitative mapping of the magnetic field generated by the writer part as a function of applied electrical current up to +/-60 mA in real conditions.

• Specific sample preparation to extract the active part of the device, without damaging the magnetic shields and the necessary elements for the current injection.

• The resulting field maps demonstrate the key features requested in magnetic recording, namely a highly directional magnetic field with a low angular spread.

• ***Use the write pole as a in situ magnet to apply a local magnetic field in a TEM. Mounting on the tip of a sample holder with piezo-electric displacements and moved close to a magnetic sample to be studied.***

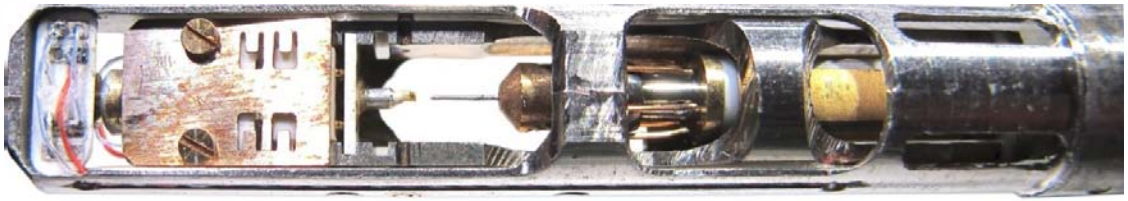

➔ **Perfect tool for performing double exposure interferometry: square signal for the current injection, frequency and amplitude can be tuned.**

Double exposure interferometry using a HDD writer

JOURNAL OF APPLIED PHYSICS VOLUME 37, NUMBER 2 FEBRUARY 1966

Holographic Interferometry*

L. O. Heflinger, R. F. Wuerker, and R. E. Brooks
TRW Systems, Redondo Beach, California
(Received 30 August 1965)

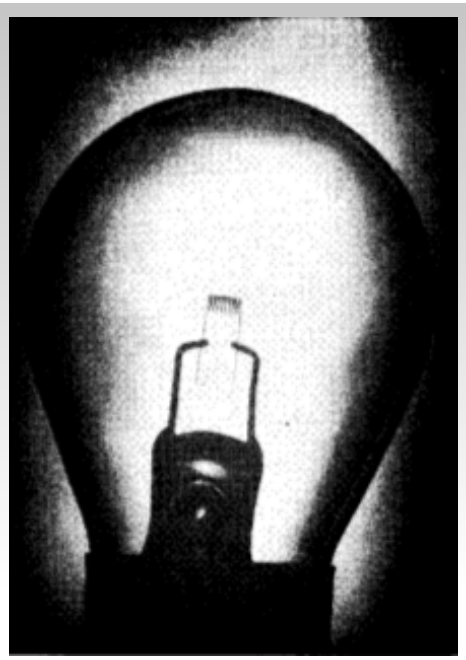

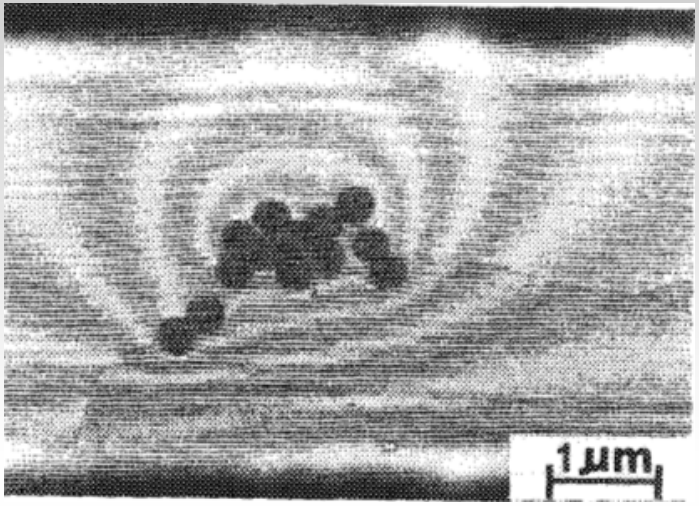

S. Frabboni, G. Matteucci & G. Pozzi
Ultramicroscopy **23**, 29–37 (1987).

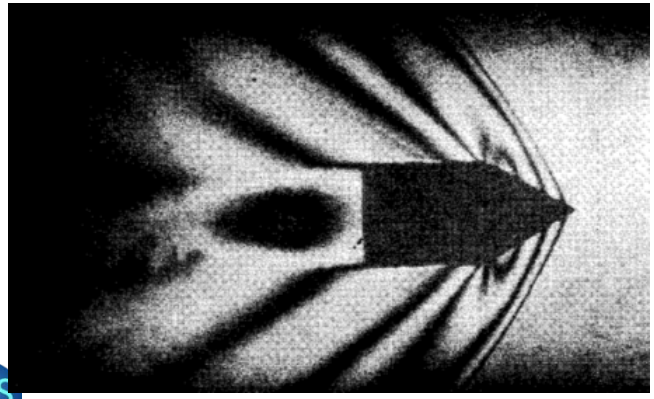

Moiré effect

Double exposure interferometry using a HDD writer

$\phi_1(\mathbf{R})$: Pole (+60 mA) + Shield + Distortions

$\phi_2(\mathbf{R})$: Shield + Distortions

$$\frac{1}{2}$$

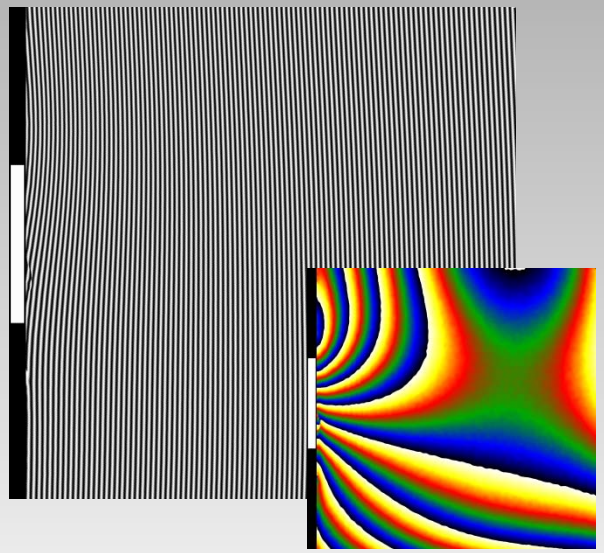

$$+$$

$$\frac{1}{2}$$

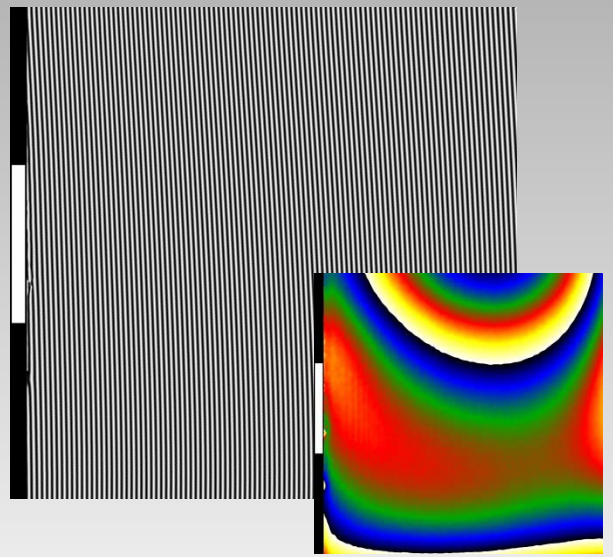

$$I_1(\mathbf{R}) = |A_0|^2 + |A(\mathbf{R})|^2 + 2\,A_0 A(\mathbf{R})\cos(k\cdot\mathbf{R} + \phi_1(\mathbf{R}))$$

$$I_1(\mathbf{R}) = |A_0|^2 + |A(\mathbf{R})|^2 + 2\,A_0 A(\mathbf{R})\cos(k\cdot\mathbf{R} + \phi_2(\mathbf{R}))$$

$$=$$

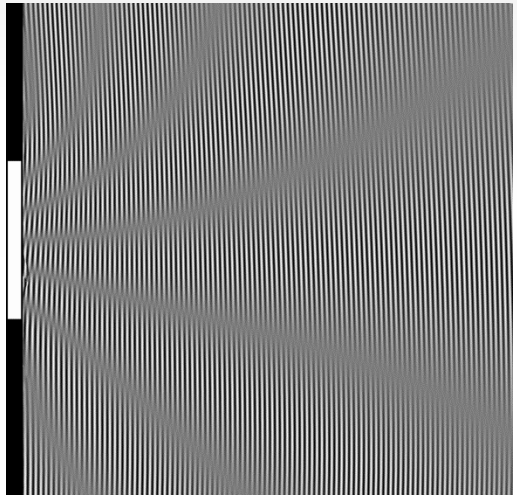

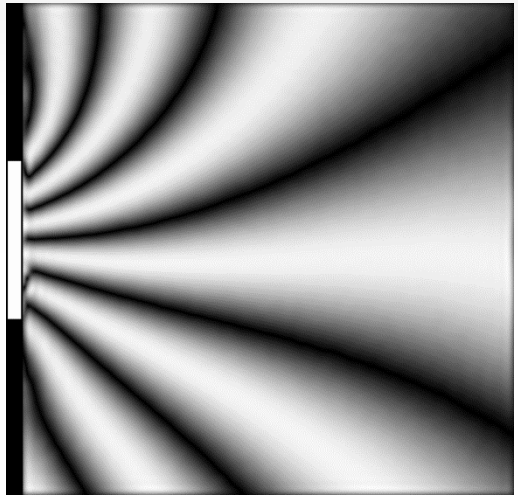

$$I_{1+2}(\mathbf{R}) = |A_0|^2 + |A(\mathbf{R})|^2 + 2\,A_0 A(\mathbf{R})\cos\left(\frac{\phi_1(\mathbf{R}) - \phi_2(\mathbf{R})}{2}\right)\cos\left(k\cdot\mathbf{R} + \frac{\phi_1(\mathbf{R}) + \phi_2(\mathbf{R})}{2}\right)$$

Amplitude

Double exposure interferometry using a HDD writer

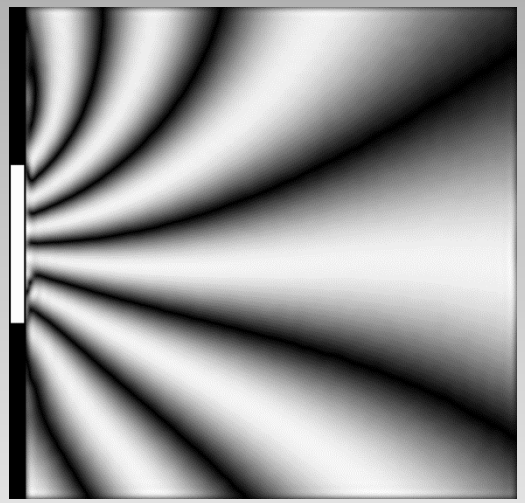

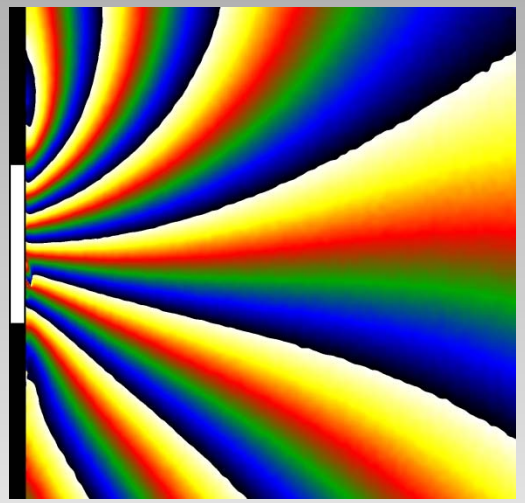

- Direct information from only pole contribution
- Other constant contributions (shield, distortions) removed

$$\text{Amplitude} \propto \cos\left(\frac{\phi_1(\mathbf{R}) - \phi_2(\mathbf{R})}{2}\right)$$

$$\propto \cos\left(\frac{\text{Pole (+60 mA)}}{2}\right)$$

Phase of pole contribution +60 mA

- Need to superimpose 2 states during the exposure time

=> Square signal for current injection

- Possibilility to change:
  - the offset
  - the amplitude
  - the frequency

Double exposure interferometry using a HDD writer

Freq = 1kHz, 4s acquisition time

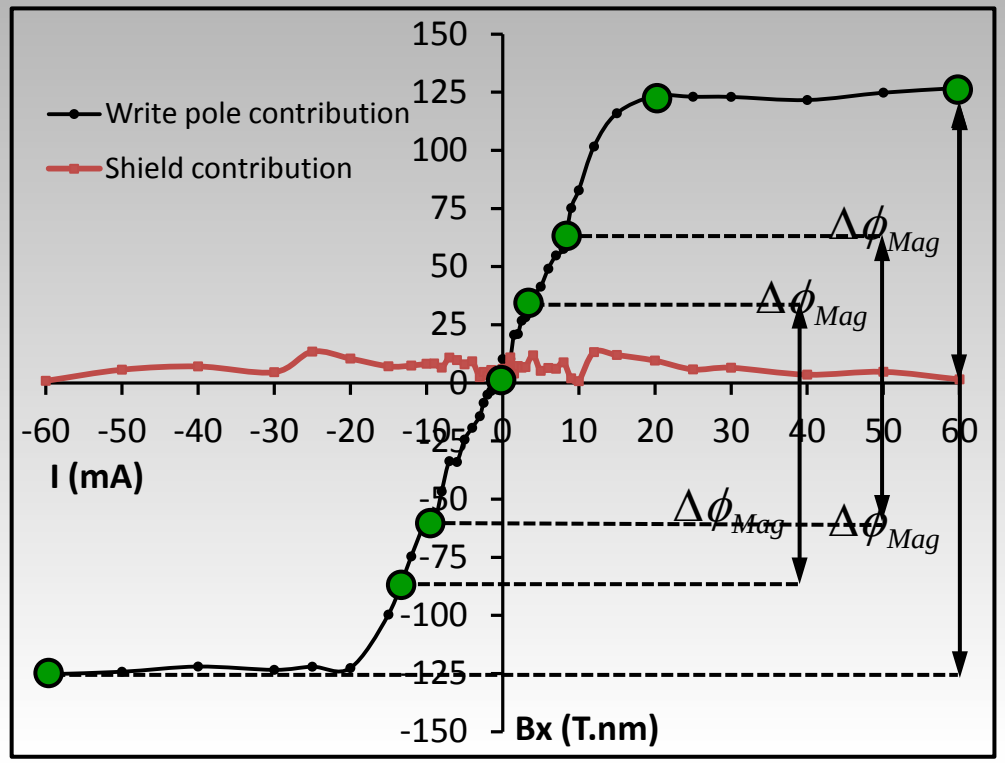

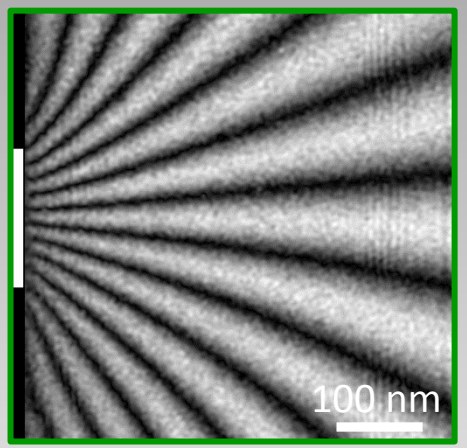

-60 to +60 mA

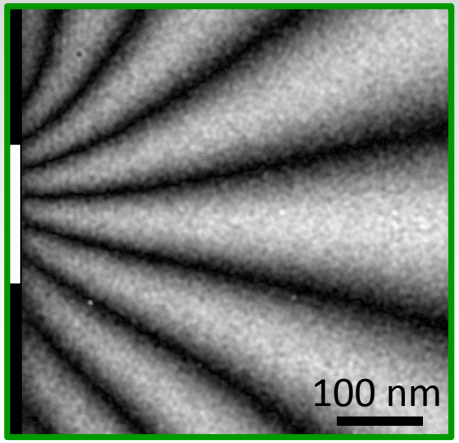

0 to +60 mA

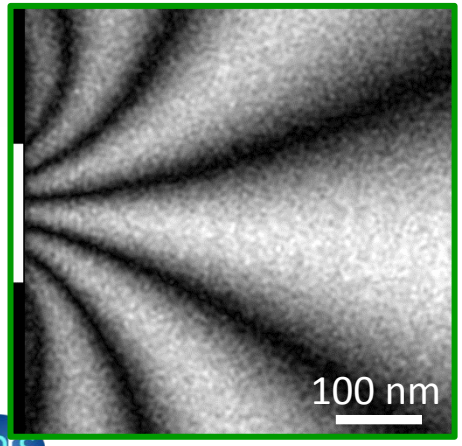

-15 to +5 mA

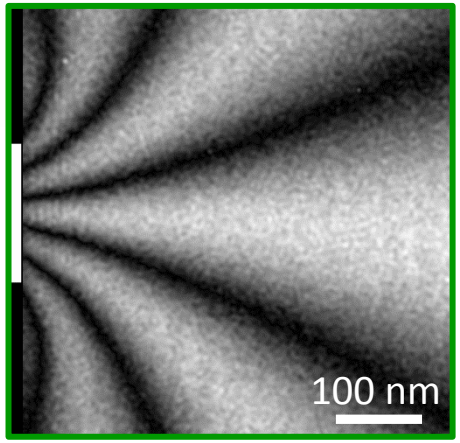

-10 to +10 mA

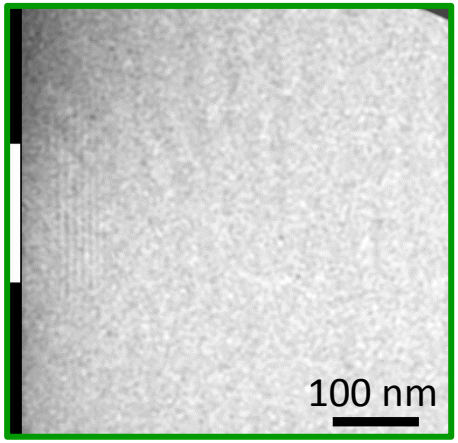

20 to +60 mA

Double exposure interferometry using a HDD writer

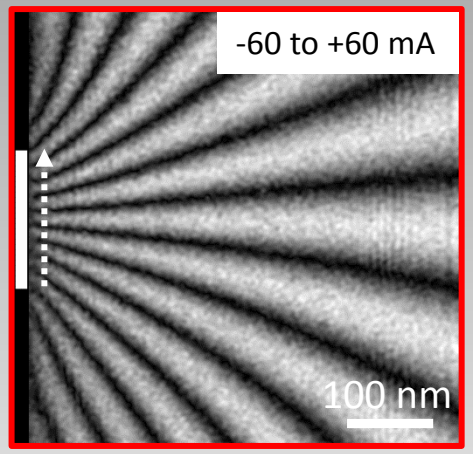

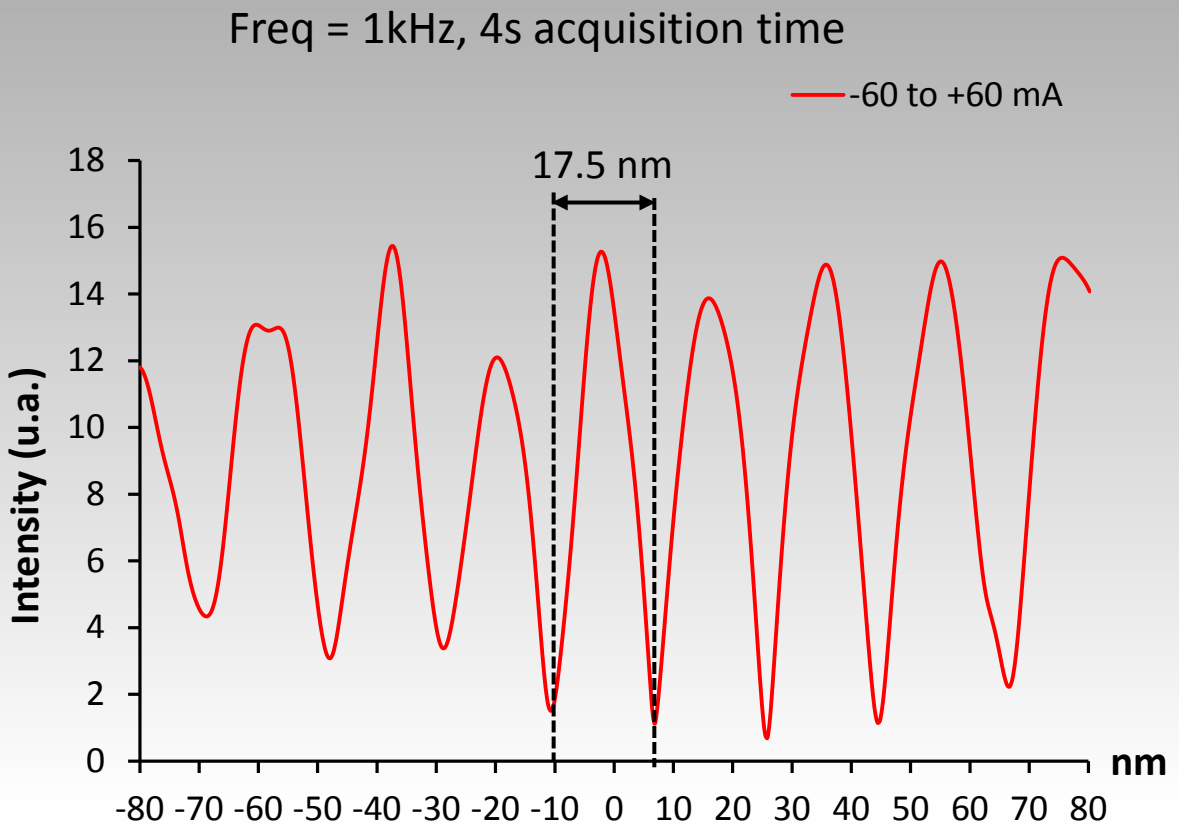

- 2π phase jump between 2 minima (or maxima)

$$\iint B_{\perp}(\mathbf{r}_{\perp}, z)\, dr\, dz = -\frac{h}{e}\Delta\phi_{Mag}(\mathbf{r}) = -\frac{h}{e} = 4.136\ 10^{-15}\ \text{Wb}$$

Length = 17.5 nm => $\int_{-\infty}^{\infty} B_y(r_{\perp}, z)\, dz \approx 236$ T.nm

-60 to 60 mA: 2 x Saturated magnetic flux => 118 T.nm

Double exposure interferometry using a HDD writer

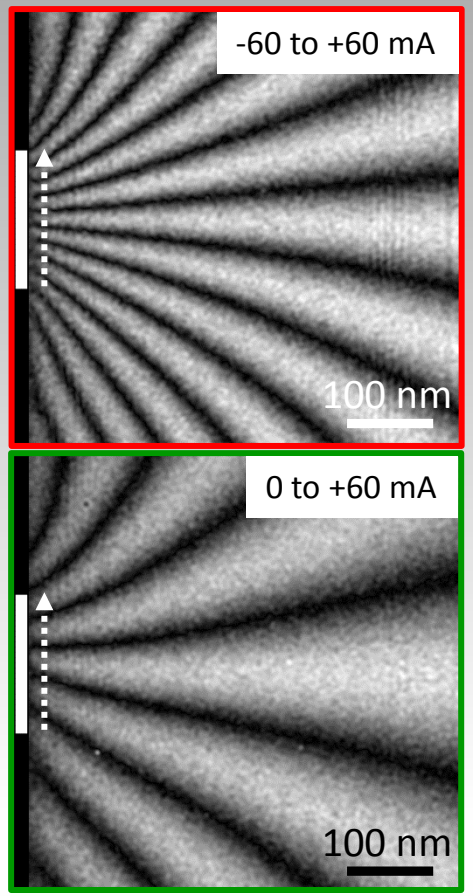

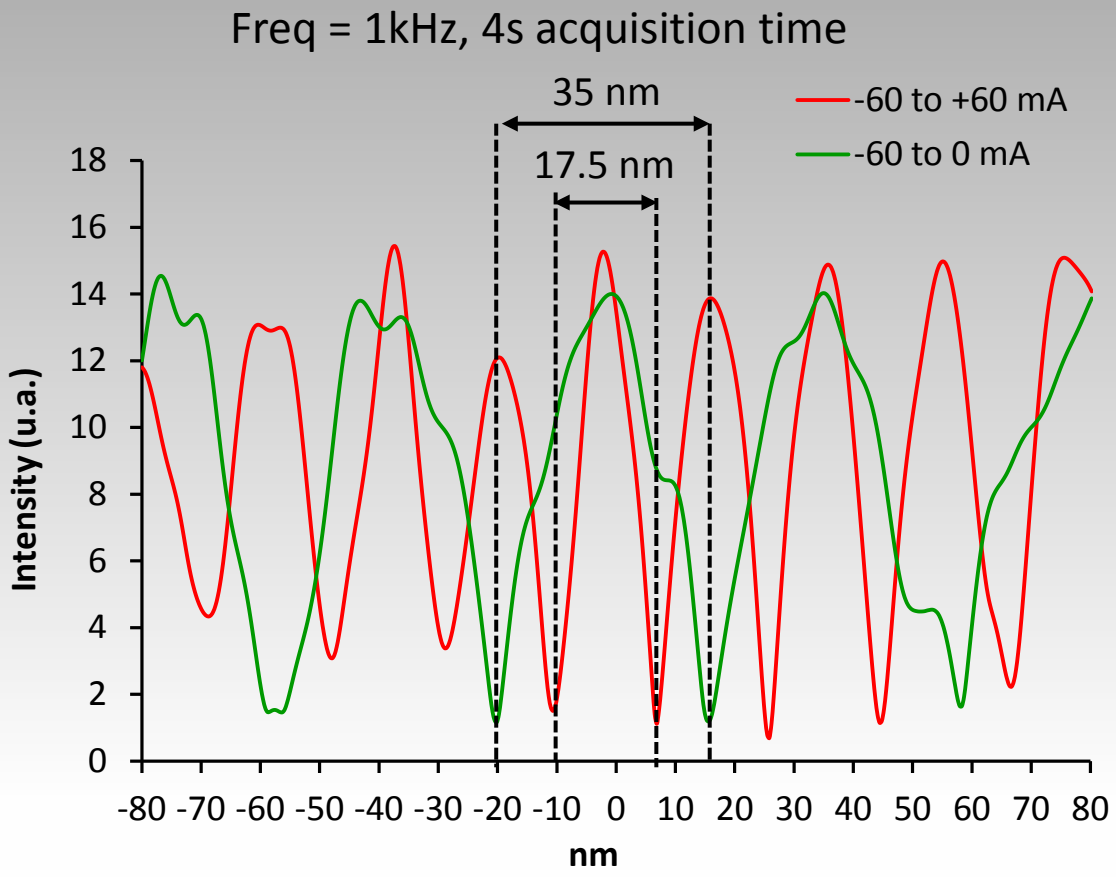

- If the amplitude of the current is divided by 2, distance between 2 minima multiplied by 2

=> <u>Magnetic flux divided by 2</u>

Double exposure interferometry using a HDD writer

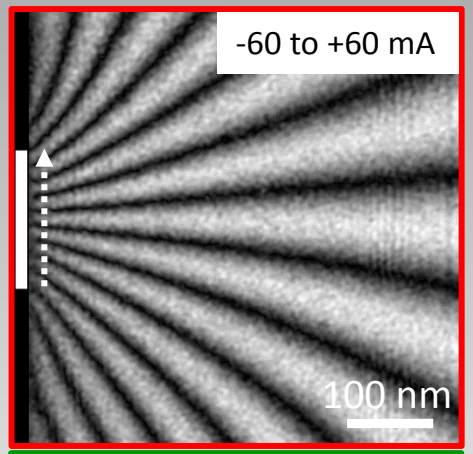

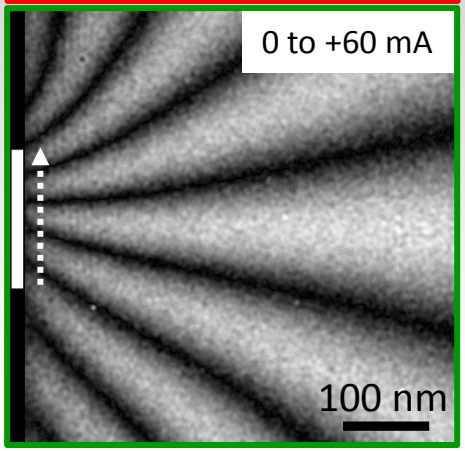

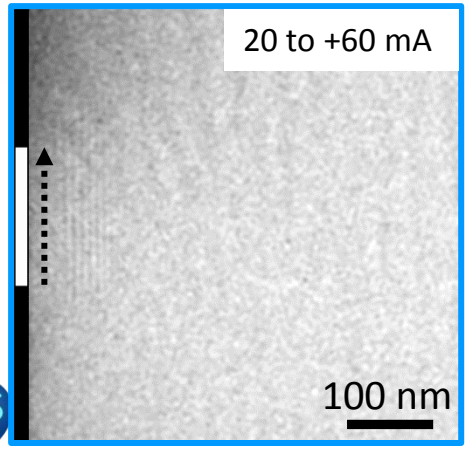

Freq = 1kHz, 4s acquisition time

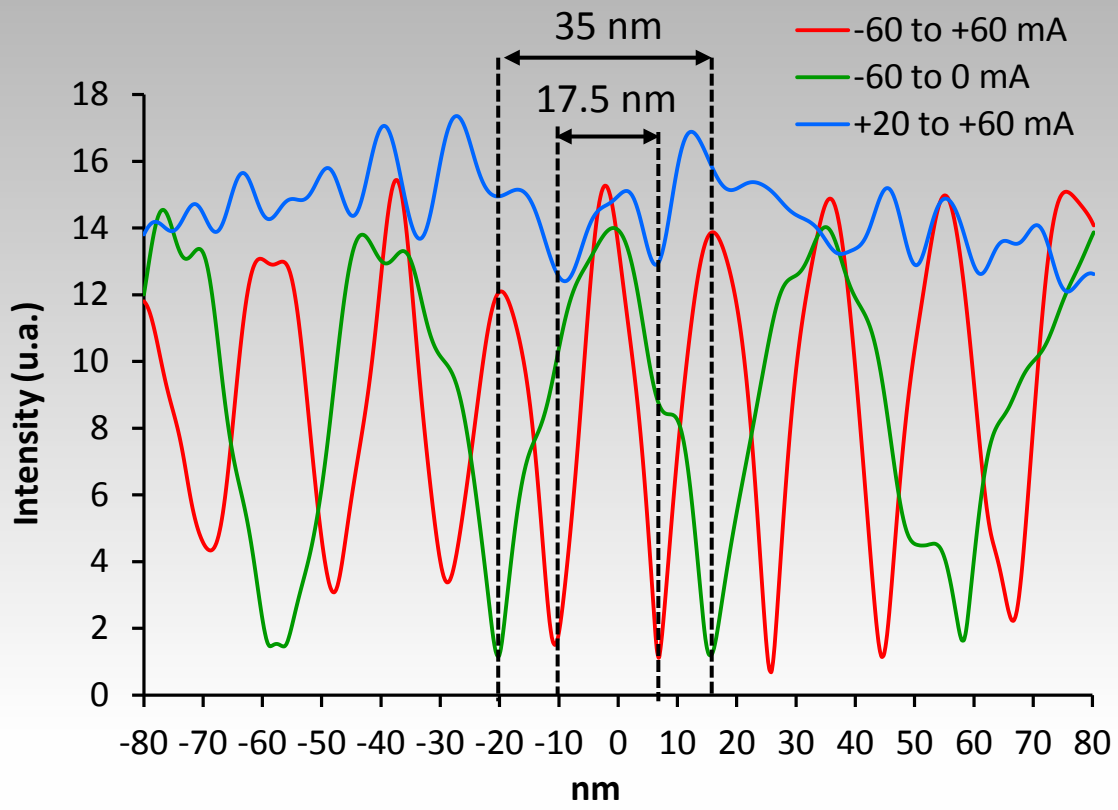

- If no variation of magnetic flux (saturation), amplitude is constant (no pronounced minima or maxima)

=> Magnetic induction can be measured and a magnetic map is obtained without reference problem

Double exposure interferometry using a HDD writer

-60 to 60 mA, 4s acquisition time

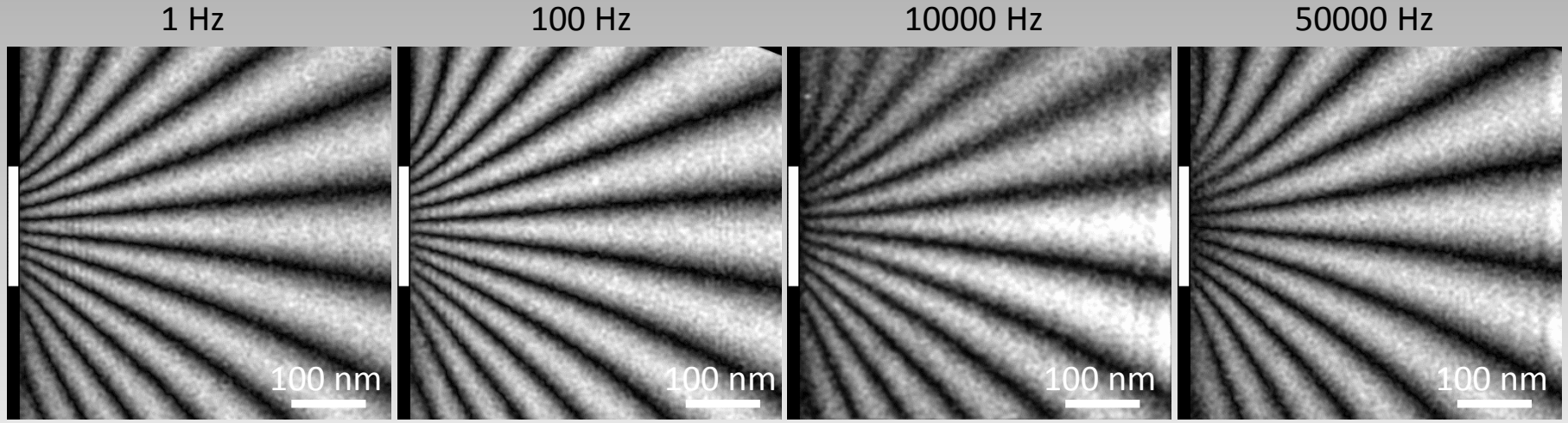

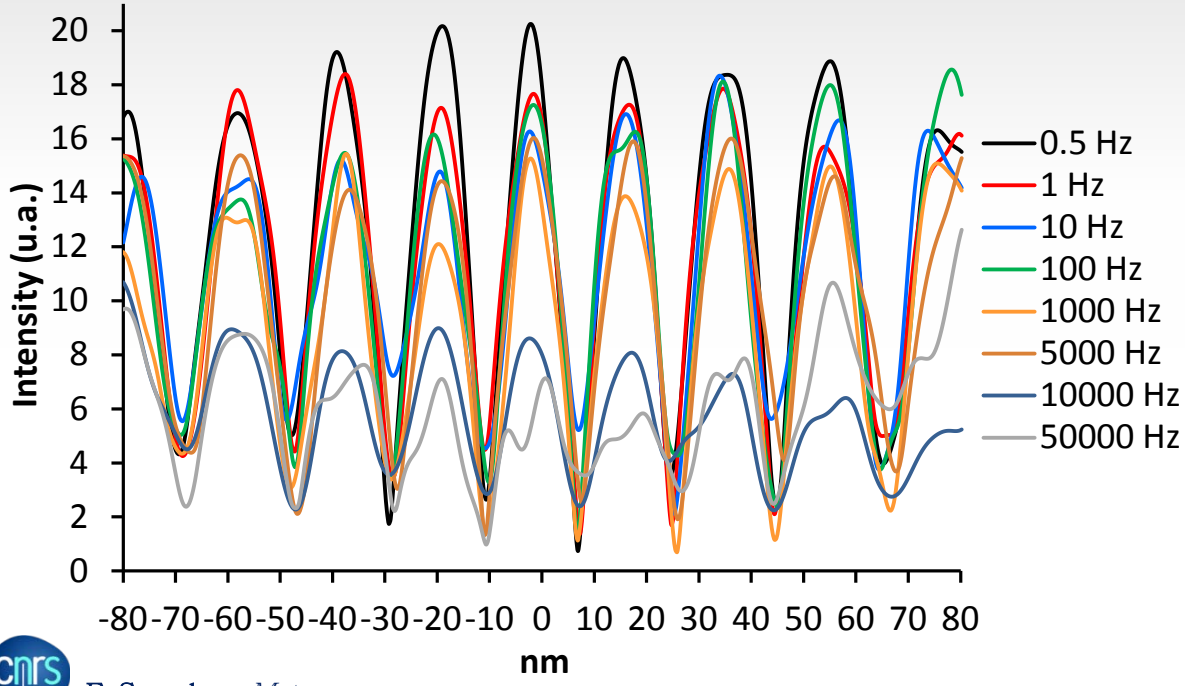

- No effect of the frequency on the amplitude of the magnetic flux
- Decrease of the amplitude of the fringes (vibration ?)
- Limitation of the electrical contacts, sample holder and source meter

Acknowledgments

• European Union under the Seventh Framework Programme under a contract for an Integrated Infrastructure Initiative Reference 312483-**ESTEEM2**.

• French National Research Agency under the "Investissement d'Avenir" program reference No. ANR-10-EQPX-38-01“: **MIMETIS**.

• This work is supported by the French national project **EMMA** (ANR12 BS10 013 01).

esteem2
european network for electron microscopy

ESTEEM2 is an

INTEGRATED INFRASTRUCTURE NETWORK

of electron microscopy facilities providing access for the academic and industrial research community in materials science to the most powerful TEM techniques available at the nanoscale.

14

European schools and workshops

to provide training in innovative methods in electron microscopy and a forum for discussing emerging techniques. (including QEM2013: www.qem2013.com)

ESTEEM2 research program

focuses on the further development of :

- electron diffraction
- imaging
- spectroscopy
- 3D methods
- time-resolved microscopy

www.esteem2.eu

SEVENTH FRAMEWORK PROGRAMME

esteem2
european network for electron microscopy

Free transnational access

to the most advanced TEM equipment and skilled operators for HR(S)TEM, EELS, EDX, Tomography, Holography and various in-situ state-of-the-art experiments.

ESTEEM2 available equipment includes:

- 19 FEI-Titan 60-300 and Tecnai G2 aberration corrected microscopes
- 6 JEOL aberration-corrected TEM
- A NION probe corrected Ultrastem 200
- The ZEISS SESAM
- The HITACHI I2TEM Cs corrected C-FEG
- Extensive FIB and sample preparation facilities.

www.esteem2.eu

SEVENTH FRAMEWORK PROGRAMME

The TEM group @ CEMES - Toulouse

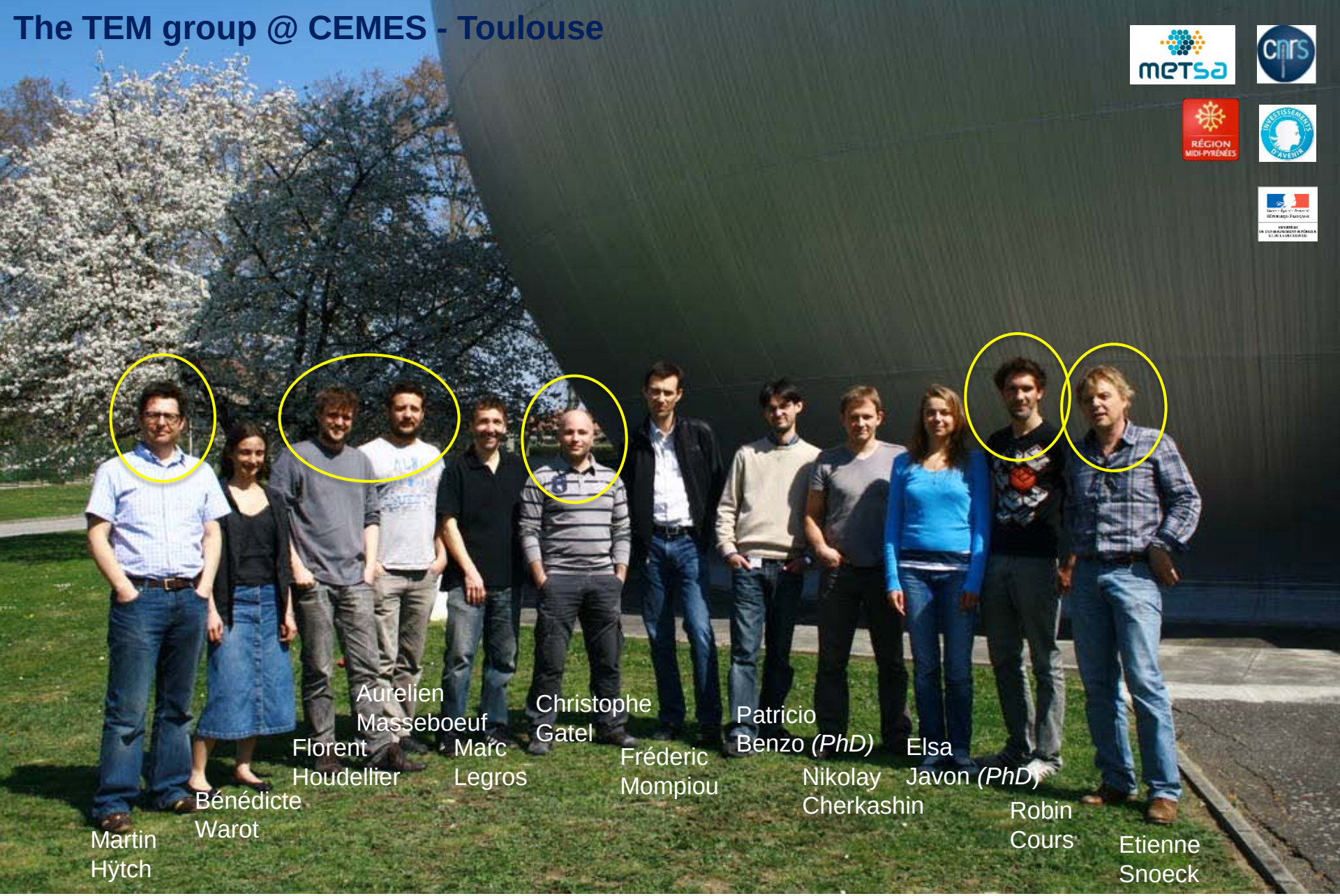

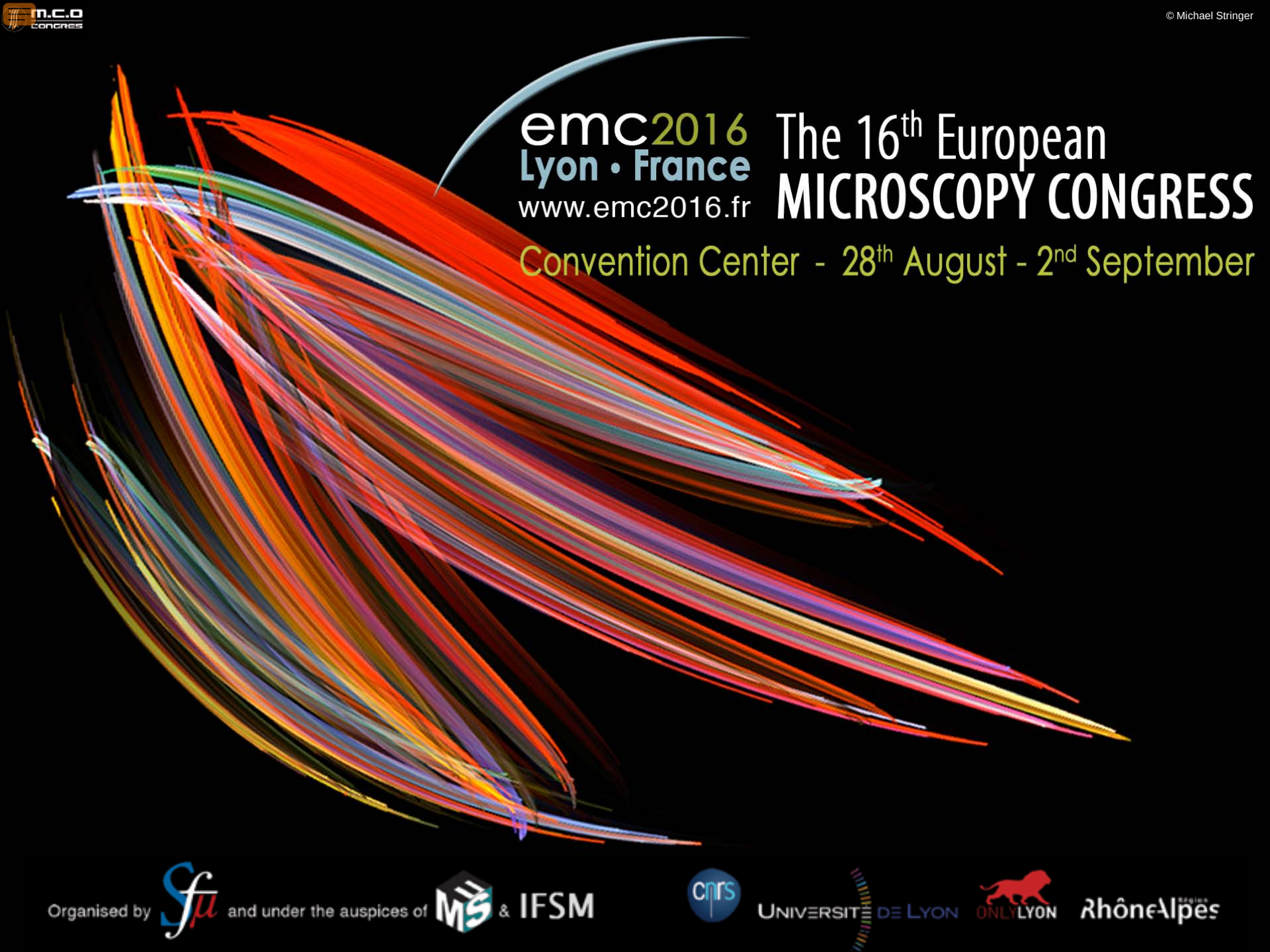

Double exposure interferometry using a HDD writer

JOURNAL OF APPLIED PHYSICS VOLUME 37, NUMBER 2 FEBRUARY 1966

Holographic Interferometry*

L. O. Heflinger, R. F. Wuerker, and R. E. Brooks
TRW Systems, Redondo Beach, California
(Received 30 August 1965)

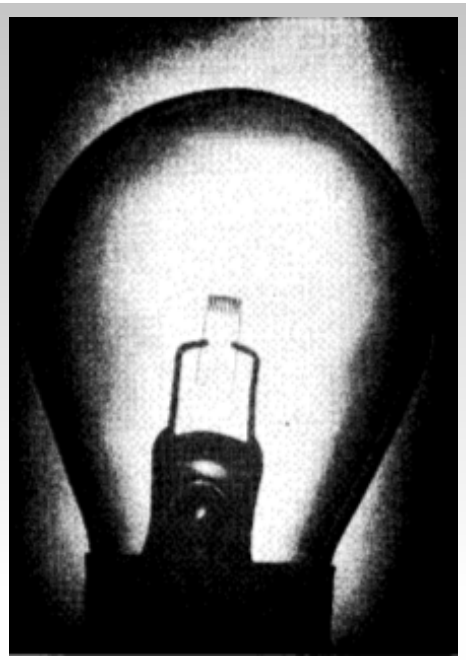

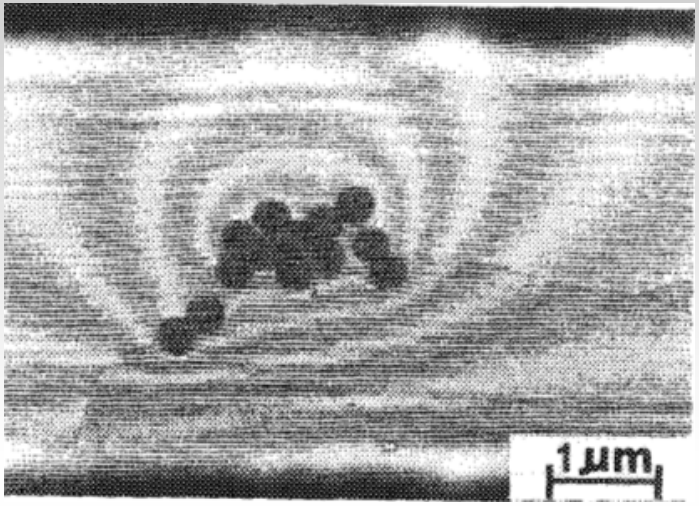

S. Frabboni, G. Matteucci & G. Pozzi
Ultramicroscopy **23**, 29–37 (1987).

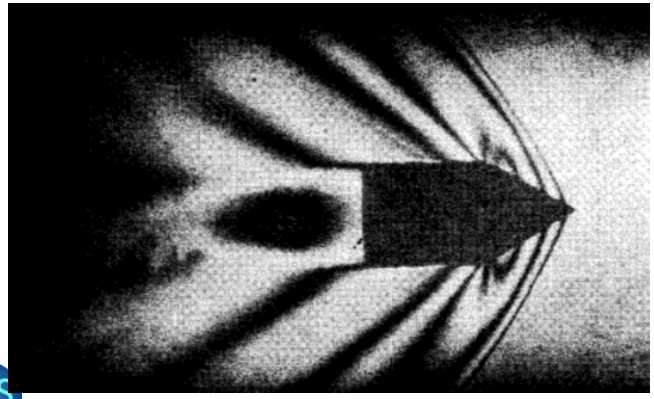

Moiré effect

Double exposure interferometry using a HDD writer

$\phi_1(\mathbf{R})$: Pole (+60 mA) + Shield + Distortions

$\phi_2(\mathbf{R})$: Shield + Distortions

$$\frac{1}{2}$$

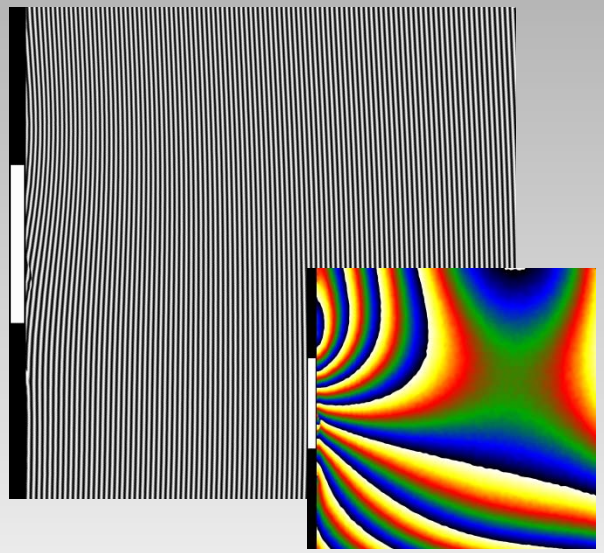

$$+$$

$$\frac{1}{2}$$

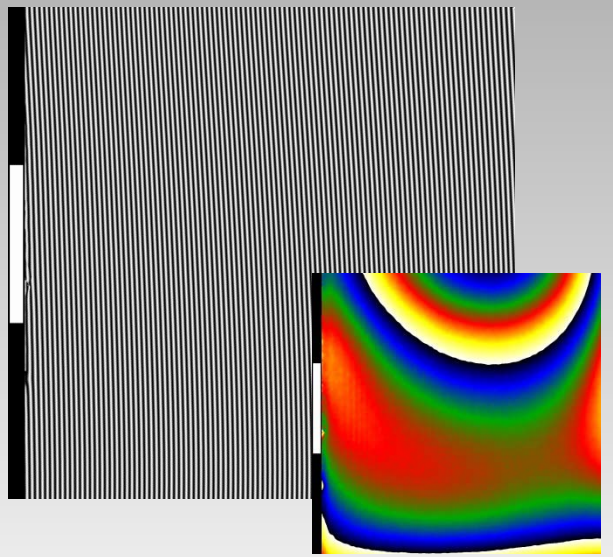

$$I_1(\mathbf{R}) = |A_0|^2 + |A(\mathbf{R})|^2 + 2\,A_0 A(\mathbf{R})\cos(k\cdot\mathbf{R} + \phi_1(\mathbf{R}))$$

$$I_1(\mathbf{R}) = |A_0|^2 + |A(\mathbf{R})|^2 + 2\,A_0 A(\mathbf{R})\cos(k\cdot\mathbf{R} + \phi_2(\mathbf{R}))$$

$$=$$

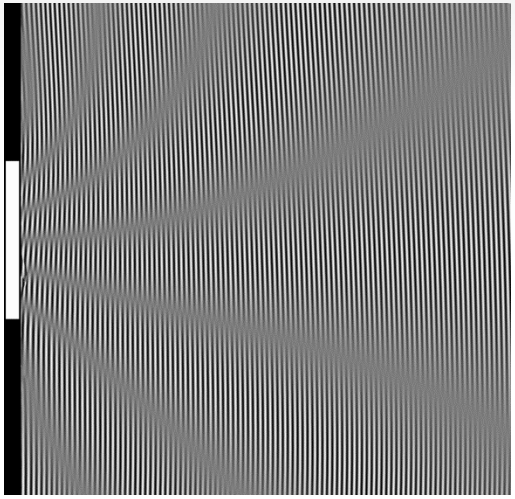

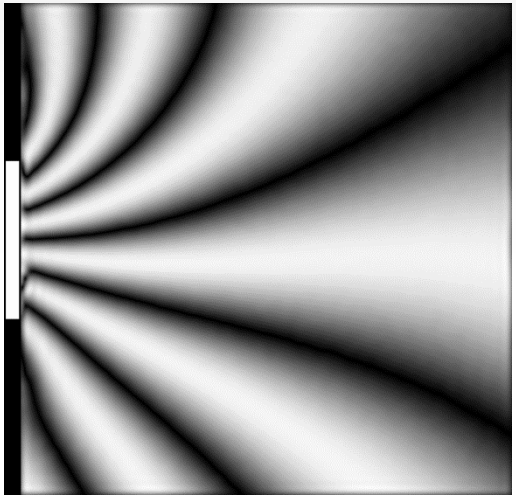

$$I_{1+2}(\mathbf{R}) = |A_0|^2 + |A(\mathbf{R})|^2 + 2\,A_0 A(\mathbf{R})\cos\left(\frac{\phi_1(\mathbf{R}) - \phi_2(\mathbf{R})}{2}\right)\cos\left(k\cdot\mathbf{R} + \frac{\phi_1(\mathbf{R}) + \phi_2(\mathbf{R})}{2}\right)$$

Amplitude

Double exposure interferometry using a HDD writer

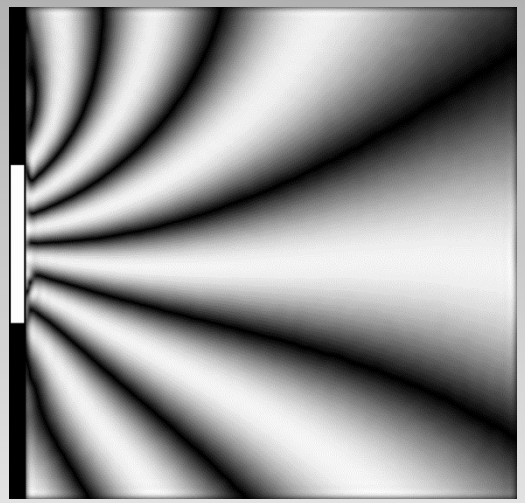

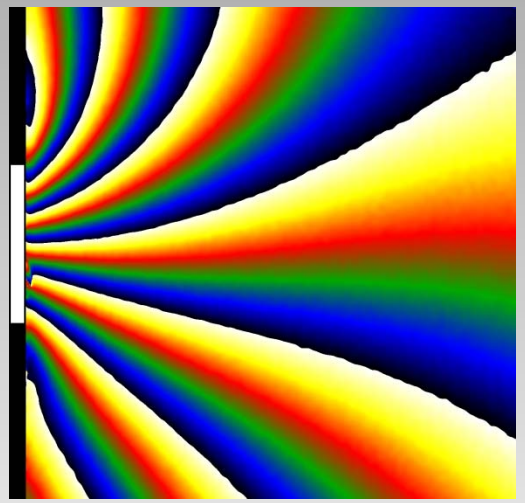

- Direct information from only pole contribution
- Other constant contributions (shield, distortions) removed

$$\text{Amplitude} \propto \cos\left(\frac{\phi_1(\mathbf{R}) - \phi_2(\mathbf{R})}{2}\right)$$

$$\propto \cos\left(\frac{\text{Pole (+60 mA)}}{2}\right)$$

Phase of pole contribution +60 mA

- Need to superimpose 2 states during the exposure time

=> Square signal for current injection

- Possibilility to change:
  - the offset
  - the amplitude
  - the frequency

Double exposure interferometry using a HDD writer

Freq = 1kHz, 4s acquisition time

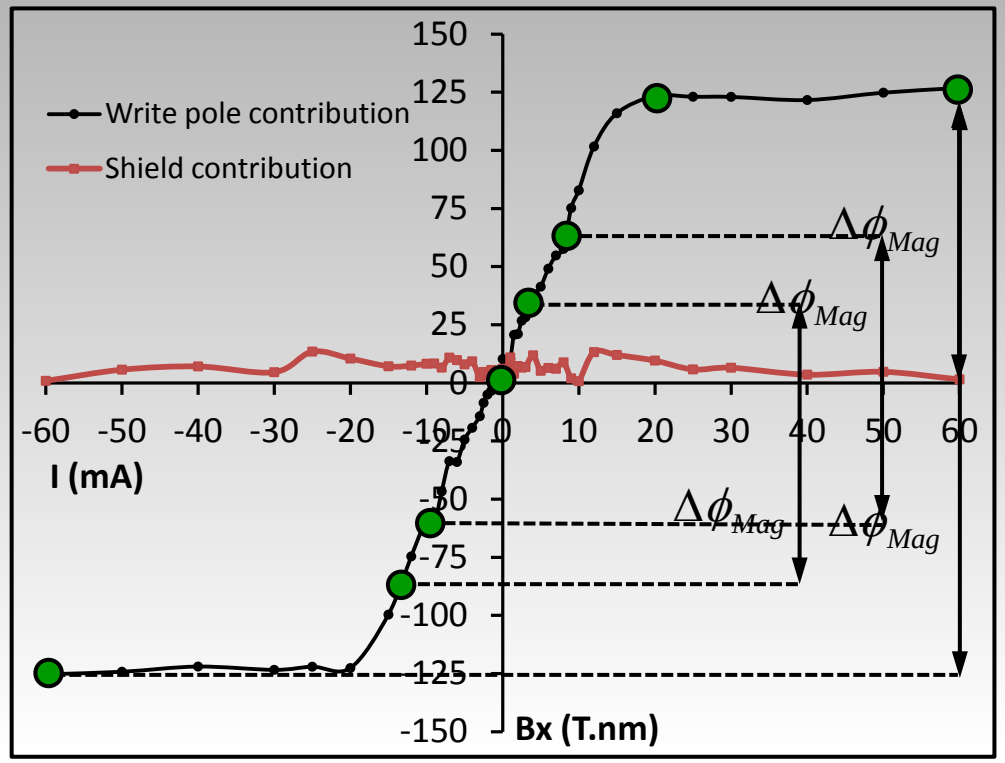

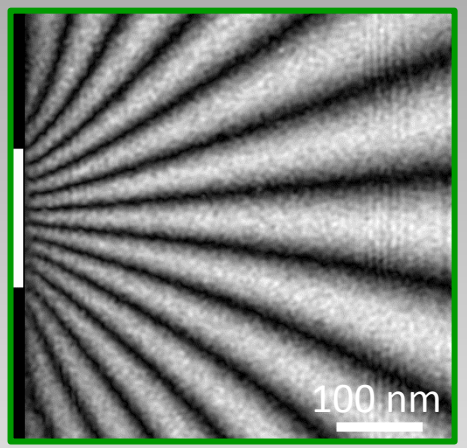

-60 to +60 mA

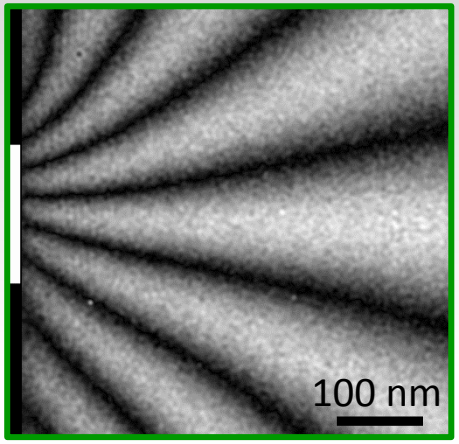

0 to +60 mA

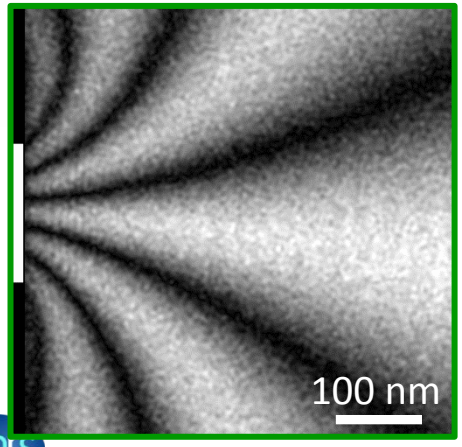

-15 to +5 mA

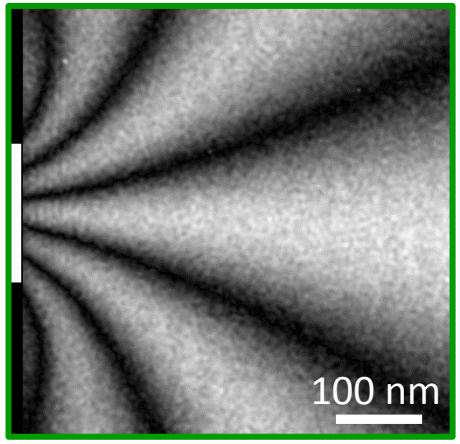

-10 to +10 mA

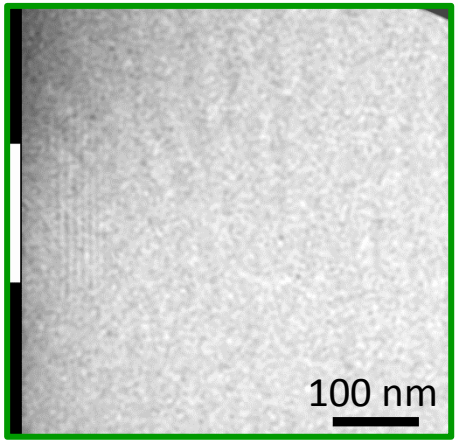

20 to +60 mA

Double exposure interferometry using a HDD writer

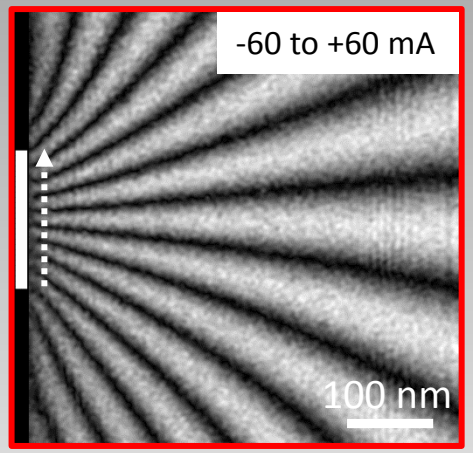

Freq = 1kHz, 4s acquisition time

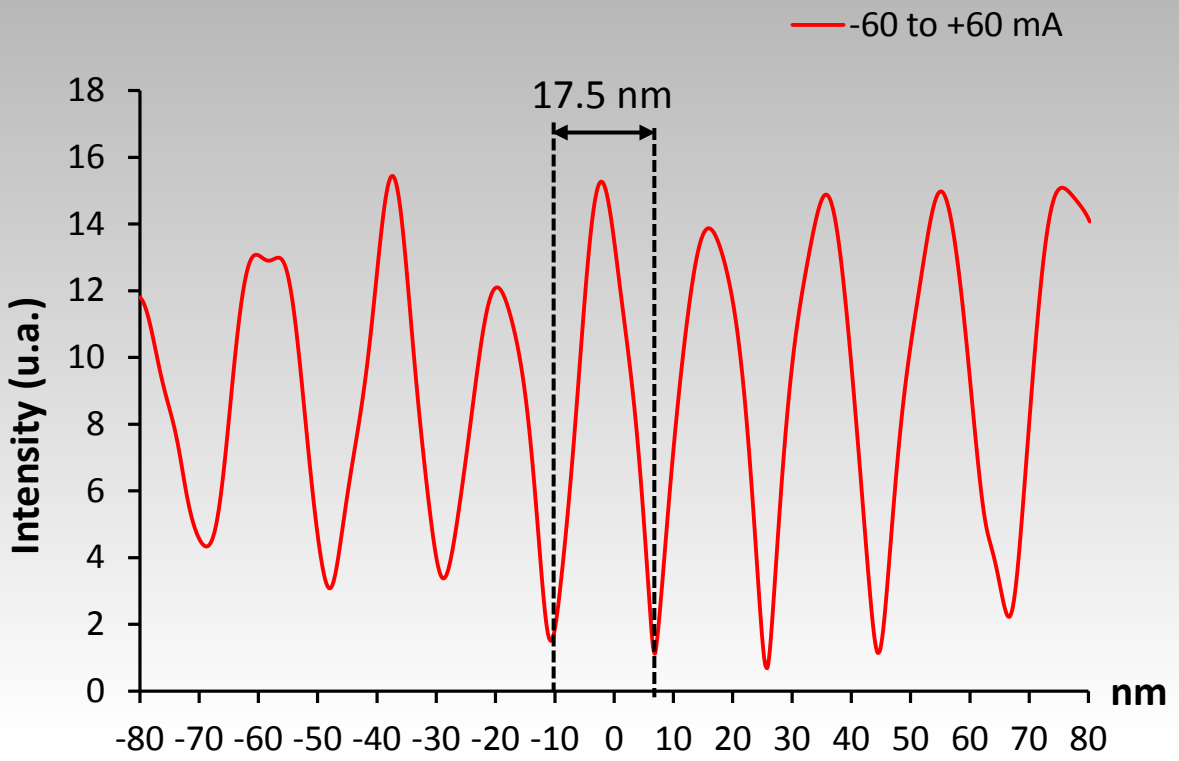

- 2π phase jump between 2 minima (or maxima)

$$\iint B_{\perp}(\mathbf{r}_{\perp}, z)\, dr\, dz = -\frac{h}{e}\Delta\phi_{Mag}(\mathbf{r}) = -\frac{h}{e} = 4.136\ 10^{-15}\ \text{Wb}$$

Length = 17.5 nm => $\int_{-\infty}^{\infty} B_y(r_{\perp}, z)\, dz \approx 236$ T.nm

-60 to 60 mA: 2 x Saturated magnetic flux => 118 T.nm

Double exposure interferometry using a HDD writer

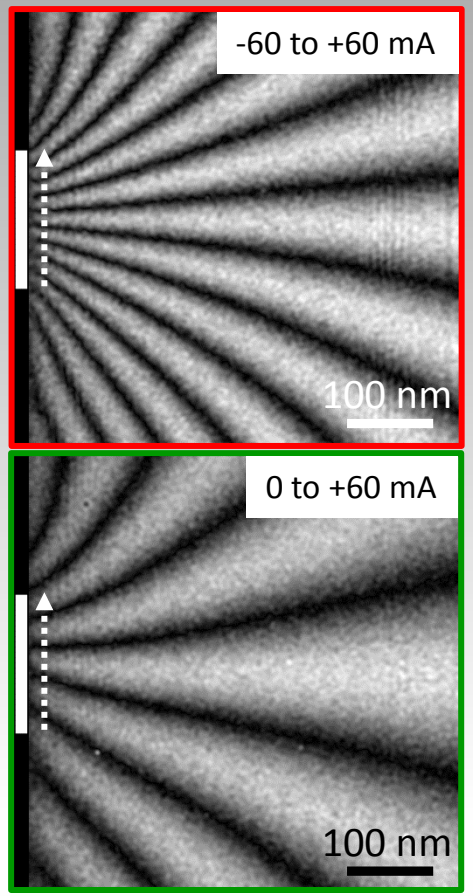

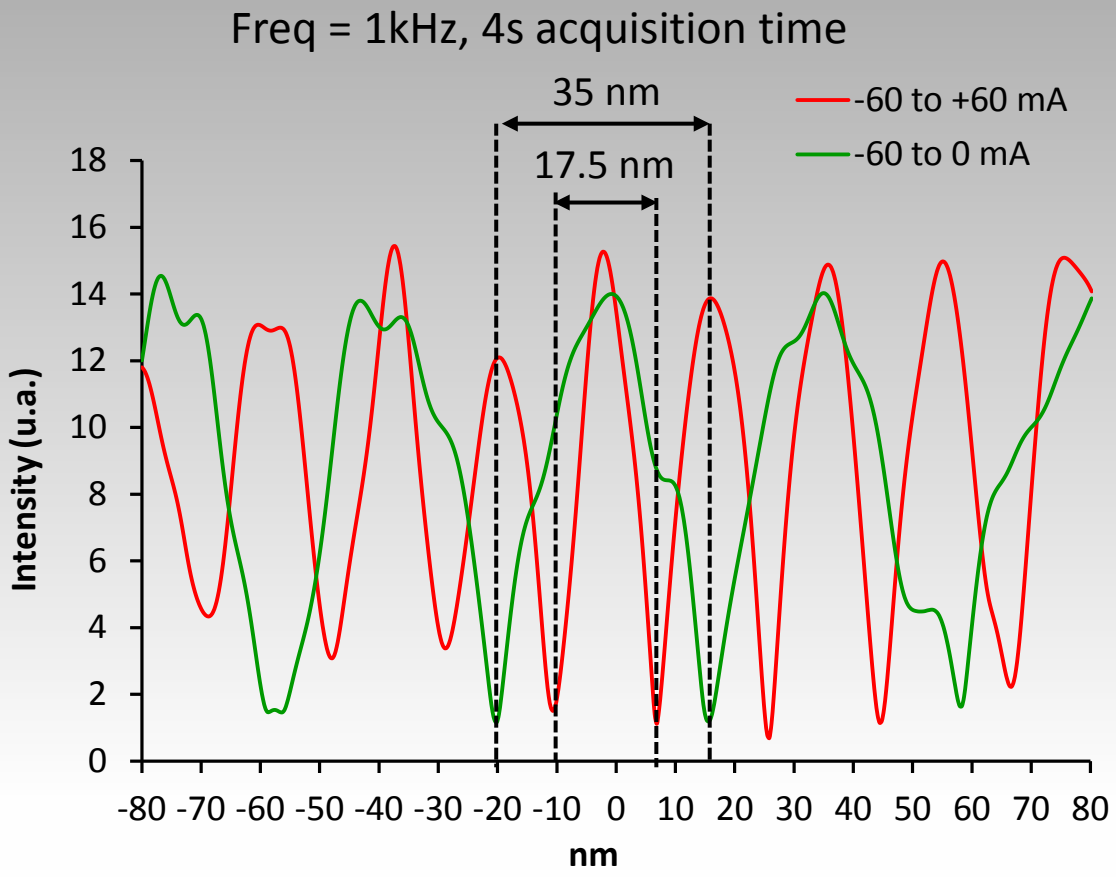

- If the amplitude of the current is divided by 2, distance between 2 minima multiplied by 2

=> <u>Magnetic flux divided by 2</u>

Double exposure interferometry using a HDD writer

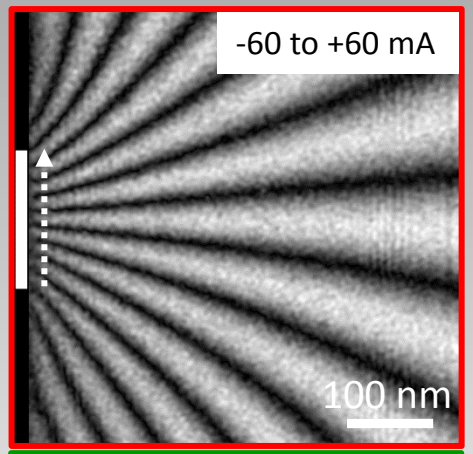

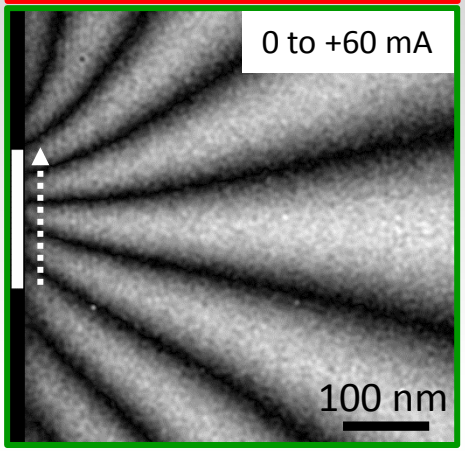

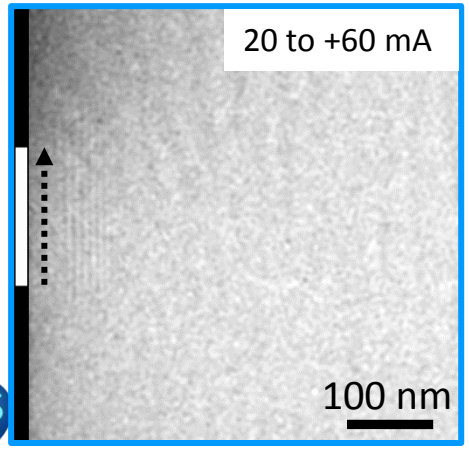

Freq = 1kHz, 4s acquisition time

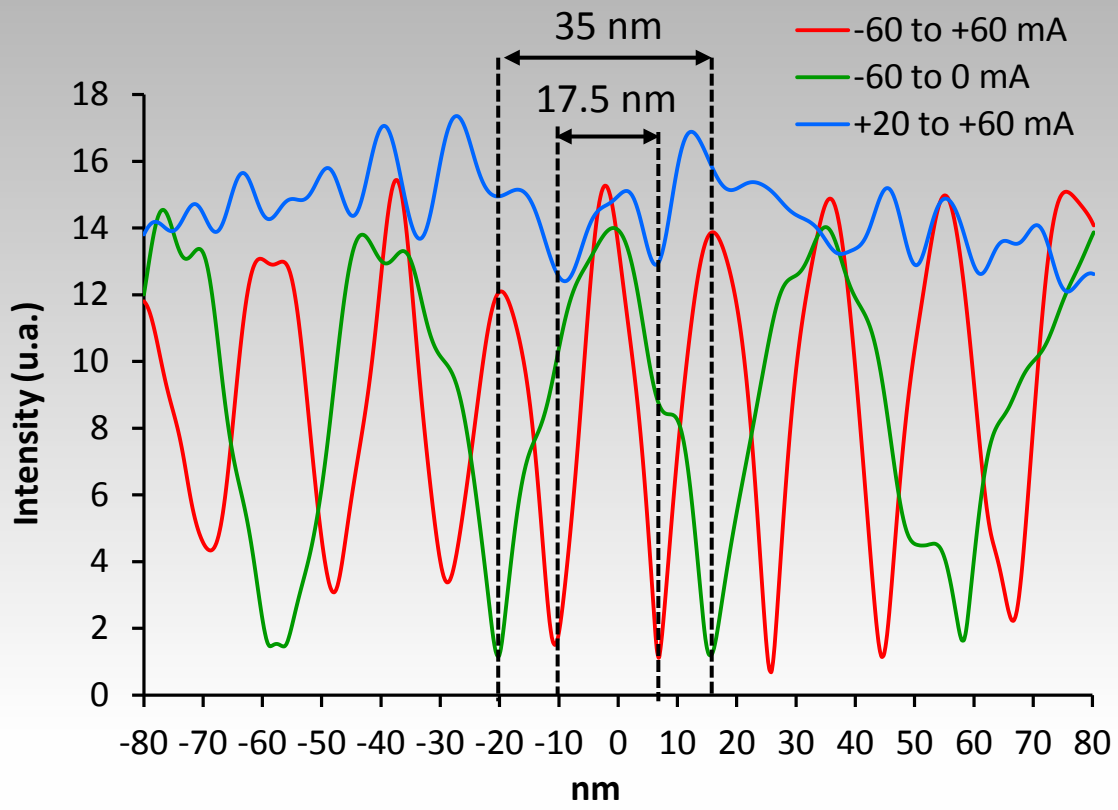

- If no variation of magnetic flux (saturation), amplitude is constant (no pronounced minima or maxima)

=> Magnetic induction can be measured and a magnetic map is obtained without reference problem

Double exposure interferometry using a HDD writer

-60 to 60 mA, 4s acquisition time

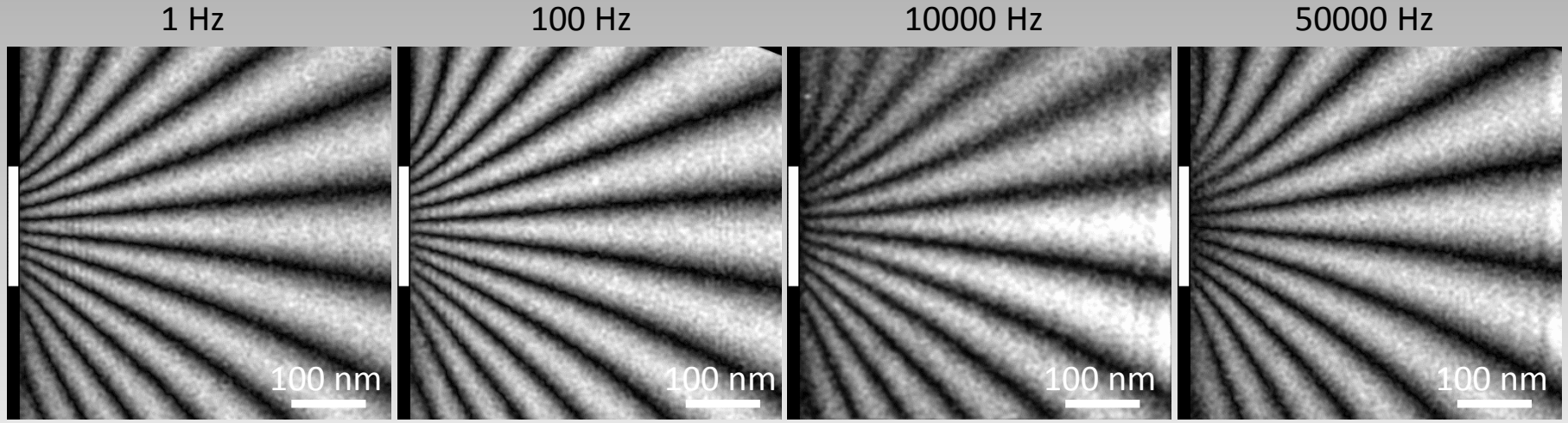

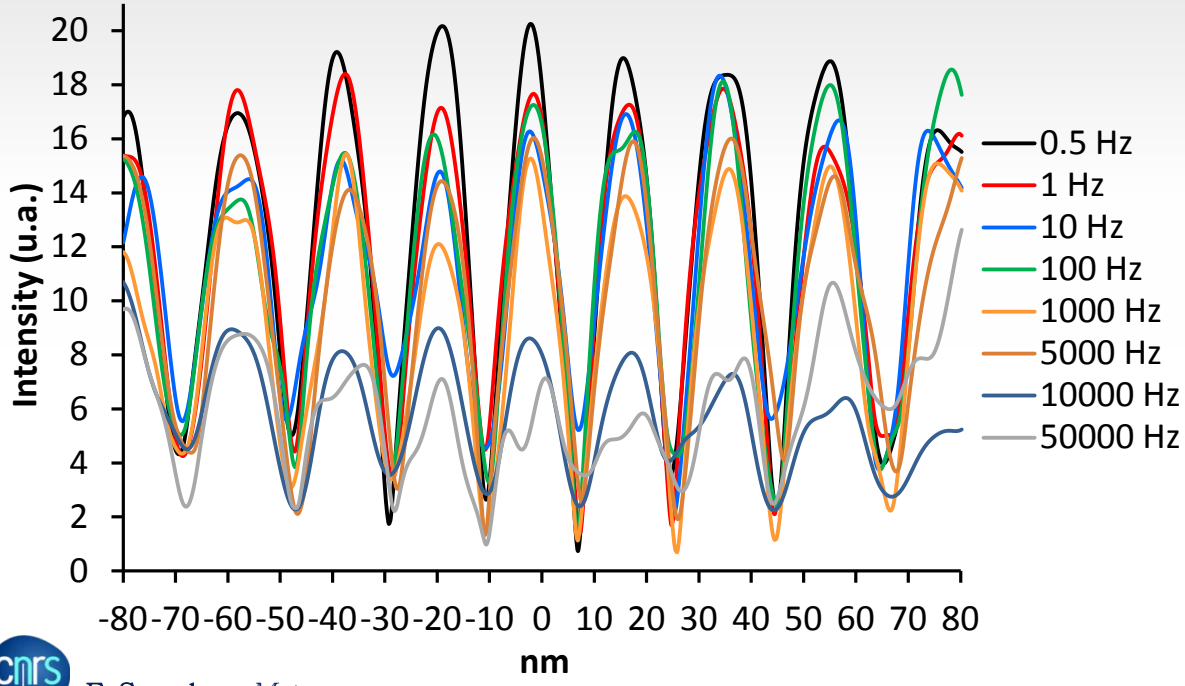

- No effect of the frequency on the amplitude of the magnetic flux
- Decrease of the amplitude of the fringes (vibration ?)
- Limitation of the electrical contacts, sample holder and source meter

Spin configurations in size controlled single Fe nanomagnets

Magnetic configuration depends on the energy minimization considering:

- the magneto-crystalline anisotropy
- the exchange constant
- the magneto-static energies

3 typical configurations in a magnetic material as a function of the size at the remnant state:

- Multidomain state: adjacent domains with magnetic walls
- Vortex (V) state: external spins rotate to achieve a flux closure, while in the vortex core, spins tilt out-of-plane
- Single-domain (SD) configuration : uniform arrangement of magnetic moments

Size ↘

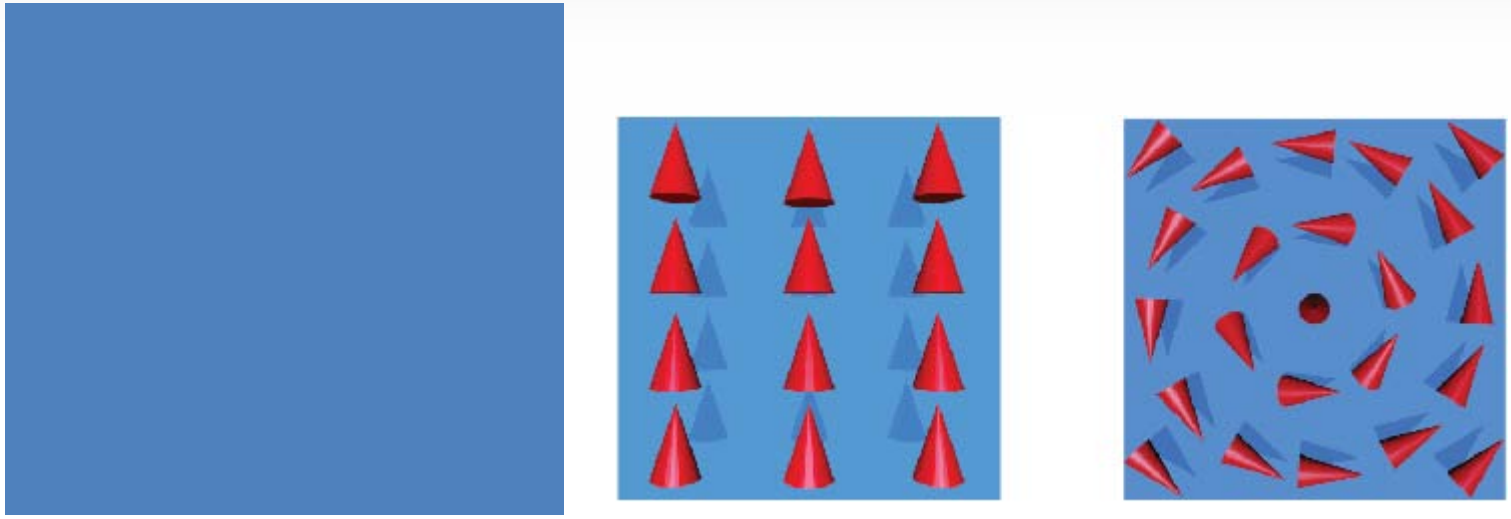

Size ↘

Spin configurations in size controlled single Fe nanomagnets

Need of model objects for the study of magnetic transition as a function of the size

=> Nanoparticles synthesized in liquid phase by organometallic chemistry

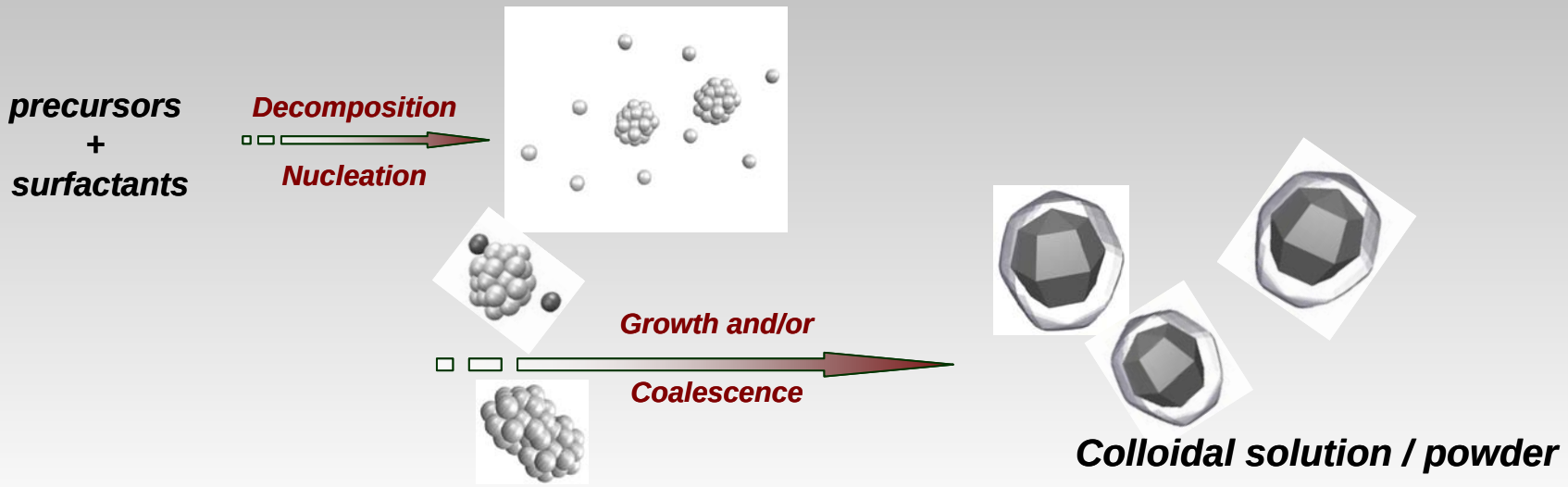

- Shape and size control through the reaction conditions : ligands, temperature, products concentration… => Spherical NPs, nanocubes, nanorods, multipods,…
- The surfactants control the nucleation and growth steps, and prevent the coalescence of the nanocrystals.
- Defect-free nanomagnets with controlled and reproducible magnetic properties allow accurate modeling and comparison with experimental investigations.

Spin configurations in size controlled single Fe nanomagnets

Examples for Co and Fe nanoparticles

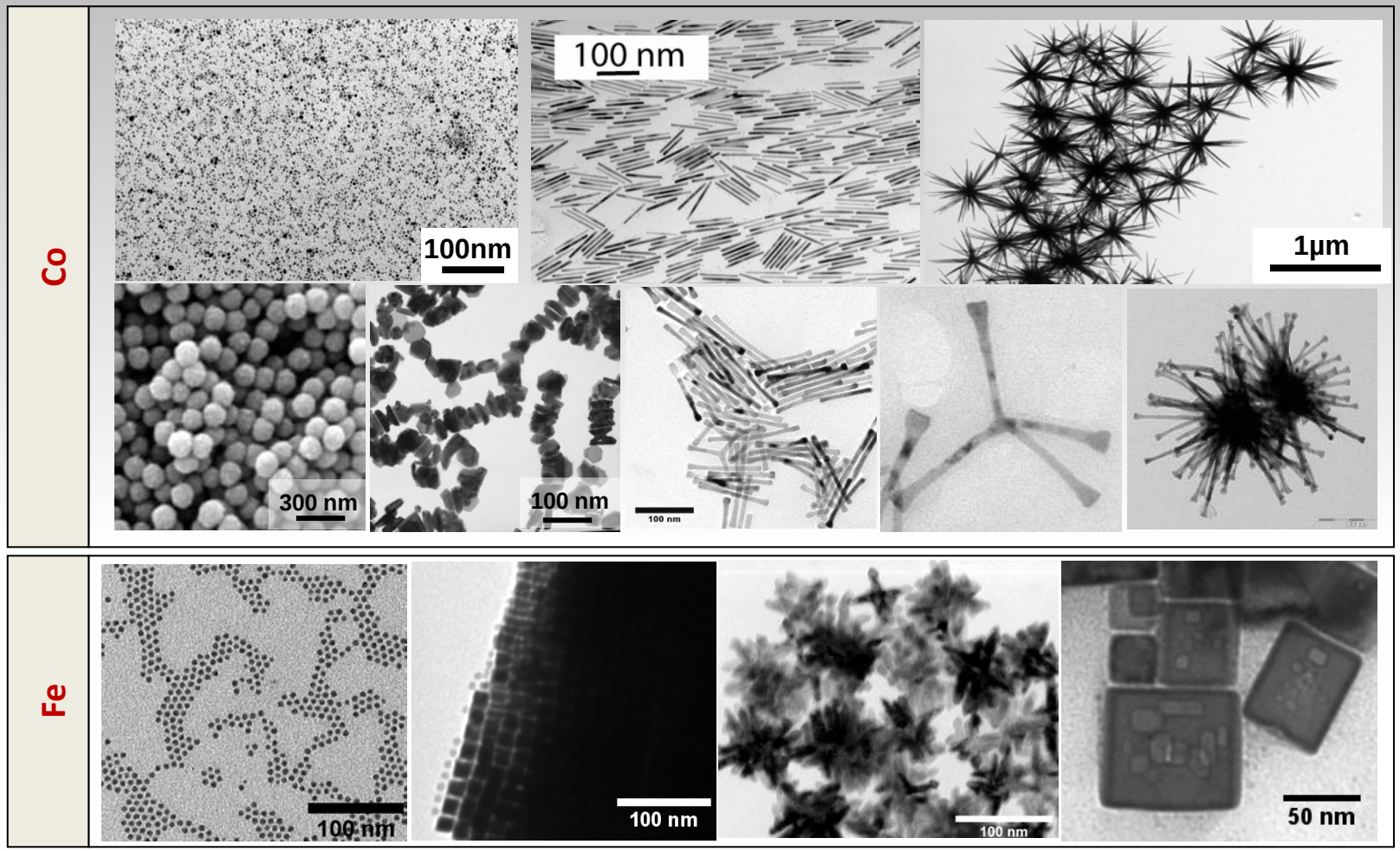

Spin configurations in size controlled single Fe nanomagnets

To study the Vortex -> Modomain transition, 3 issues have to be solved:

- Isolated nano-objects are mandatory to prevent any artefacts in the transition determination such as dipolar interactions

=> Need to find isolated magnetic particles

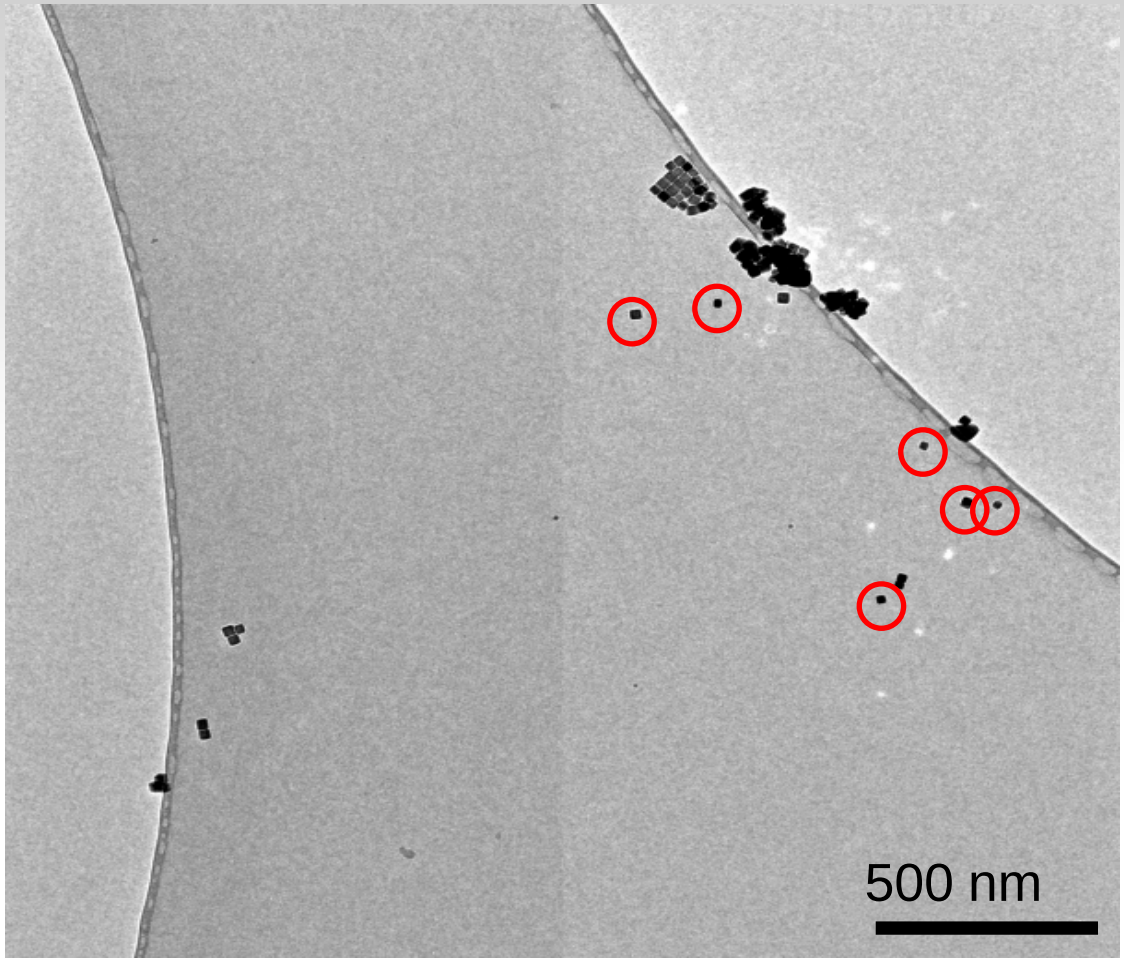

Spin configurations in size controlled single Fe nanomagnets

Several configurations of nanocubes: Study of their dipolar interactions

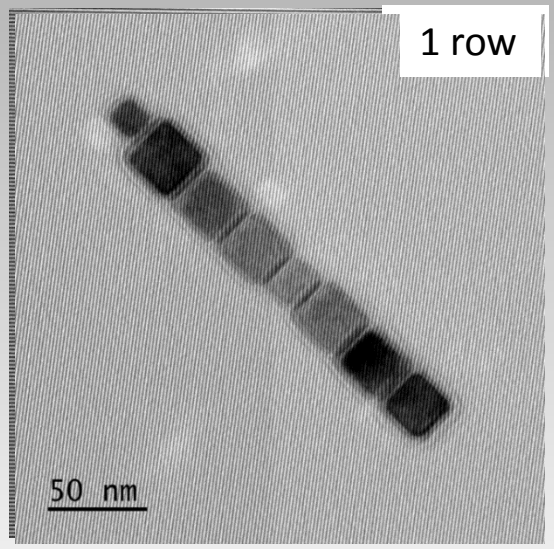

Hologram

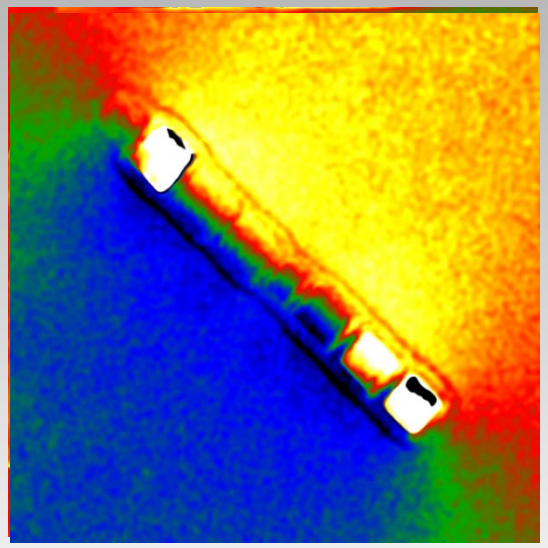

Magnetic Phase Shift

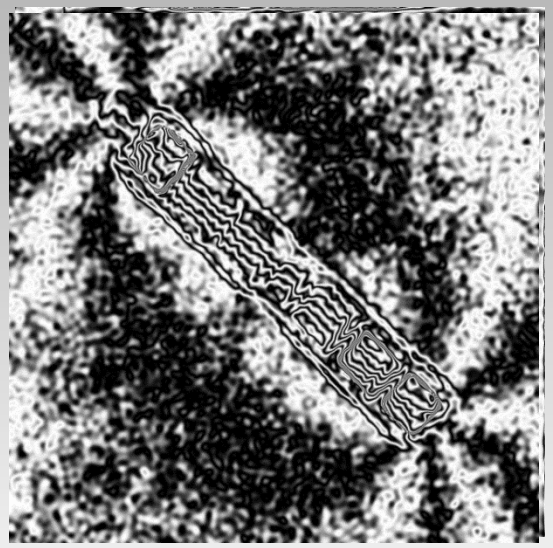

Cosine of Magnetic Phase

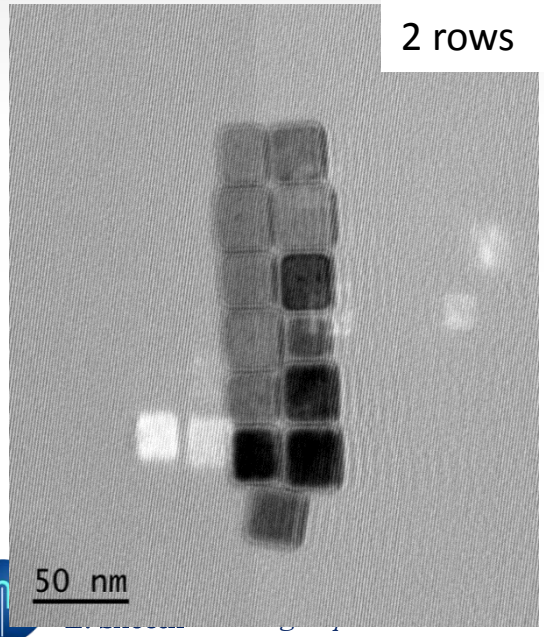

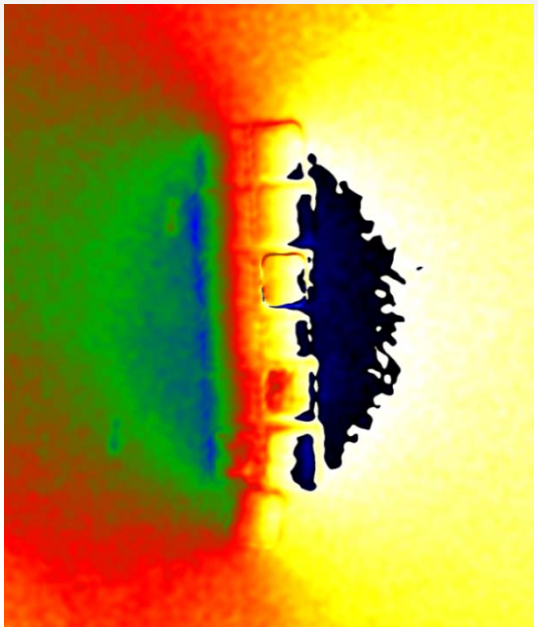

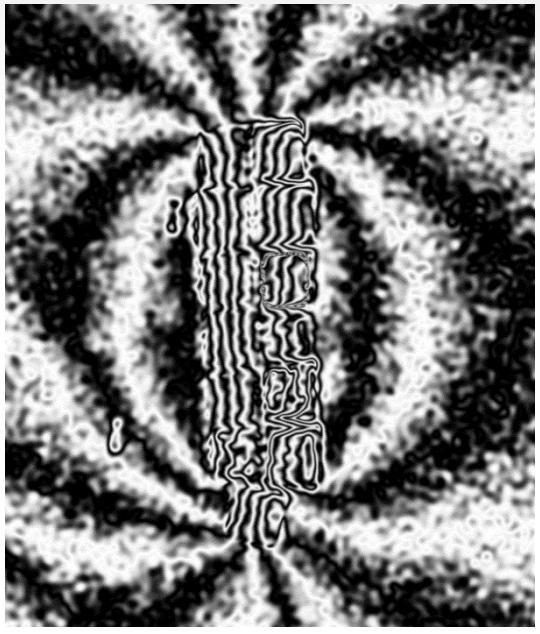

Induction profile and tilt problem

Y component, D dataset, -60 mA

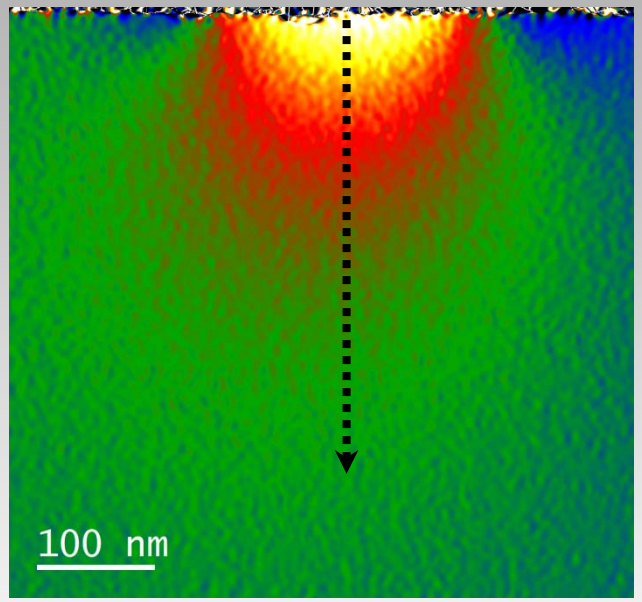

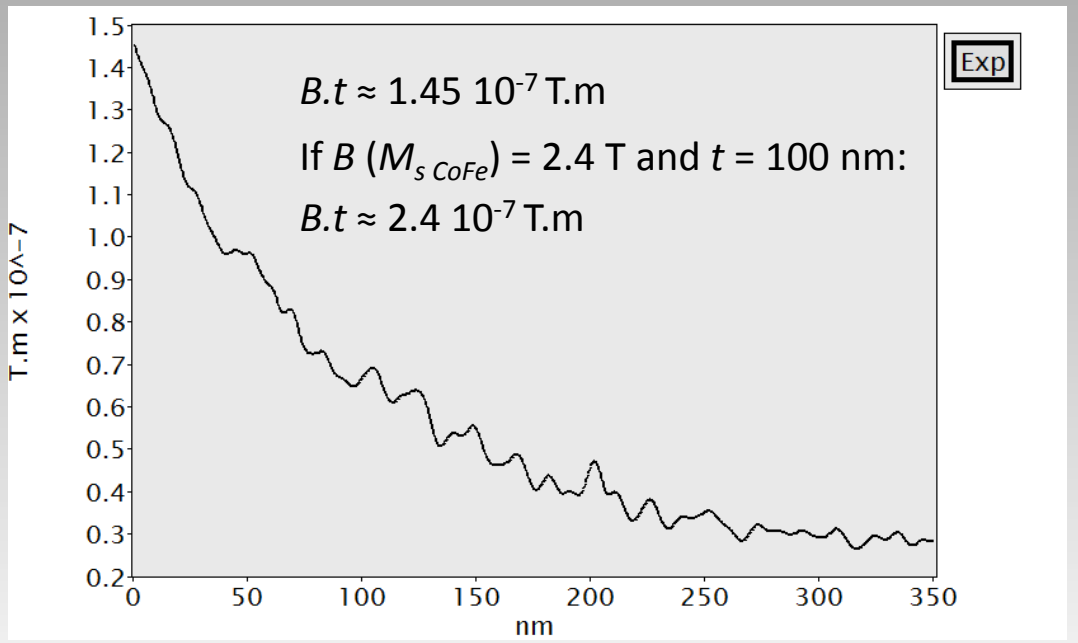

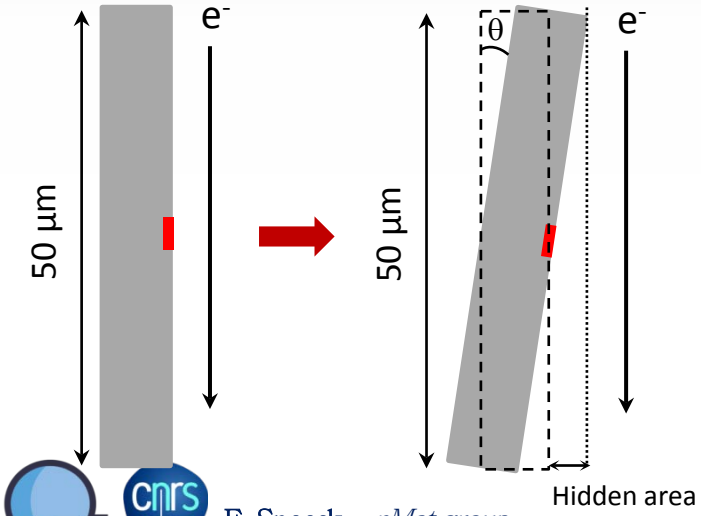

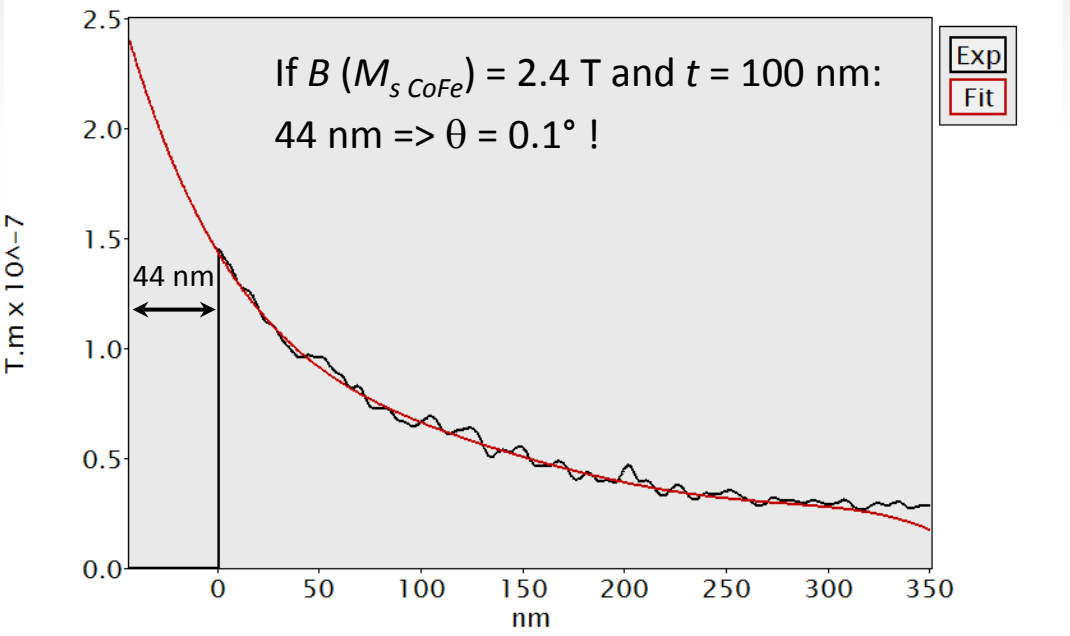

Domain wall imaging in Ni Nanowire

- Studying transition between vortex to transverse walls as a function of diameter
- Concept of « massless » DW [1,2]

Cylindrical symmetry => High propagation velocity of TW

=> Interest for spintronic logic devices

- Very few experimental observations of DW in cylinders

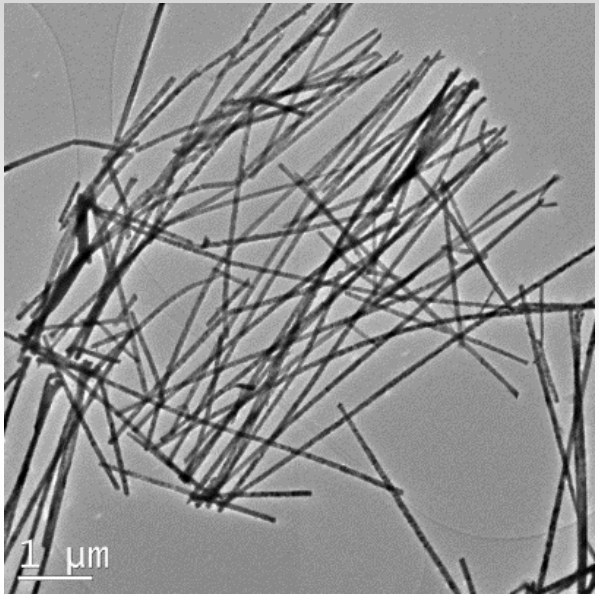

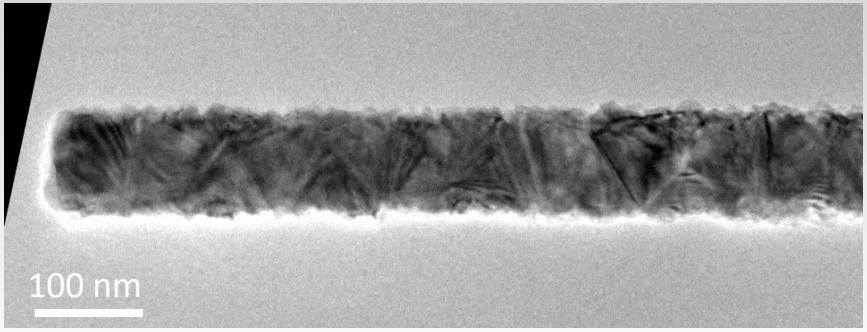

- Electro-deposition in commercial Poly-Carbonate (PC) membranes Polycrystalline nanocylinder
- Easy and low cost
- Mean diameter : 50, 80 or 110 nm
- Hundreds of nanowires on a TEM grid

$\mu_0 H_0 = 1T$

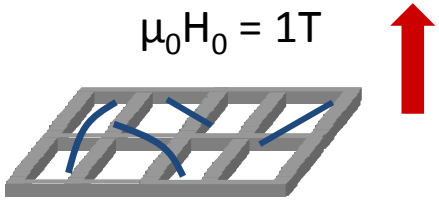

[1] M. Yan *et al.,* PRL **104**, 057201,(2010)
[2] M. Yan *et al.,* APL. **100**, 252401 (2012)

Domain wall imaging in Ni Nanowire

Without DW

With DW

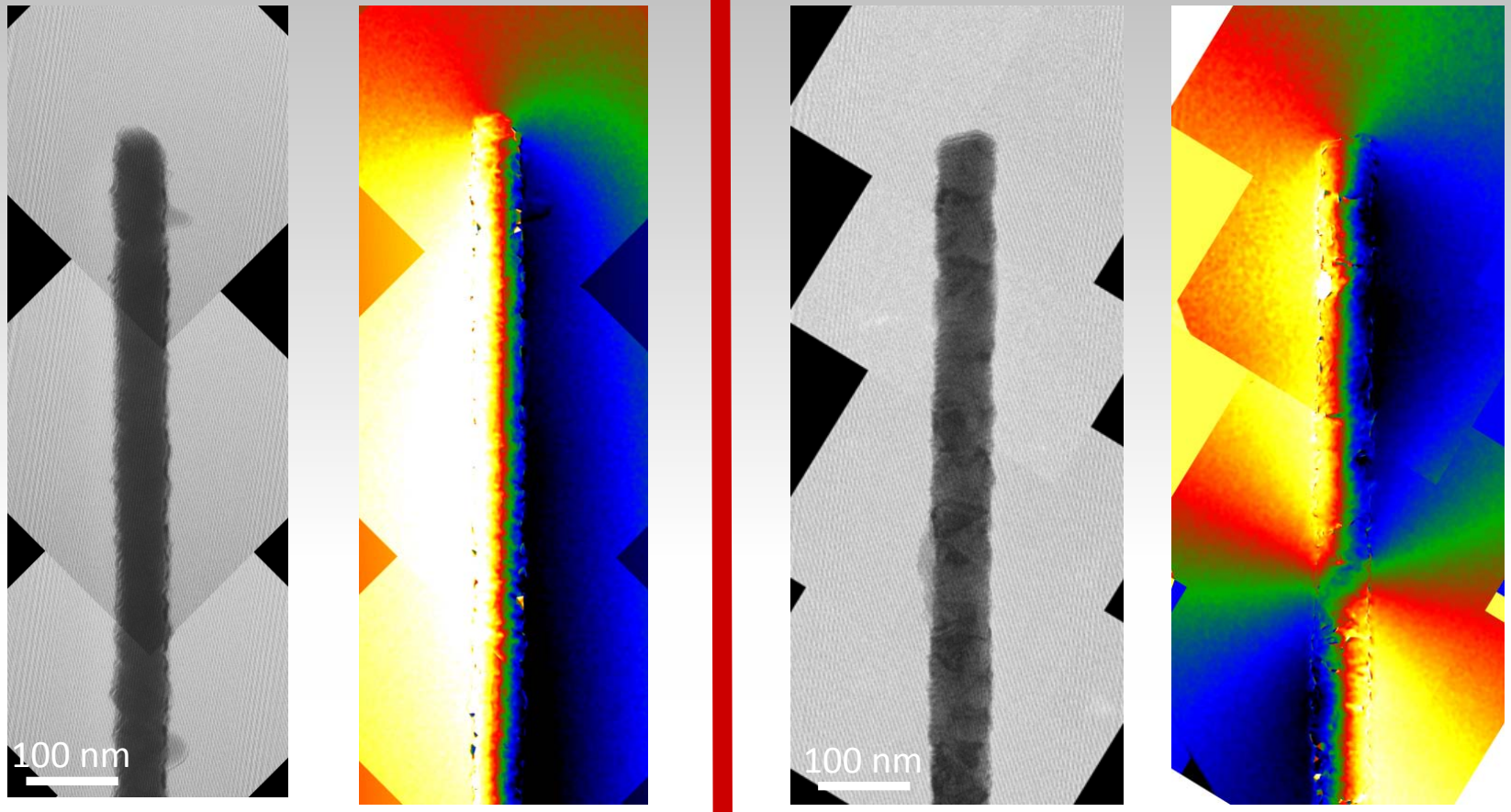

Local field lines outside the nanowire + asymmetry inside
=> Presence of a DW

Nanoletters, ***13,*** *2053-2057 (2013)*

Domain wall imaging in Ni Nanowire

3D OOMMF software: Cell size 2.5 x 2.5 x 2.5 nm^3

Universe size 500 x 500 x 2000 nm^3

Generation of grains with random orientation

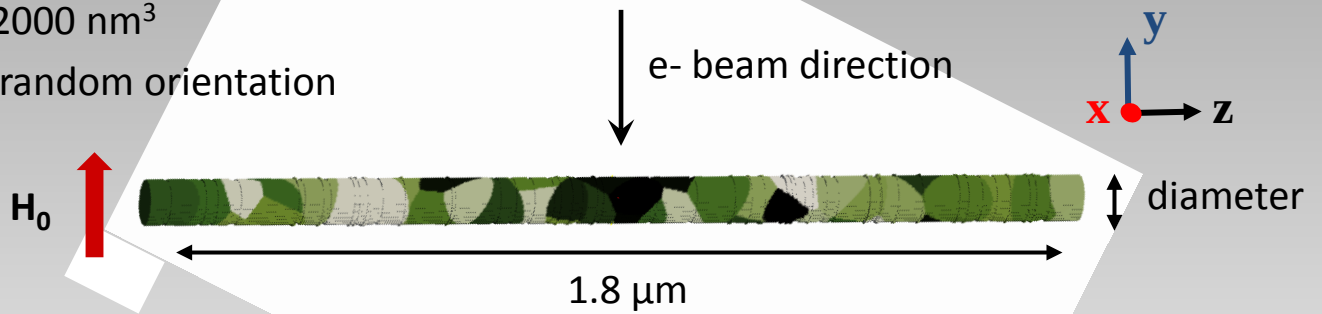

M_y component

ϕ = 48 nm

ϕ = 85 nm

ϕ = 92 nm

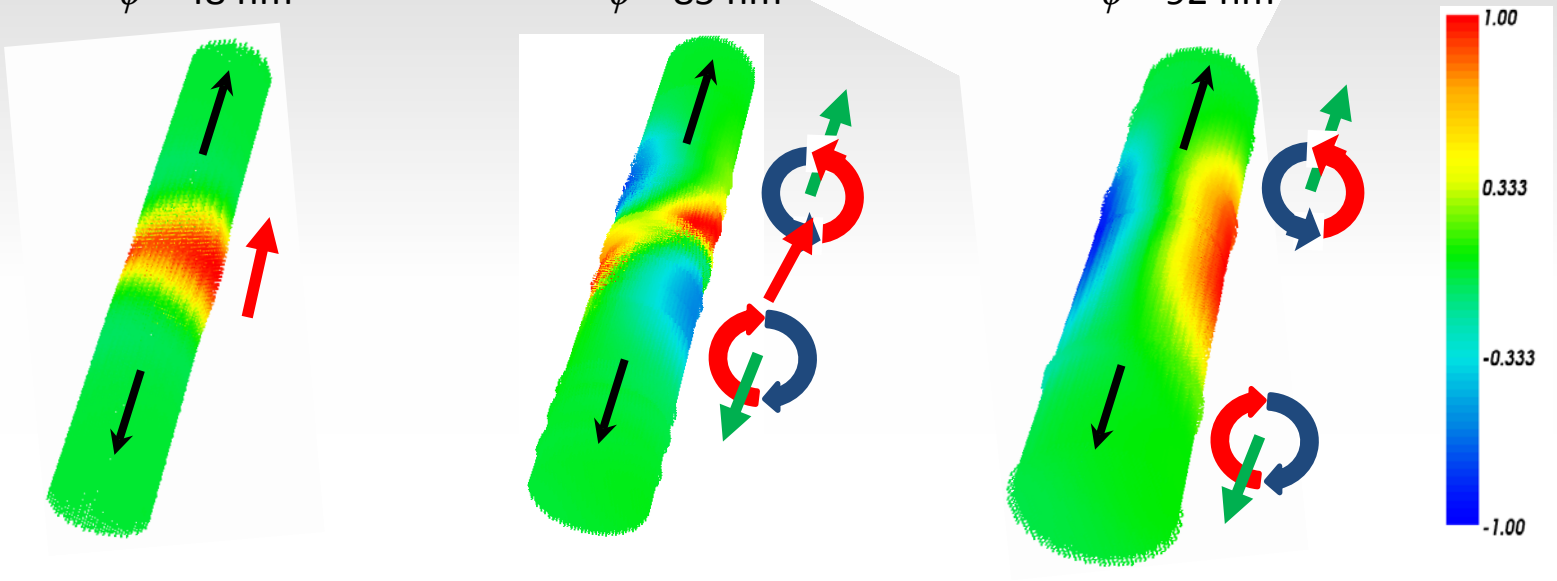

Tranverse → Hybrid → Vortex

diameter

Domain wall imaging in Ni Nanowire

Phase

Cos(phase)

Experimental phase

Diameter = 55 nm

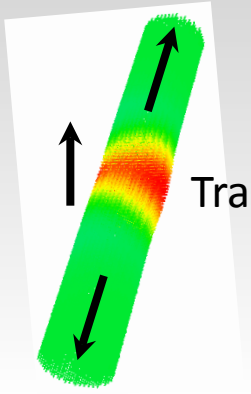

Transverse wall

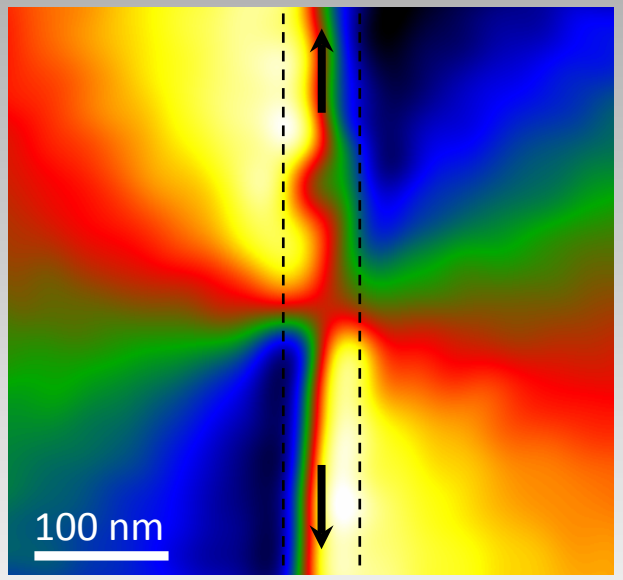

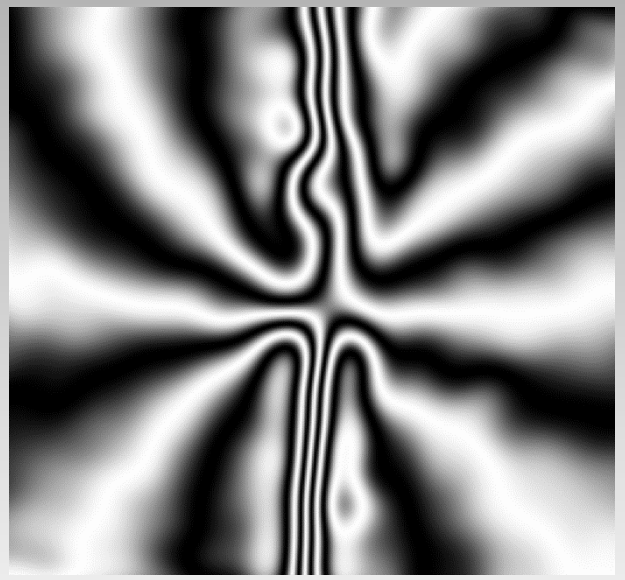

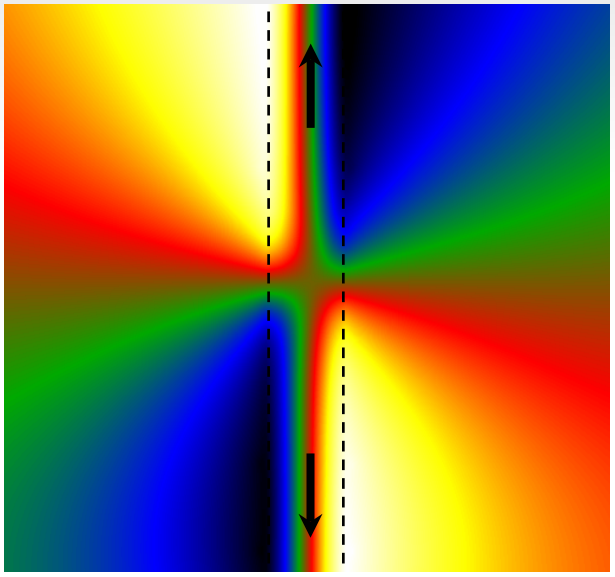

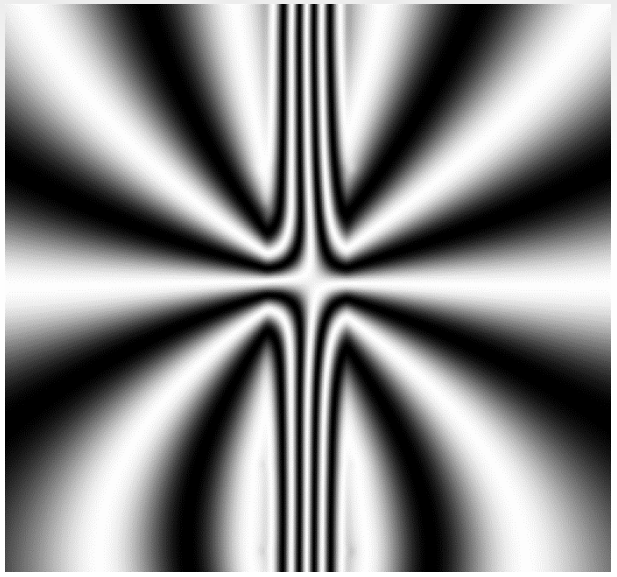

Simulated phase

Very good agreement between simulation and experiments

Domain wall imaging in Ni Nanowire

Phase

Cos(phase)

Experimental phase

Diameter = 85 nm

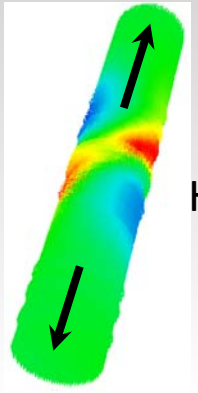

Hybrid wall

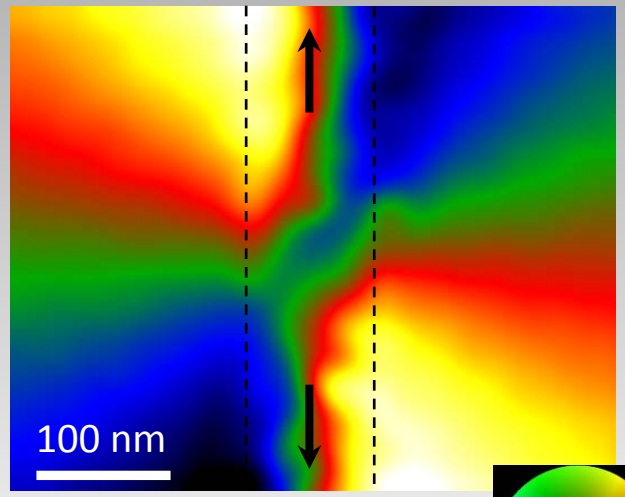

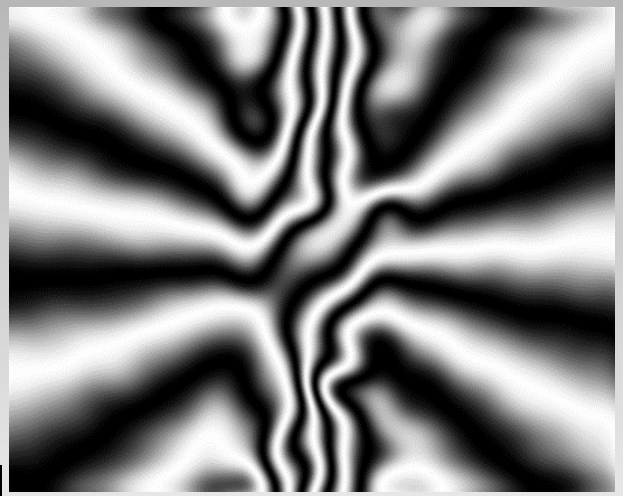

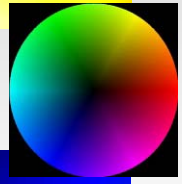

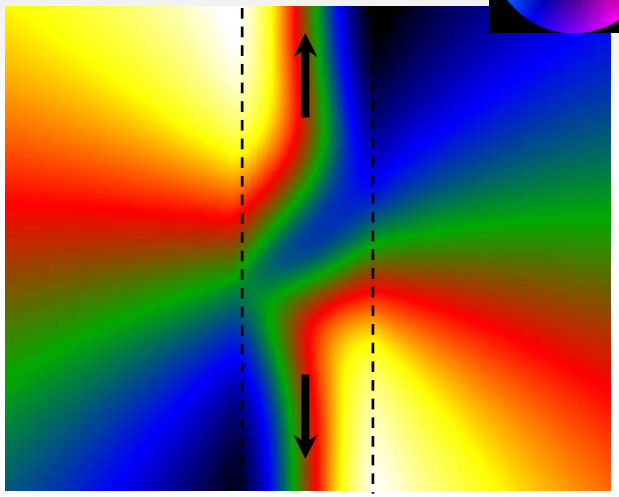

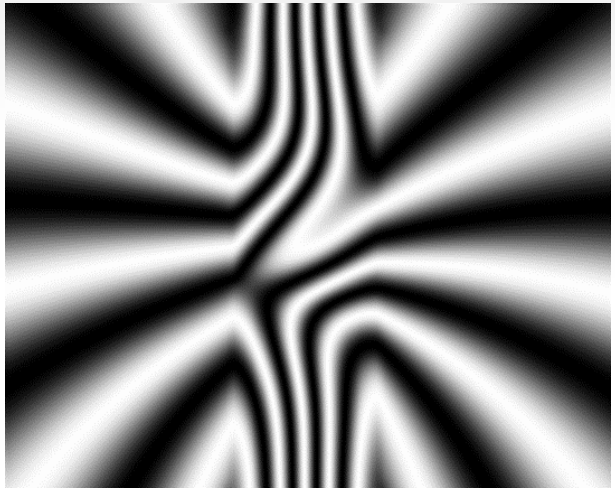

Simulated phase

Very good agreement between simulation and experiments

- Need to combine experimental phase and micromagnetic simulations
  => Determination of the magnetic configuration inside nano-objets

- New Hitachi I2TEM => Study of Fe Nanocubes (and other particles) with smaller dimensions. Next step: Study of the superparamagnetic transition

- Magnetic transition: function of the size, but possibility to change the temperature, to inject a current

- For nanowires: different domain walls have been observed. In future, study of nanowires with Co/Cu multilayers

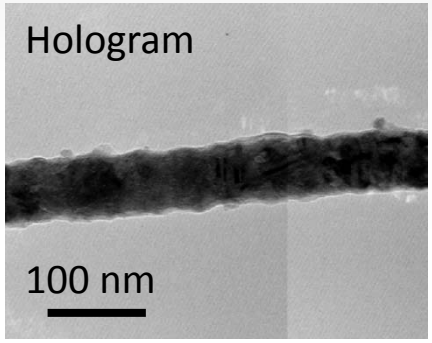

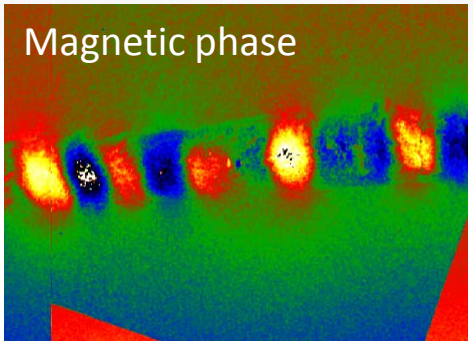

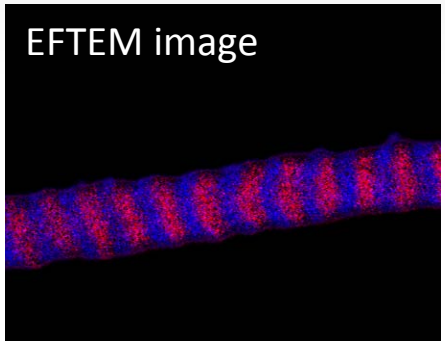

Special acknowledgments to ESTEEM2 Project and MIMETIS Equipex

I2TEM: Spatial Resolution

Observation modes	Aberration	Stage	Focusing	Cs	Cc	Resolution	Mag. at SA	Dark field
OBJ off observation Lorentz mode	Uncorrected	Standard	Int 1	770 mm	50 mm	1.0 nm	-	NA
	Corrected (Aplanatic)	Standard	TL11	0 mm	164 mm	0.56 nm	8.8	NA
Double stage (single focus Lorentz mode)	Uncorrected	Upper	Objective (weak)	3.2 m	63 mm	1.43 nm	3.8	NA
	Corrected (Aplanatic)	Upper	Objective (weak)	0 m	115 mm	0.48 nm		
Double stage (double focus Lorentz mode)	Uncorrected	Upper	Objective (strong)	241 m	1.1 m	4.2 nm	4.1	Available
	Corrected (Aplanatic)	Upper	Objective (strong)	0 m	1.7 m	1.8 nm	3.8	Available
High resolution mode	Uncorrected	Standard	Objective	2.3 mm	2.4 mm	0.24 nm	61	Available
	Corrected (Aplanatic)	Standard	Objective	0 mm	3.7 mm	0.084 nm	99 (Changeable)	Available

Very good spatial resolution

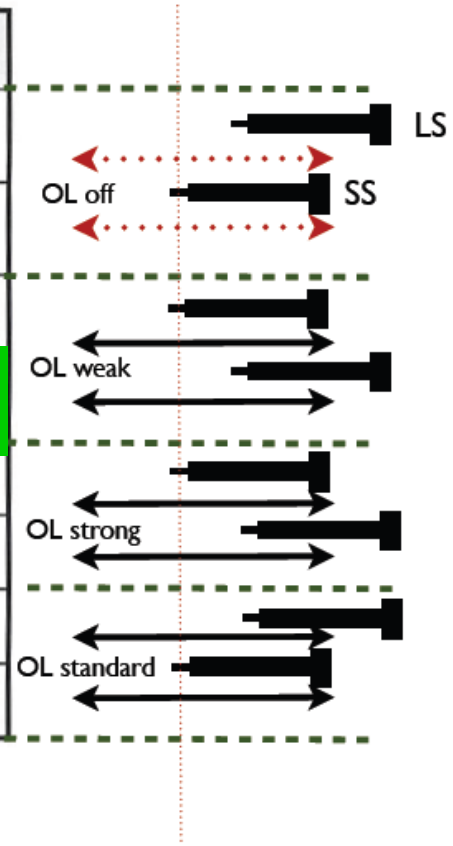

Accelerating voltage : 300kV
Pole piece : Wide gap

- ✓ 3 corrected Lorentz mode
- ✓ Various resolution and object magnification on the hologram
- ✓ 0.8A resolution in standard mode despite wide pole piece gap

Aharonov-Bohm effect: Phase shift of the beam due to the electromagnetic field

W. Ehrenberg, R.E. Siday, *Proc. Phys. Soc.* **B62**, 8 (1949)

Y. Aharonov, Y. D. Bohm , *Phys. Rev.* **115**, 485 (1959)

Y. Aharonov, Y. D. Bohm , *Phys. Rev.* **123**, 1511 (1961)

A. Tonumora *et al.*, *Phys. Rev. Letter* **48**, 1443 (1982)

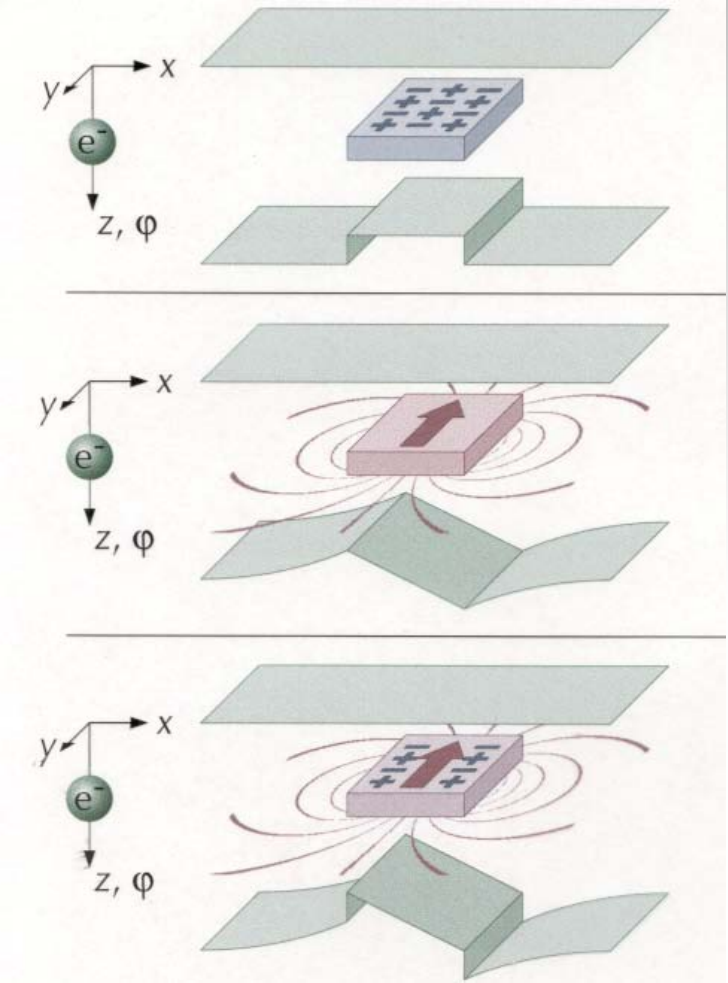

Phase shift introduced by the local electrostatic potential

$$\phi_{MIP,Elec}(\mathbf{R}) = C_E \int V(\mathbf{r})\, dz$$

Phase shift introduced by the magnetic field

$$\phi_{Mag}(\mathbf{R}) = -\frac{e}{h}\int A_z(\mathbf{r},z)\, dz$$

$$= -\frac{e}{h}\iint \mathbf{B}_{\mathbf{R}}(\mathbf{R}_\perp, z)\, dR\, dz$$

Total phase shift

$$\phi_{Total}(\mathbf{R}) = \phi_{MIP,Elec}(\mathbf{R}) + \phi_{Mag}(\mathbf{R})$$

Integration of the projected potential

Magnetic components from ϕ_{Mag}

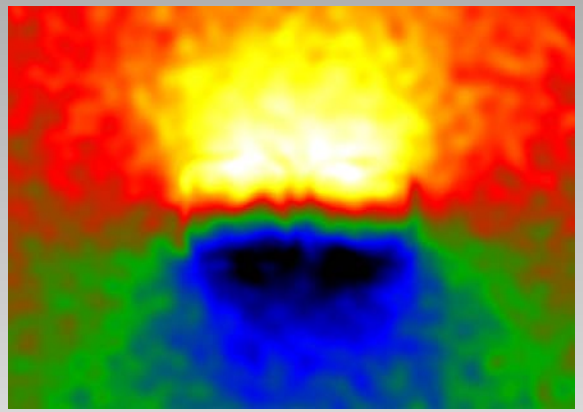

- Phase gradient proportional to the component in the plane of **B**

=> Isophase contours correspond to B direction

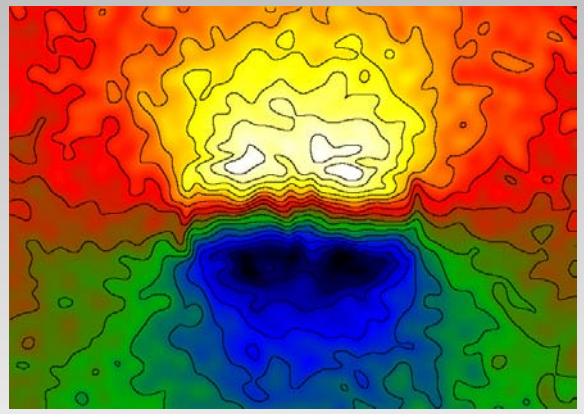

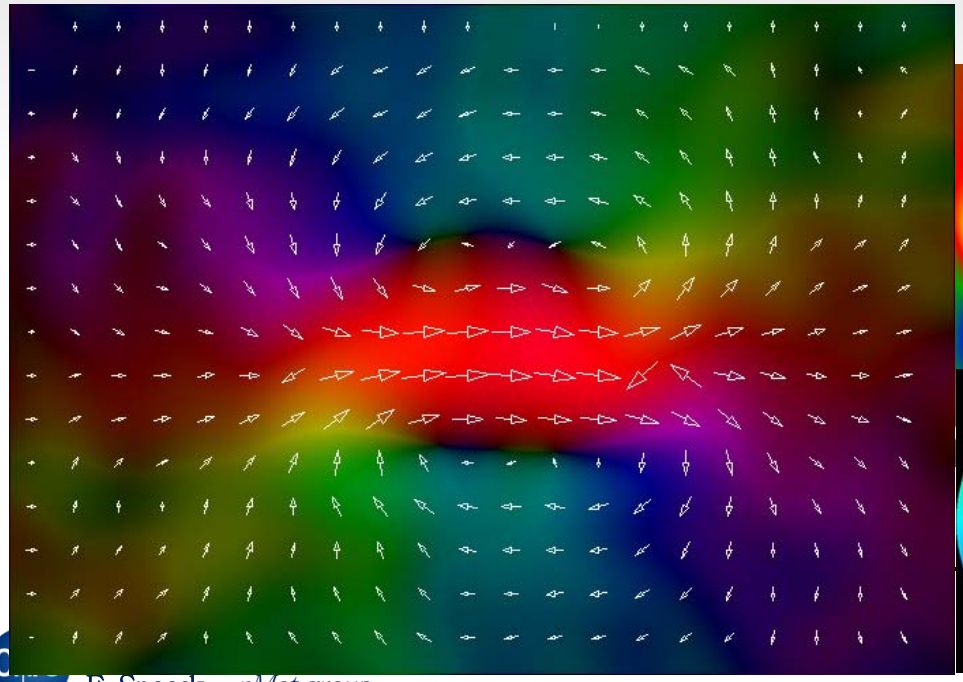

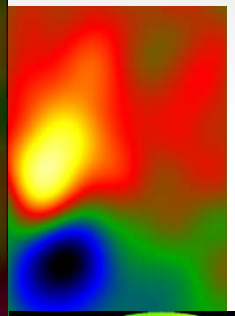

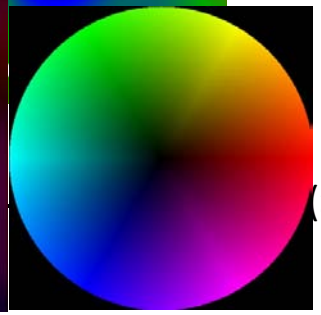

- <u>Only planar induction can be studied !</u>
- Complicated data treatment

(t = thickness)

Electro-deposition in commercial Poly-Carbonate (PC) membranes

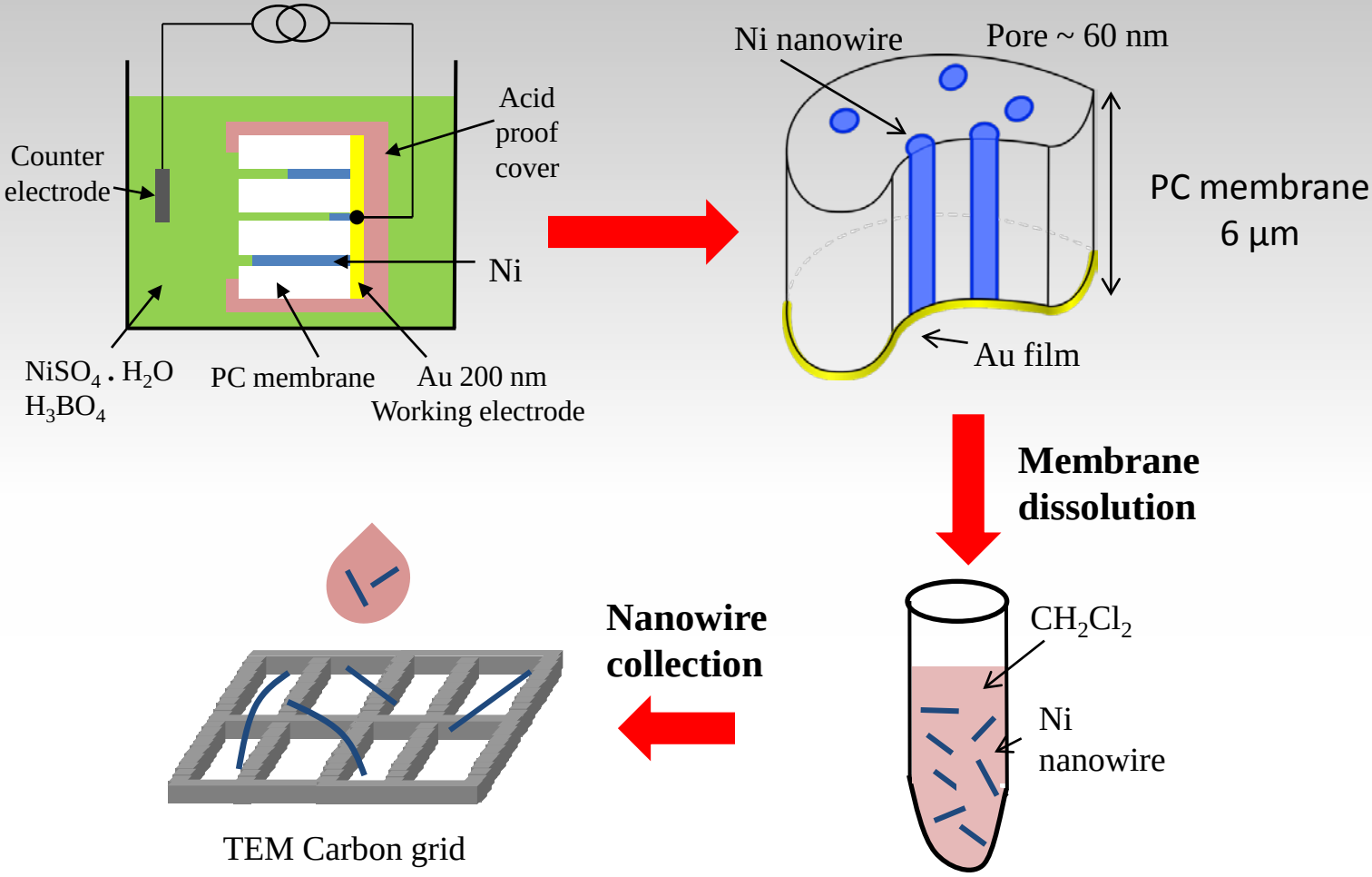

What does Φ contain ?

$\phi =$ ϕ_{MIP} + ϕ_{Elec} + ϕ_{Mag} + ϕ_{G}

Mean Inner Potential | Electric Field | Magnetic Induction | Geometrical Phase

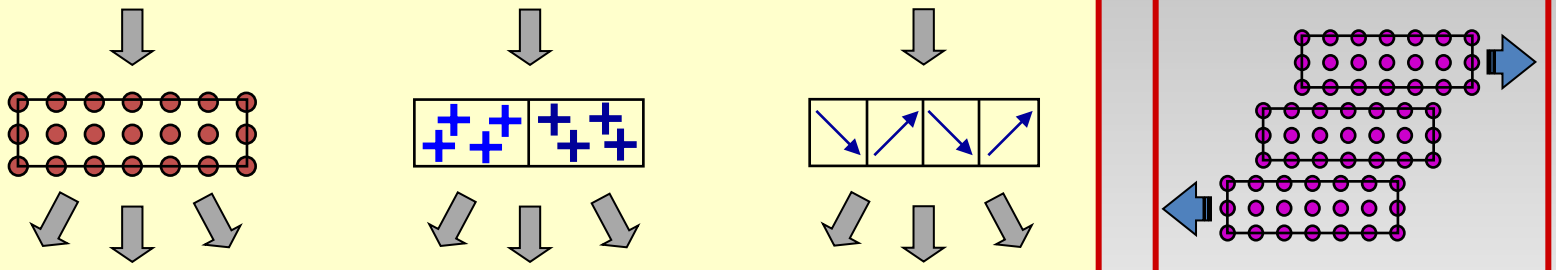

$$\phi_{MIP}(\mathbf{R}) = C_E \int V_{MIP}(\mathbf{r})\,\mathrm{dz} \quad \text{with} \quad C_E = \left(\frac{2\pi}{\lambda}\right)\left(\frac{E+E_0}{E(E+2E_0)}\right)$$

$$\phi_{Elec}(\mathbf{R}) = C_E \int V_{Elec}(\mathbf{r})\,\mathrm{dz} = C_E \iint E(\mathbf{r})\,\mathrm{dS}$$

(Samples with charges or Ferroelectric materials)

$$\phi_{Mag}(\mathbf{R}) = -\frac{e}{h}\int A_z(\mathbf{r},z)\,\mathrm{dz} = -\frac{e}{h}\iint \mathbf{B}_{\mathbf{R}}(\mathbf{R}_{\perp},z)\,\mathrm{dR}\,\mathrm{dz}$$

(Aharanov-Bohm effect)

For ϕ_G : peculiar case due to the periodic arrangement of atoms

Phase shift extraction

30nm Fe nanocubes

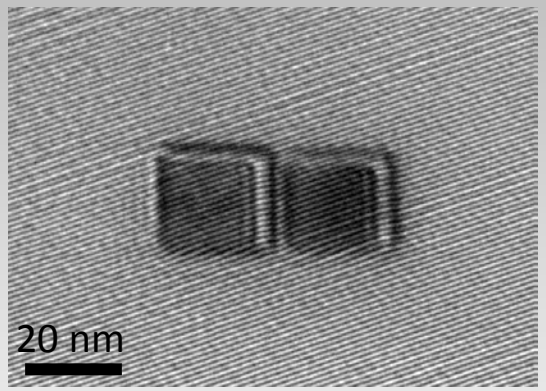

Hologram

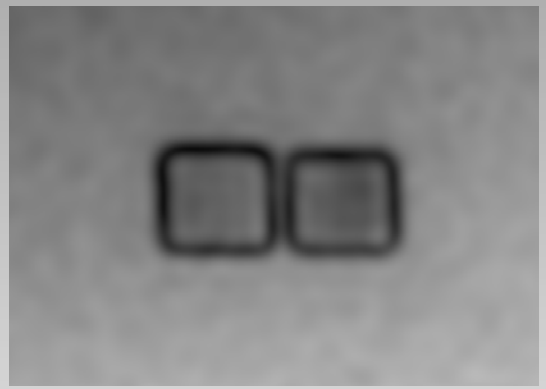

Amplitude image

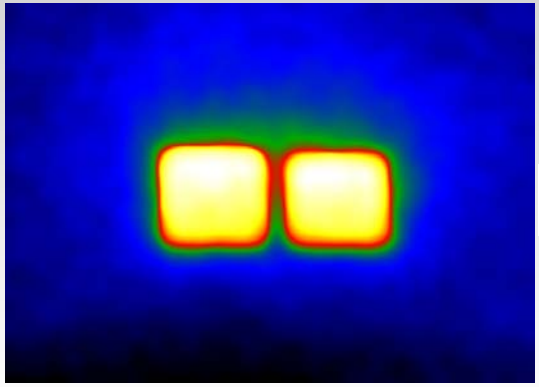

Phase image

$$\phi_{MIP,Elec}(\mathbf{R}) + \phi_{Mag}(\mathbf{R})$$

- Different methods to separate the contributions
- Need to record many holograms

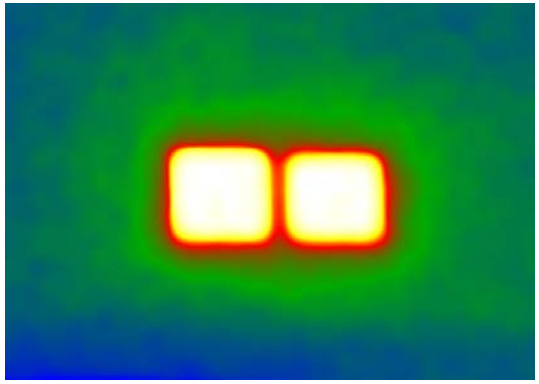

$$\phi_{MIP,Elec}(\mathbf{R}) = C_E \int V(\mathbf{r})\, dz \qquad \phi_{Mag}(\mathbf{R}) = -\frac{e}{h}\iint \mathbf{B}_{\mathbf{R}}(\mathbf{R}_{\perp}, z)\, dR\, dz$$

30nm Fe nanocubes

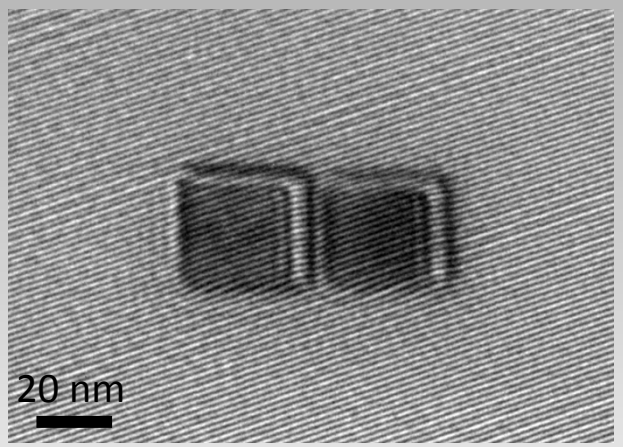

FFT

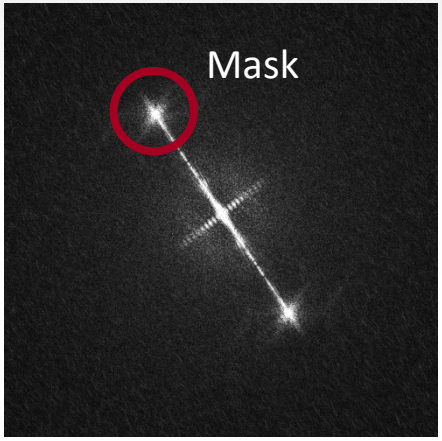

FFT^{-1}

Hologram Image

Interference between a reference wave and the wave through the sample

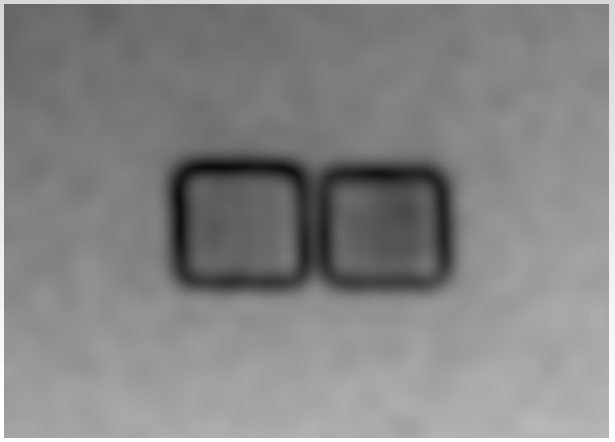

Amplitude image

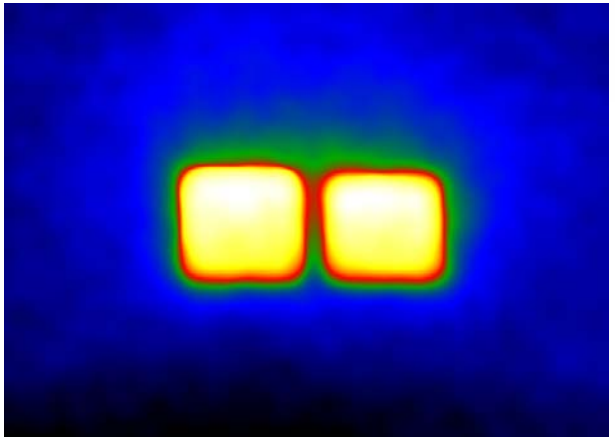

Phase image

Phase shift extraction and different contributions

30nm Fe nanocubes

$$\phi(\mathbf{R}) = \phi_{MIP,Elec}(\mathbf{R}) + \phi_{Mag}(\mathbf{R})$$

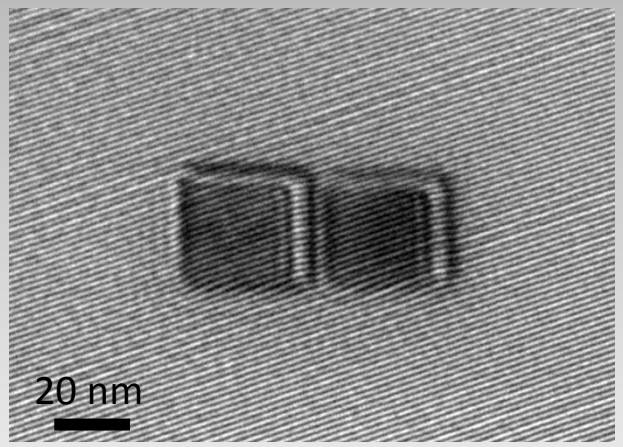

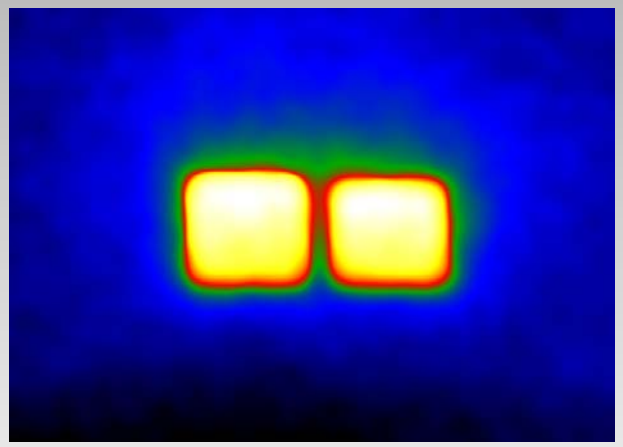

- Different methods to separate the contributions
- Need to record many holograms

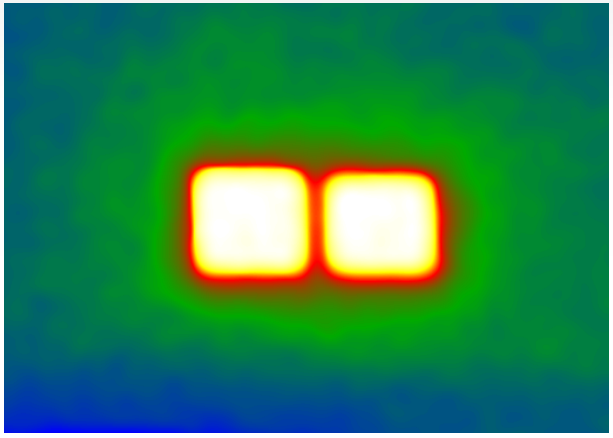

$$\phi_{MIP,Elec}(\mathbf{R}) = C_E \int V(\mathbf{r})\,\mathrm{dz}$$

$$\phi_{Mag}(\mathbf{R}) = -\frac{e}{h}\iint \mathbf{B}_{\mathbf{R}}(\mathbf{R}_{\perp}, z)\,\mathrm{dR}\,\mathrm{dz}$$

Incident beam $\psi_0 = \exp(i\mathbf{k}.\mathbf{r})$

↓

After the sample $\psi(\mathbf{r}) = A(\mathbf{R})\exp i\big((\mathbf{k}.\mathbf{r}) + \phi(\mathbf{R})\big)$

↓

After the objective lens $\Psi(\mathbf{r}) = A_S(\mathbf{R})\exp i\big((\mathbf{k}.\mathbf{r}) + \phi_S(\mathbf{R})\big)$

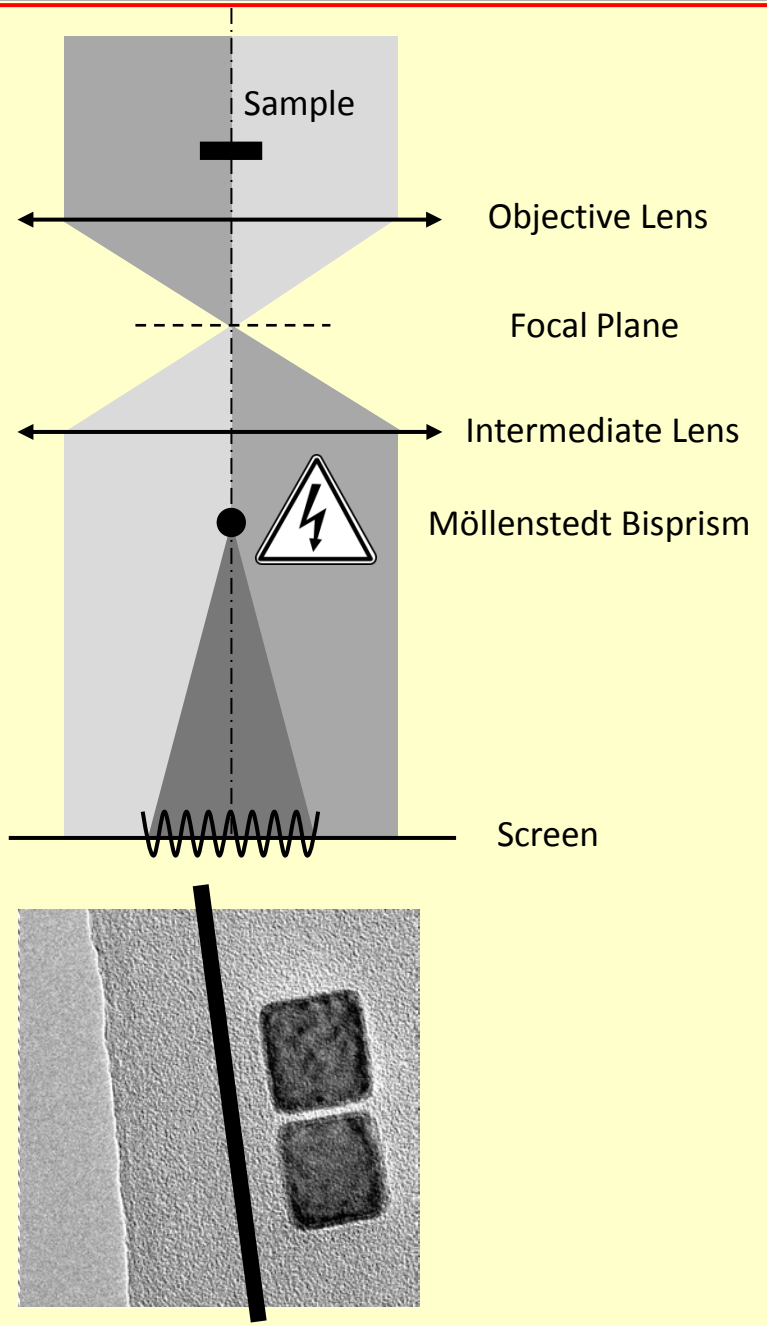

Image intensity

~~$I(\mathbf{R}) \propto |\Psi|^2 \propto A_S{}^2(\mathbf{R})$~~ → $\phi(\mathbf{R})$ is lost !

$$I_{Holo} = |\Psi_0 + \Psi^*|^2 \quad \text{+ background}$$
$$= 1 + A_s{}^2(\mathbf{R})$$
$$+ 2A_s(\mathbf{R}).\cos(2\pi R_0.x + \phi_S(\mathbf{R}))$$
$$+ I_{Inélast}(\mathbf{R})$$

Several configurations of nanocubes: Study of their dipolar interactions

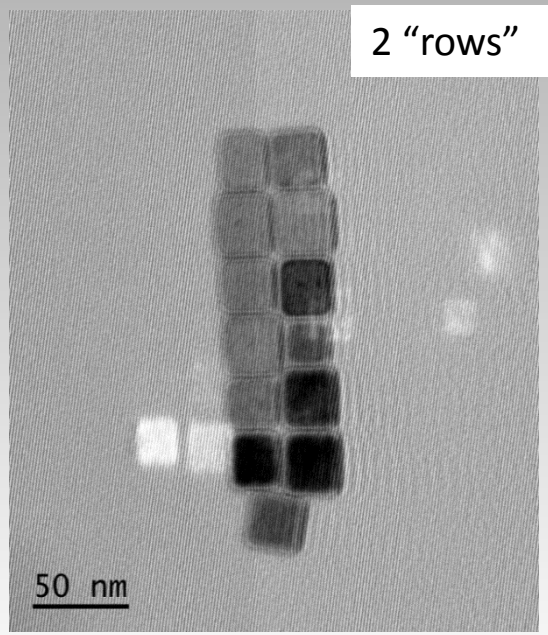

Hologram

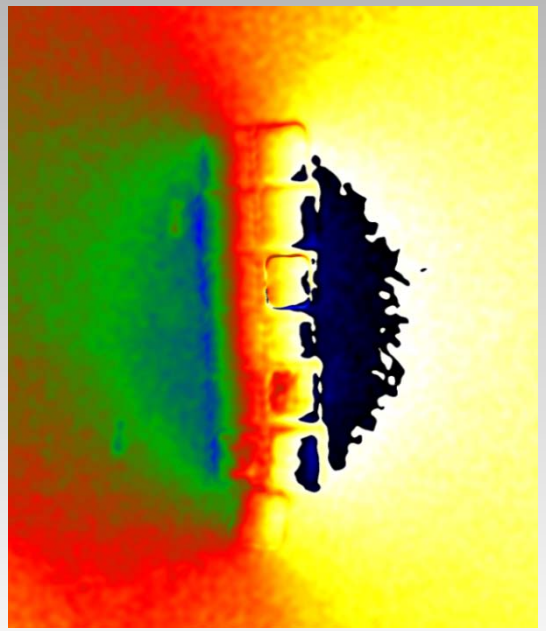

Magnetic Phase Shift

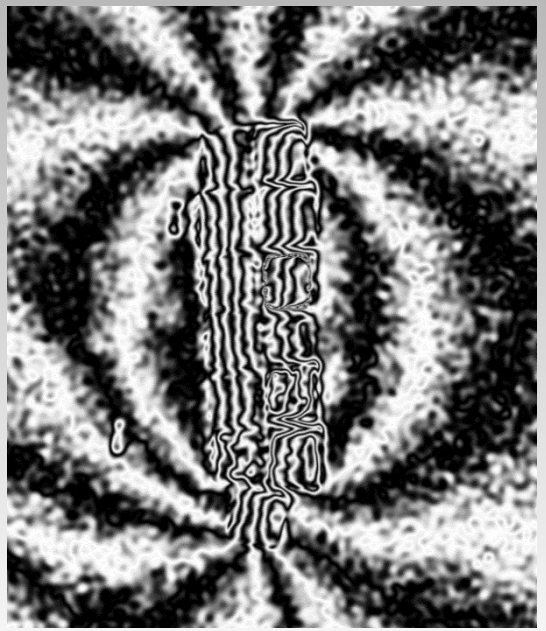

Cosine of Magnetic Phase

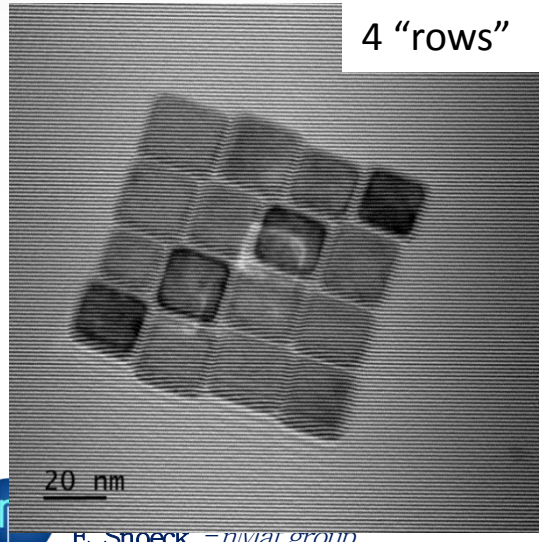

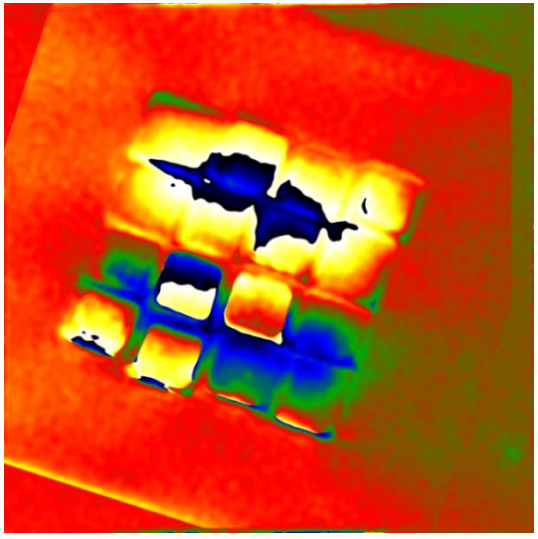

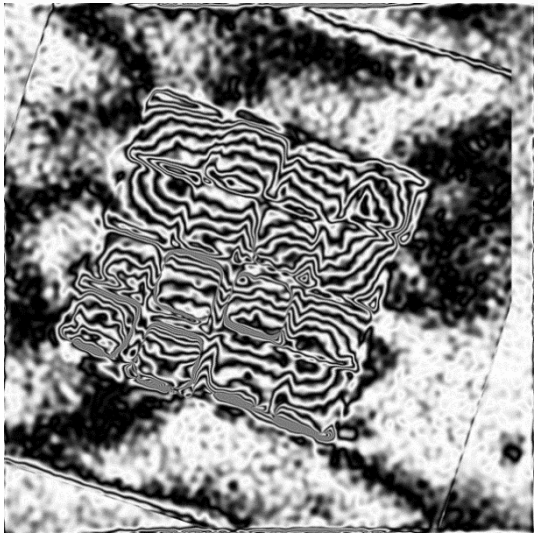

Variation of the radiated regions located at 5 nm in front of the pole as a function of the applie current

Angular spread